

# **Biocatalytic Production of Bioactive Dipeptides**

Von der Naturwissenschaftlichen Fakultät der  
Gottfried Wilhelm Leibniz Universität Hannover

zur Erlangung des Grades

**Doktor der Naturwissenschaften (Dr. rer. nat.)**

genehmigte Dissertation

von

**Sven Ingo Bordewick, M.Sc.**

2022

Referent: Prof. Dr. rer. nat. Dr.-Ing. habil. Ralf Günter Berger

Korreferent: apl. Prof. Dr. rer. nat. Sascha Beutel

Korreferent: Prof. Dr. rer. nat. habil. Lutz Fischer

Tag der Promotion: 15.12.2022

## Danksagung

Zuerst möchte ich mich ganz herzlich bei meinem Doktorvater Herrn Prof. Dr. Dr. Berger bedanken für die Bereitstellung dieses spannenden Themas und den Freiraum dieses ganz nach meinen Wünschen und Vorstellungen zu bearbeiten. Dieses große entgegengebrachte Vertrauen und die ständige Bereitschaft für Diskussionen und seine Ratschläge haben wesentlich dazu beigetragen, auch die schwierigen Phasen der Promotion zu überwinden und somit die vorliegende Arbeit erst möglich gemacht.

Bei Herrn Prof. Dr. Sascha Beutel und bei Herrn Prof. Dr. Lutz Fischer bedanke ich mich für die Übernahme des Korreferats und ebenso danke ich Herrn PD Dr. Krings für die Übernahme des Vorsitzes der Promotionskommission.

Allen ehemaligen und aktuellen Kollegen am LCI möchte ich für die sehr angenehme Atmosphäre und die große Hilfsbereitschaft danken. Insbesondere möchte ich mich bei Frau Dr. Franziska Ersoy bedanken für die jederzeit „offene Tür“ und die wertvollen fachlichen und sprachlichen Ratschläge.

Ich danke Alex, Selina, Lara, Hermine, Manuel und Franzi, deren Bachelor-Arbeiten ich betreuen durfte, für das Interesse an meiner Forschung, ihr engagiertes Arbeiten im Labor und die wertvolle Erfahrung, Wissen vermitteln zu können. Besonders bedanken möchte ich mich bei Alex, der mich auch nach seiner Bachelorarbeit noch lange als „HiWi“ tatkräftig unterstützt hat.

Dem Bundesministerium für Ernährung und Landwirtschaft (BMEL) danke ich für die Förderung unserer Forschungsarbeiten zu Salzgeschmacksverstärkern.

Meinen Freunden gilt mein größter Dank für die Unterstützung in den schwierigen Momenten und die vielen schönen und lustigen Momente: David, Ben, Lars, Andy, Hubertus und Ludwig. Besonders danke ich außerdem ML für das Zuhören und die unzähligen wertvollen Ratschläge.

Vanessa danke ich für ihre Liebe und Unterstützung, ohne die sowohl die Promotion als auch das Durchleben der Pandemie unvorstellbar schwieriger gewesen wäre. Ebenso möchte ich mich bei ihrer Familie für die freundliche Aufnahme und Unterstützung bedanken.

Zum Schluss und am allerwichtigsten möchte ich mich bei meiner Mutter bedanken für die bedingungslose Liebe, das Vertrauen und die Unterstützung in allen Lebenslagen. Vielen, vielen Dank!

## Zusammenfassung

Dipeptide sind eine vielversprechende Substanzklasse mit einer großen Bandbreite verschiedener Bioaktivitäten. Für N-terminale Arginyldipeptide (Arg-X) wurden sowohl salzgeschmacksverstärkende (u. a. Arg-Ser) als auch antihypertensive Eigenschaften (Arg-Phe) nachgewiesen. Eine neuartige biokatalytische Strategie für die spezifische Synthese dieser Dipeptide ist die Nutzung von L-Aminosäureligasen wie RizA aus *B. subtilis*, welche es ermöglicht Arg-X Dipeptide direkt aus den Aminosäuren zu synthetisieren. Hindernisse für einen industriellen Einsatz sind allerdings die Abhängigkeit von dem teuren Kofaktor ATP (Adenosintriphosphat), niedrige Produktausbeuten, die Bildung von unerwünschtem Arg-Arg als Nebenprodukt und die potenziell hohen Enzymkosten.

Um den Bedarf an ATP zu senken, wurde eine Strategie zur ATP-Regenerierung aus Acetylphosphat mittels Acetatkinase aus *E. coli* (AckA) etabliert. Bis zu 5.9 g/L Arg-Ser wurden produziert, was einer ATP-Effizienz von 23 g Arg-Ser pro Gramm ATP entsprach (ohne Regenerierung maximal 0.5 g Arg-Ser/g ATP). Als nächstes wurden Varianten von RizA erzeugt, um die Substratspezifität zu beeinflussen. Insgesamt 21 RizA-Varianten wurden mittels positionsgerichteter Mutagenese von acht Positionen in der Substratbindetasche erzeugt. Weitere 14 Varianten wurden durch Kombination verschiedener Mutationen erzeugt. Varianten mit verbesserter Aktivität und Spezifität wurden für alle fünf betrachteten Aminosäurekombinationen (Arg + Arg, Asp, Ser, Ala oder Phe) gefunden. Der größte Unterschied wurde für K83F\_S156A erhalten, welches die Produktbildung von Arg-Phe im Vergleich zum Wildtypenzym versechsfachte und die Spezifität mehr als verzehnfachte. Schließlich wurde eine Ko-Immobilisierung von RizA und ausgewählten Varianten mit AckA durchgeführt, um die Wiederverwendbarkeit dieses biokatalytischen Systems zu ermöglichen. Immobilisate von T81F\_A158S produzierten bis zu 3,0 g/L Arg-Ser und Immobilisate von K83F\_S156A produzierten bis zu 3.8 g/L Arg-Phe und konnten beide mehrfach wiederverwendet werden.

Diese Arbeit stellt die erste umfassende wissenschaftliche Untersuchung zur Etablierung einer Regenerierung von ATP für eine L-Aminosäureligase und die Ko-Immobilisierung eines solchen Systems dar und hat das Wissen über das *engineering* der Substratspezifität von L-Aminosäureligasen wesentlich erweitert.

**Schlagerworte:** Biokatalyse; bioaktive Dipeptide; Salzgeschmacksverstärker; Antihypertensivum; L-Aminosäureligasen; ATP-Regenerierung; *protein engineering*; Ko-Immobilisierung

## Abstract

Dipeptides are a promising substance class with a large variety of bioactivities. N-terminal arginyl dipeptides (Arg-X) have been shown to exhibit both salt-taste enhancing (Arg-Ser among others) and antihypertensive properties (Arg-Phe). A novel biocatalytic strategy for the specific synthesis of these dipeptides is the application of L-amino acid ligases like RizA from *B. subtilis*, which enables production of Arg-X dipeptides directly from their amino acids. However, challenges for an industrial application are the dependence on the expensive cofactor ATP (adenosine triphosphate), low product yields, formation of the undesired side product Arg-Arg and the potentially high enzyme costs.

In order to reduce the need for ATP, a strategy for ATP regeneration from acetyl phosphate was established using acetate kinase from *E. coli* (AckA). Up to 5.9 g/L Arg-Ser were produced, corresponding to an ATP efficiency of 23 g Arg-Ser per gram ATP (without regeneration max. 0.5 g Arg-Ser/g ATP). Next, variants of RizA were created to alter the substrate specificity. A total of 21 RizA variants were created by site-directed mutagenesis of eight positions in the substrate binding pocket. Additional 14 variants were created by combination of different mutations. Variants with improved activity and specificity were identified for all five examined amino acid combinations (Arg + Arg, Asp, Ser, Ala, Phe). The largest change was observed for K83F\_S156A, which improved the product formation of Arg-Phe six-fold and improved specificity more than ten-fold. Finally, co-immobilization of RizA and selected variants with AckA was performed to enable reusability of this biocatalytic system. Immobilisates of T81F\_A158S produced up to 3.0 g/L Arg-Ser and immobilisates of K83F\_S156A produced up to 3.8 g/L Arg-Phe and could both be reused several times.

This thesis represents the first extensive scientific investigation into establishing ATP regeneration for an L-amino acid ligase and co-immobilization of such a biocatalytic system, and substantially expanded the knowledge about engineering the substrate specificity of L-amino acid ligases.

**Keywords:** biocatalysis; bioactive dipeptides; salt-taste enhancer; antihypertensive; L-amino acid ligase; ATP regeneration; protein engineering; co-immobilization

---

**Table of Contents**

Danksagung .....	I
Zusammenfassung .....	II
Abstract.....	III
Table of Contents .....	IV
List of Tables.....	VII
List of Sequences.....	VII
List of Figures.....	VII
List of Abbreviations.....	IX
1 Introduction .....	1
1.1 Biocatalysis.....	1
1.1.1 Development.....	1
1.1.2 Engineering of Biocatalytic Reactions.....	3
1.1.3 Regeneration of ATP .....	6
1.1.4 Immobilization.....	10
1.2 Bioactive Dipeptides .....	11
1.2.1 Properties .....	11
1.2.2 Applications of Arginyl Dipeptides .....	12
1.3 Production of Dipeptides .....	15
1.3.1 Strategies.....	15
1.3.2 L-Amino Acid Ligases .....	17
2 Aim of This Thesis .....	20
3 Preamble to the Publication “Recombinant Production of Arginyl Dipeptides by L-Amino Acid Ligase RizA Coupled with ATP Regeneration”.....	21
4 Recombinant Production of Arginyl Dipeptides by L-Amino Acid Ligase RizA Coupled with ATP Regeneration .....	22
4.1 Abstract.....	22
4.2 Introduction .....	23
4.3 Results and Discussion .....	24
4.3.1 Influence of Substrate Concentrations .....	24
4.3.2 Influence of Cofactor Concentrations .....	25
4.3.3 Influence of Enzyme Concentrations.....	26
4.3.4 Influence of Temperature and pH.....	27
4.3.5 Time Course of Formation of Arg-Ser, Arg-Ala, Arg-Gly and Arg-Arg .....	28
4.4 Materials and Methods .....	30
4.4.1 Chemicals, Reagents and Strains .....	30
4.4.2 Construction of pET28a_his6-rizA and pET28a_his6-ackA Constructs.....	31

---

4.4.3	Cultivation and Expression .....	31
4.4.4	Purification.....	31
4.4.5	Biocatalysis .....	32
4.4.6	Analysis .....	32
4.5	Conclusions .....	32
4.6	Supplementary Materials .....	33
4.7	Disclosures .....	34
5	Preamble to the Publication “Mutagenesis of the L-Amino Acid Ligase RizA Increased the Production of Bioactive Dipeptides” .....	36
6	Mutagenesis of the L-Amino Acid Ligase RizA Increased the Production of Bioactive Dipeptides.....	37
6.1	Abstract.....	37
6.2	Introduction .....	38
6.3	Results and Discussion .....	39
6.3.1	Selection of Mutations .....	39
6.3.2	Biocatalytic Performance of RizA Variants With Different Substrates .....	42
6.3.3	Effects of Mutations on the Substrate Specificity and Biocatalytic Productivity of RizA .....	46
6.4	Materials & Methods .....	52
6.4.1	Chemicals, Reagents and Strains .....	52
6.4.2	Mutagenesis of RizA .....	52
6.4.3	Cultivation and Purification.....	52
6.4.4	Biocatalysis.....	53
6.4.5	Analysis .....	53
6.5	Conclusions .....	53
6.6	Supplementary Materials .....	54
6.7	Disclosures .....	58
7	Preamble to the publication “Co-Immobilization of RizA Variants with Acetate Kinase for the Production of Bioactive Arginyl Dipeptides” .....	59
8	Co-Immobilization of RizA Variants with Acetate Kinase for the Production of Bioactive Arginyl Dipeptides .....	60
8.1	Abstract.....	60
8.2	Introduction .....	61
8.3	Results and Discussion .....	63
8.3.1	(Co-)Immobilization Conditions.....	63
8.3.2	Co-Immobilization of RizA Variants.....	65
8.3.3	Characterization of the Immobilisates .....	69
8.4	Materials & Methods .....	74
8.4.1	Chemicals, Reagents and Strains .....	74

---

8.4.2	Mutagenesis .....	74
8.4.3	Production of Soluble Enzymes.....	75
8.4.4	Immobilization.....	75
8.4.5	Biocatalysis.....	75
8.4.6	Analysis .....	76
8.5	Conclusions .....	76
8.6	Supplementary Materials.....	77
8.7	Disclosures .....	77
9	Conclusion and Outlook .....	79
10	References .....	82
11	Lebenslauf .....	93
12	Liste der wissenschaftlichen Publikationen.....	94



## List of Tables

<b>Table 1-1.</b> Challenges in designing a biocatalytic process and methods for solving them. ..5	
<b>Table 1-2.</b> Effects of a selection of bioactive dipeptides. .... 12	12
<b>Table 1-3.</b> Overview of biocatalytic methods to produce dipeptides. .... 16	16
<b>Table 1-4.</b> Overview of characterized LALs. .... 19	19
<b>Table 6-1.</b> Variants with the highest biocatalytic performance for the production of Arg-X dipeptides..... 49	49
<b>Table 8-1.</b> Comparison of the biocatalytic performances of the RizA immobilisates..... 72	72
<b>Supporting Table 6-1.</b> Primer pairs for mutagenesis..... 56	56
<b>Supporting Table 8-1.</b> Primer pairs for mutagenesis..... 77	77

## List of Sequences

<b>Supporting Sequence 4-1.</b> DNA sequence of his6-rizA..... 34	34
<b>Supporting Sequence 4-2.</b> DNA sequence of his6-ackA ..... 34	34

## List of Figures

<b>Figure 1-1.</b> Strategies employed in protein engineering dependent on the necessary amount of data on the enzyme and screening capabilities..... 3	3
<b>Figure 1-2.</b> Structure and ATP-dependent processes. .... 7	7
<b>Figure 1-3.</b> Selection of phosphorylation reactions forming ADP or ATP. .... 8	8
<b>Figure 1-4.</b> ATP regeneration from ADP and acetyl phosphate using acetate kinase..... 9	9
<b>Figure 1-5.</b> Classification of immobilization methods. .... 10	10
<b>Figure 1-6.</b> Covalent immobilization using a carrier activated with NHS-ester groups. .... 11	11
<b>Figure 1-7.</b> Proposed mechanism for LALs. .... 18	18
<b>Figure 4-1.</b> Graphical abstract of the publication (Bordewick et al., 2021b). .... 22	22
<b>Figure 4-2.</b> Reaction scheme for the RizA/AckA system for regeneration of ATP from acetyl phosphate for synthesis of Arg-Ser from arginine and serine. .... 24	24
<b>Figure 4-3.</b> Effect of substrate amino acids (AA) and acetyl phosphate on the Arg-Ser production..... 25	25
<b>Figure 4-4.</b> Effect of the two cofactors ATP and Mg <sup>2+</sup> on Arg-Ser production..... 26	26
<b>Figure 4-5.</b> Effect of two enzymes RizA and AckA on Arg-Ser production. .... 27	27
<b>Figure 4-6.</b> Effect of the temperature and buffer pH on Arg-Ser production..... 28	28

---

<b>Figure 4-7.</b> Time course of dipeptide formation with optimized reaction conditions.....	29
<b>Figure 6-1.</b> Graphical abstract of the publication (Bordewick et al., 2021a). .....	37
<b>Figure 6-2.</b> Mutated residues of RizA (green) in the C- (red) and N-terminal (blue) binding pocket .....	40
<b>Figure 6-3.</b> Residues in the C-terminal binding pocket.....	41
<b>Figure 6-4.</b> Residues in the N-terminal binding pocket.....	42
<b>Figure 6-5.</b> Formation of Arg-Arg by the RizA variants.....	43
<b>Figure 6-6.</b> Formation of Arg-Asp and Arg-Arg by the RizA variants.....	44
<b>Figure 6-7.</b> Formation of Arg-Ser and Arg-Arg by the RizA variants. ....	45
<b>Figure 6-8.</b> Formation of Arg-Ala and Arg-Arg by the RizA variants.....	45
<b>Figure 6-9.</b> Formation of Arg-Phe and Arg-Arg by the RizA variants. ....	46
<b>Figure 6-10.</b> Change in product formation with RizA variants compared to the wild type with each substrate.....	47
<b>Figure 8-1.</b> Graphical abstract of the publication (Bordewick et al., 2022). .....	60
<b>Figure 8-2.</b> Immobilization of RizA in comparison to co-immobilization of RizA and AckA. ....	63
<b>Figure 8-3.</b> Effect of different ratios of RizA and AckA during co-immobilization.....	65
<b>Figure 8-4.</b> Production of Arg-X dipeptides by soluble variants containing two mutations. ....	66
<b>Figure 8-5.</b> Co-immobilization of RizA variants.....	68
<b>Figure 8-6.</b> Effect of reaction temperature and pH.....	69
<b>Figure 8-7.</b> Effect of reaction temperature .....	71
<b>Supporting Figure 4-1.</b> Comparison of reaction with or without regeneration.....	33
<b>Supporting Figure 6-1.</b> 3D bar chart of dipeptide formation. ....	54
<b>Supporting Figure 6-2.</b> Change in product formation of RizA. ....	55
<b>Supporting Figure 6-3.</b> Exemplary chromatogram with gradient program 1 for measurement of Arg-Ser. ....	55
<b>Supporting Figure 6-4.</b> Exemplary chromatogram with gradient program 2 for measurement of Arg-Phe. ....	56
<b>Supporting Figure 8-1.</b> Reusability of the immobilisates when using coupling buffer for washing.....	77

---

**List of Abbreviations**


---

<b>Abbreviation</b>	<b>Meaning</b>
× g	Times gravity / relative centrifugal force
°C	Degrees Celsius
μM	μmol/L
1,3-BPG	1,3-Bisphosphoglycerate
AA	Amino acid(s)
ACE	Angiotensin I-cleaving enzyme
AckA	Acetate kinase from <i>E. coli</i>
AcP	Acetyl phosphate
ADP	Adenosine diphosphate
AMP	Adenosine monophosphate
APPA	2-Amino-5-phosphono-3- <i>cis</i> -pentenoic acid
ATP	Adenosine triphosphate
<i>B. subtilis</i>	<i>Bacillus subtilis</i>
BLE	<i>Bundesanstalt für Landwirtschaft und Ernährung</i> (german)
BMEL	<i>Bundesministerium für Ernährung und Landwirtschaft</i> (german)
Boc	<i>tert</i> -Butyloxycarbonyl
Bzl	Benzyl
cAMP	Cyclic adenosine monophosphate
CAST	Combinatorial active-site saturation test
Cbz	Carboxybenzyl
CCK	Cholecystokinin
CDP-choline	Cytidine diphosphate-choline
CLEA	Cross-linked enzyme aggregate
Da	Dalton
DNA	Deoxyribonucleic acid
<i>E. coli</i>	<i>Escherichia coli</i>
<i>e.g.</i>	<i>Exempli gratia</i> (latin) / for example
EC	Enzyme Commission number
EDTA	Ethylenediaminetetraacetic acid
ENaC	Epithelium sodium channel
FACS	Fluorescence-activated cell sorting

---

FAD	Flavin adenine dinucleotide
Fmoc	Fluorenylmethyloxycarbonyl
fw	Forward
GC	Gas chromatography
HIV	Human immunodeficiency virus
HPLC	High performance liquid chromatography
<i>i.e.</i>	<i>Id est</i> (latin) / that is
IPTG	Isopropyl $\beta$ -D-1-thiogalactopyranoside
$K_m$	Michaelis-Menten constant
LB	Lysogeny broth
M	mol/L
mM	mmol/L
MTP	Microtiter plate
n.i.	not identified
NADH	Nicotinamide dinucleotide
NADPH	Nicotinamide dinucleotide phosphate
NCD	Non-communicable diseases
NHS	<i>N</i> -hydroxysuccinimide
Ni-NTA	Nickel-nitriloacetic acid
PCR	Polymerase chain reaction
PDB	Protein Data Bank
pH	"Potential of hydrogen"
$P_i$	Inorganic phosphate
pI	Isoelectric point
$PP_i$	Pyrophosphate
PPK	Polyphosphate kinase
ProSAR	Protein structure-activity relationship
QM/MM	Quantum mechanical/molecular mechanics
RizA	<i>L</i> -Amino acid ligase RizA from <i>B. subtilis</i>
RNA	Ribonucleic acid
RP	Reversed-phase
rpm	Revolutions per minute
RT	Room temperature
rv	Reverse

---

SAM	<i>S</i> -Adenosylmethionine
SHR	Spontaneously hypertensive rats
SLP	Substrate-level phosphorylation
TB	Terrific broth
<i>t</i> -Bu	<i>tert</i> -Butyl
TRIS	Tris(hydroxymethyl)aminomethane
TβL	Tabtoxinine β-lactam
WHO	World Health Organization

---

For amino acids, the IUPAC 3-letter or 1-letter abbreviations are used. If no configuration is stated, an L-configuration is intended. Two or more amino acids connected by hyphens (*e.g.* Arg-Ser) denote a peptide sequence starting with the N-terminal amino acid. Amino acid substitutions in enzymes are given by their original amino acid and position followed by the substitution (*e.g.* T81F); in the case of multiple substitutions, these are separated by underscores (*e.g.* T81F\_A158S).

## 1 Introduction

### 1.1 Biocatalysis

#### 1.1.1 Development

For thousands of years, humanity has wielded nature's potential for bioconversions to produce and conserve foods like bread, cheese, beer, vinegar or wine through fermentation (Sheldon & Pereira, 2017). For example, the earliest evidence for cereal-based beer brewing was found in a cave in Israel dating back 11,700 to 13,700 years (Liu et al., 2018). Since then, the usage of living organisms or parts thereof to produce goods has significantly shaped humanity's development and has grown into the field of biotechnology, which can be defined as "the application of scientific and engineering principles to the processing of materials by biological agents" (Buchholz & Collins, 2013; Gavrilescu & Chisti, 2005). The discovery that bioconversions are not dependent on the presence of living cells was made by Eduard Buchner, who used cell-free yeast extracts to convert sugars to ethanol (Buchner, 1897). He was later awarded the Nobel Prize in Chemistry in 1907 for his work (Jaenicke, 2007). Ludwig Rosenthaler is widely regarded as the father of the field of biocatalysis for his usage of plant extracts containing hydroxynitrile lyase to selectively synthesize (*R*)-mandelonitrile from benzaldehyde and hydrogen cyanide (Rosenthaler, 1909; Yi et al., 2021).

Fermentation can be distinguished from biocatalysis in that the former is usually a whole-cell bioconversion, in which production of the biocatalyst and the desired reaction are coupled, while they are independent in biocatalysis and the enzyme or resting whole cells are prepared beforehand. Biocatalysis can be classified further depending on whether resting cells, isolated enzymes or immobilized enzymes are used. The usage of resting cells has the inherent risk of side reactions possibly degrading substrates or products or leading to undesired reactions. Additionally, the cell membrane needs to be permissible for the substrates. The usage of isolated enzymes circumvents these issues but complicates separation of the enzyme from the reaction solution and its reuse. This can be improved through the use of immobilized enzymes (Reetz, 2013b).

Biocatalysis has many advantages due to the often very high specificity of enzymes, mild reaction conditions and less requirement for using hazardous solvents or reagents (Bell et al., 2021; Bornscheuer et al., 2012). Additionally, enzymes are a non-toxic and inherently biodegradable, renewable resource and thus are generally environmentally-friendly catalysts. They possess great potential for the sustainable production of a wide range of products in the

chemical, pharmaceutical, food and other related industries (Sheldon & Woodley, 2018). Apart from the application of enzymes as detergent ingredients for over 30 years, one of the earlier and most economically significant biocatalytic applications is the usage of nitrile hydratase to produce acrylamide from acrylonitrile on a thousands of tons per year scale (Bell et al., 2021; Kirk et al., 2002; Yamada & Kobayashi, 1996). In the production of esters for the cosmetics industry (*e.g.* myristyl myristate) by Evonik, the enzymatic process outperformed the chemical one: Despite high enzyme costs, usage of immobilized and reusable CAL-B lipase at reduced temperatures (60 to 80 °C) was more cost-efficient than the chemical process, which incurred higher energy expenditures due to the high reaction temperature (>180 °C) and costly downstream processing to remove malodorous by-products (Thum, 2004; Wu et al., 2021b). An important example from the pharmaceutical industry is the application of an (*R*)-selective transaminase for the synthesis of sitagliptin, an anti-diabetic compound (Choi et al., 2015). The last step of the chemical process is a reductive amination using rhodium-catalyzed asymmetric hydrogenation followed by crystallization. The hydrogenation step required high pressure equipment, removal of the transition metal from the product, and had low stereoselectivity, which in turn necessitated the crystallization step to obtain optically pure product. With the application of an engineered transaminase, the overall yield and productivity were improved, less waste was produced and the crystallization step could be omitted (Desai, 2011; Savile et al., 2010). Another example is the application of a ketoreductase for regio-specific hydroxylation in the synthesis of a precursor of atorvastatin, which is used in treating abnormally high lipid levels in the blood (Choi et al., 2015; Huisman & Collier, 2013; Ma et al., 2010).

In earlier biocatalysis, mostly hydrolases were used, mainly for the kinetic resolution of chiral alcohols, amines and carboxylic acids, or ketoreductases for the asymmetric reduction of prochiral ketones. Today, this has expanded to encompass enzymes from nearly all classes. In addition, the development of a biocatalytic process has shifted from optimizing the reaction conditions to suit an enzyme towards engineering an enzyme to suit the desired purpose and reaction conditions (Wu et al., 2021b; Yi et al., 2021). Thus, the development of biocatalysis is closely tied to that of protein engineering.

### 1.1.2 Engineering of Biocatalytic Reactions

The development of biocatalysis was described by Bornscheuer et al. (2012) to proceed in three distinct waves: In the first wave, starting with the work by Rosenthaler (Chapter 1.1.1), biocatalytic reactions were performed with extracts and isolated enzymes and thus depended on the availability of suitable enzymes in nature and arduous screening and isolation procedures. After the establishment of recombinant DNA (deoxyribonucleic acid) technology increased the availability of enzymes through the ability to produce them recombinantly (Reetz, 2013b), the second wave in the 1980s and 1990s was based on the emergence of protein engineering. Early rational design approaches focused on changing single amino acids based on structural information about the enzyme. In the third wave of biocatalysis, a new approach was developed, in which random mutations were introduced into enzymes followed by selection of improved variants. Due to its similarities to Darwinian evolution, it was coined “directed evolution”. It was pioneered in the late 1990s by Pim Stemmer and Frances Arnold, the latter of which received the 2018 Nobel Prize in Chemistry for her contributions, while the former had unfortunately already passed away (Bornscheuer et al., 2019; Jones, 2018). Today, a whole spectrum of protein engineering methods exists (Figure 1-1).

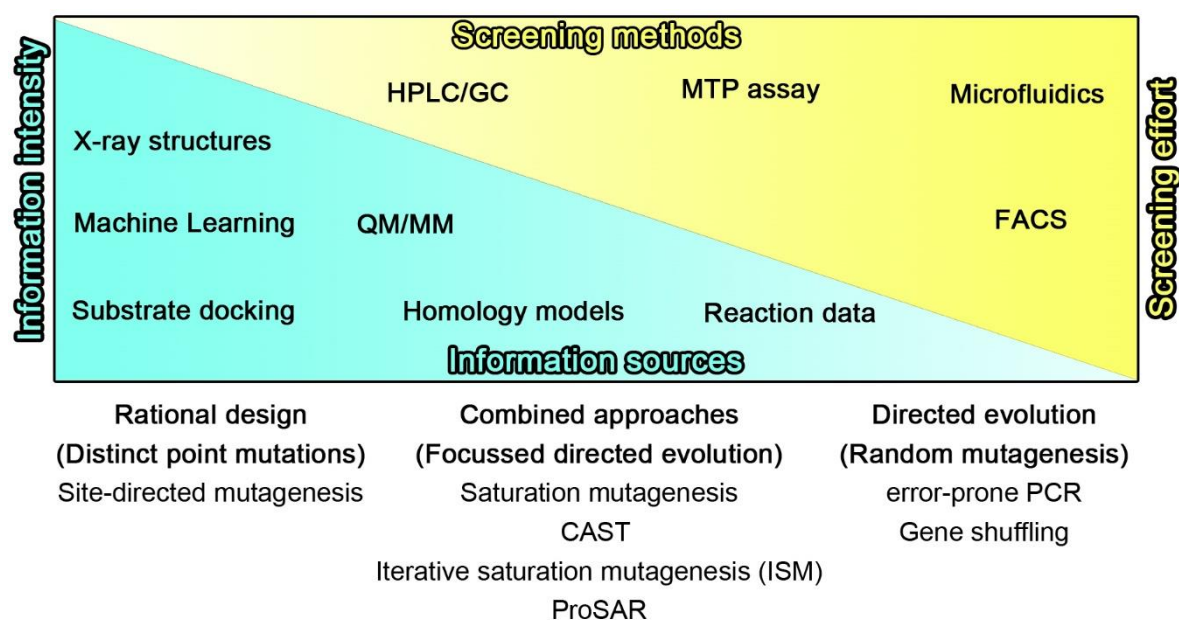


**Figure 1-1.** Strategies employed in protein engineering dependent on the necessary amount of data on the enzyme and screening capabilities. Adapted from Behrens et al. (2011) and modified with information from Bornscheuer et al. (2012) and Yi et al. (2021). CAST: Combinatorial active-site saturation test; FACS: fluorescence-activated cell sorting; GC: gas chromatography; HPLC: high performance liquid chromatography; MTP: microtiter plate; PCR: polymerase chain reaction; ProSAR: Protein structure-activity relationship; QM/MM: quantum mechanical/molecular mechanics.



In rational design, single amino acids are substituted by site-directed mutagenesis based on a known or predicted effect certain mutations have at the targeted position. Consequently, rational design requires the largest amount of knowledge about the enzyme's structure and the reaction mechanism. While homology models can be created from structures of related enzymes, their quality varies and a crystallographic structure of the target enzyme provides the best basis (Behrens et al., 2011; Kazlauskas & Bornscheuer, 2009). Since these structures offer only static "snapshots" of the structure, they can be used as the basis for computer modelling to simulate substrate binding and orientation in docking studies or more complex simulations with a QM/MM (quantum mechanical/molecular mechanics) approach. Increasingly, machine learning is also applied on biocatalytic datasets to predict mutations for rational design (Behrens et al., 2011; Yi et al., 2021). Since only a relatively small number of variants are created, the screening effort is low and can be managed with any assay or analytical method suitable for the examined reaction.

On the other end of the spectrum, directed evolution requires the least amount of information on the enzyme. Conversely, it requires the largest screening effort due to the large number of variants created. First, libraries of genes containing random mutations are created using methods like error-prone PCR or gene shuffling. The resulting enzymes are then screened for variants with the desired properties by high-throughput methods like microtiter plate assays (either by hand or automated using a robotic platform), fluorescence-activated cell sorting (FACS) or microfluidics (Arnold, 2018; Yi et al., 2021). In order to reduce the screening effort, a wide variety of combined techniques has been developed that use prior knowledge about the enzyme to create "smart" libraries (Behrens et al., 2011; Bornscheuer et al., 2012). When targeting only one residue already known for its importance, for example in directing stereoselectivity, instead of changing it to one specific amino acid, saturation mutagenesis can be performed to examine every possible amino acid at this position. In the combinatorial active-site saturation test (CAST), multiple amino acids in the active site are targeted by saturation mutagenesis. Choosing the best variants of a CAST round and using them iteratively as templates for the next round is called iterative saturation mutagenesis (ISM). In the protein structure-activity relationship (ProSAR) approach, statistical analysis on the effect of mutations is performed to guide the selection of the next round of mutations (Kazlauskas & Bornscheuer, 2009; Lutz, 2010).

Apart from protein engineering, many different aspects of biocatalytic reactions can be engineered to deal with the challenges that can be encountered in the design of a biocatalytic process (Table 1-1).

**Table 1-1.** Challenges in designing a biocatalytic process and methods for solving them. Compiled from Wu et al. (2021b), Sheldon and Woodley (2018) and Behrens et al. (2011).

Challenge	Methods
High cost of enzymes	Recombinant production Immobilization
Low stability of enzymes	Protein Engineering Immobilization <i>in silico</i> screening
Low activity/specificity	Protein Engineering High-throughput screening <i>in silico</i> screening
High cost of cofactors	Cofactor regeneration Engineering the cofactor specificity Cofactor immobilization
Multi-step reactions	Enzymatic cascades Bioinformatics-guided retrobiosynthesis

Apart from protein engineering, many properties of enzymes and most notably the stability can be improved by immobilization (Chapter 1.1.4). Another benefit is the possibility to recycle the enzymes and therefore reduce enzyme costs. Apart from improving a certain enzyme to suit the desired purpose, a related enzyme already possessing the desired properties can be identified either by high-throughput screening or *in silico* screening (Table 1-1). For example, when searching for enzyme variants with high stability under harsh conditions (*e.g.* high temperature, salt, low/high pH), screening for related enzymes in extremophilic organisms can be a suitable strategy (Demirjian et al., 2001; Elleuche et al., 2014; Schiraldi & De Rosa, 2002).

In addition to the cost of the enzyme, many reactions require additional cofactors in stoichiometric amounts to provide reduction equivalents/electrons to the reaction (for example by nicotinamide adenine dinucleotide (phosphate) or short NAD(P)H) or phosphorylate/activate the substrates (ATP). Generally, these are very expensive and have to be regenerated (Chapter 1.1.3) for the reaction for it to be economically viable. The costs can also be reduced by immobilizing the cofactor or, in the case of NAD(P)H, engineering the

specificity of the enzyme from NADPH to NADH, which is ten times less expensive (Beier et al., 2016; Velasco-Lozano et al., 2017).

Finally, many compounds, especially for pharmaceutical applications, are too complex to be produced by a single reaction/enzyme. Similar to the method of retrosynthesis in organic chemistry, a target for biocatalytic synthesis can be separated into different precursors in a retrobiosynthetic analysis. Aided by bioinformatic tools like RetroBioCat (Finnigan et al., 2021; Gao et al.) or machine learning approaches (Probst et al., 2022), enzymatic cascades with multiple enzymes can be planned and assembled much faster (Yi et al., 2021). In a recent example, the potential HIV (human immunodeficiency virus) treatment islatravir was produced in a three-step reaction utilizing a cascade containing five main enzymes and four auxiliary enzymes (Huffman et al., 2019). All five main enzymes were engineered through directed evolution towards accepting unnatural substrates. The auxiliary enzymes were used to remove unwanted side products like hydrogen peroxide and phosphate and to provide ATP regeneration. Additionally, three enzymes were immobilized. This provides a good example how modern biocatalysis integrates different techniques and disciplines to build reactions that resemble the biosynthesis of natural, complex compounds.

### 1.1.3 Regeneration of ATP

ATP (adenosine triphosphate) was discovered through the isolation of muscle tissue independently by Lohmann (1929) and Fiske and Subbarow (1929), with its structure being fully elucidated during the following 16 years (Lythgoe & Todd, 1945; Maruyama, 1991). It is composed of an adenine moiety bound through a  $\beta$ -*N*-glycosidic bond to the C1 carbon of D-ribose (Figure 1-2). The 5'-hydroxy group of D-ribose is esterified to triphosphate containing two reactive anhydride bonds between the  $\alpha$ ,  $\beta$  and  $\gamma$  phosphate groups. In biochemical systems, the latter two groups are often coordinated by divalent cations like  $Mg^{2+}$  (Andexer & Richter, 2015). ATP is best known as the universal energy currency of the cell, but this description only highlights part of its many functions in living cells (Figure 1-2).

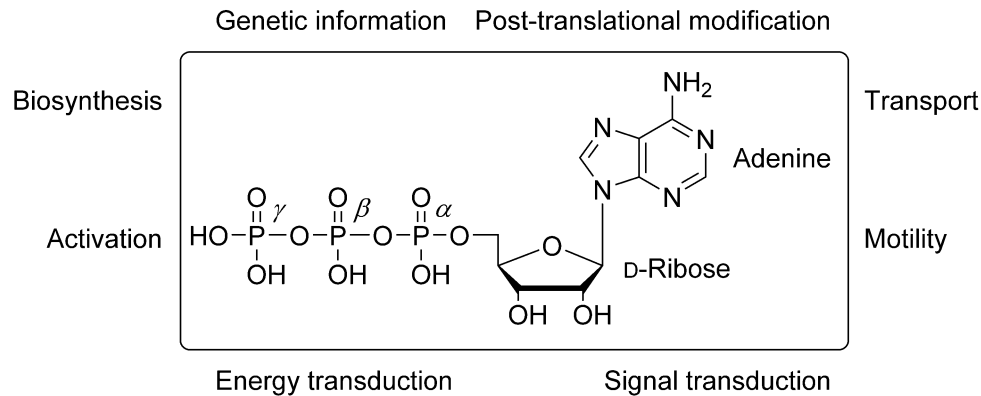


**Figure 1-2.** Structure and ATP-dependent processes. Compiled from Chen and Zhang (2021) and Andexer and Richter (2015).

Apart from its function in energy transduction, it is involved in the activation of molecules for metabolic reactions and is a building block for the biosynthesis of DNA/RNA and other cofactors like flavin adenine dinucleotide (FAD), NADH, and *S*-adenosylmethionine (SAM). It is used for the active transport of molecules through cellular membranes and drives mechanical motility both in bacterial flagella and the actin/myosin system in muscle tissues. It is used for post-translational modification of proteins and in signal transduction pathways, for example as the second messenger cyclic AMP (cAMP) and used for phosphorylation by protein kinases (Andexer & Richter, 2015; Chen & Zhang, 2021). The central reactions of ATP are either the hydrolysis of the  $\beta$ - $\gamma$  anhydride bond to yield ADP (adenosine diphosphate) and  $P_i$  (inorganic phosphate) or the hydrolysis of the  $\alpha$ - $\beta$  anhydride bond to yield AMP (adenosine monophosphate) and  $PP_i$  (pyrophosphate) (Figure 1-3). The free energy of the hydrolysis of the anhydride bonds provides the driving force for biochemical reactions and substrates can be activated for further reaction steps by phosphorylation due to phosphate being a good leaving group (Andexer & Richter, 2015).

The most energy-efficient processes producing ATP in living cells are the cellular respiration and photosynthesis, in which ATP is produced either by oxidative phosphorylation or photophosphorylation utilizing the accumulated proton motive force across the membrane to drive ATP synthesis through an  $F_0F_1$  ATP synthase (Chen & Zhang, 2021; Jia & Li, 2019; Junge & Nelson, 2015). The third principle is substrate-level phosphorylation (SLP), in which ADP or AMP are phosphorylated through the direct transfer of a phosphate group from a donor molecule. Examples include the generation of ATP during glycolysis by phosphoglycerate kinase and pyruvate kinase as well as ATP formation in muscle tissue from creatine phosphate catalyzed by creatine kinase (Figure 1-3). Most ADP/ATP regeneration strategies (Figure 1-3 bold) are based on SLP (Chen & Zhang, 2021). Apart from using

distinct enzymes, other strategies include the usage of whole cells, in which the metabolism of the cells can be utilized to regenerate ATP. However, only strategies employing purified enzymes will be examined further in this introduction.

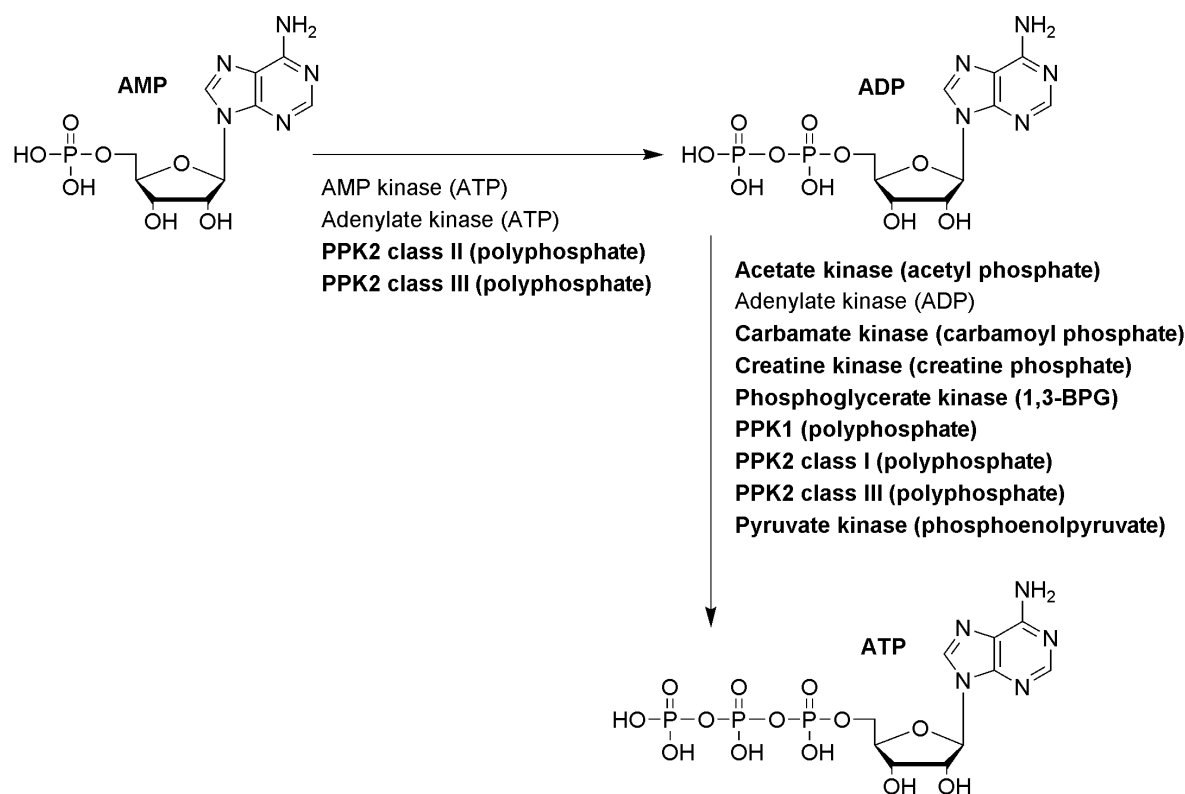


**Figure 1-3.** Selection of phosphorylation reactions forming ADP or ATP. Possible regeneration reactions are highlighted in **bold**. Enzymes catalyzing the designated reactions are shown with the donor substrate in parentheses. PPK: Polyphosphate kinase, 1,3-BPG: 1,3-bisphosphoglycerate. Compiled from Chen and Zhang (2021) and Andexer and Richter (2015).

The two major substrates used for ATP regeneration are inorganic polyphosphate and phosphorylated organic donor molecules like acetyl phosphate (Figure 1-3). The former is used by polyphosphate kinases (PPKs), which are classified into two families (PPK1 and PPK2), the latter of which is further separated into classes I to III based on phylogenetic analyses and substrate preferences (Tavanti et al., 2021). Both PPK1 and PPK2 class I enzymes can catalyze the regeneration of ATP from ADP and polyphosphate, while PPK2 class II enzymes catalyze the formation of ADP from AMP and polyphosphate. Finally, PPK2 class III are bifunctional enzymes that catalyze both reactions and are thus capable of regenerating ATP from AMP (Tavanti et al., 2021). Another strategy for regeneration from AMP is the combination of adenylate kinase and acetate kinase with acetyl phosphate as the donor (Langer et al., 1977). ATP regeneration using polyphosphate is a promising strategy due to its low cost and higher stability in comparison to organic phosphor donors. However, organic donors have been researched for many decades (Nakajima et al., 1978), while usage

of PPKs is a relatively novel approach and applicability for industrial use and issues like possible inhibition of enzymes by polyphosphate still have to be examined on a wider scale (Tavanti et al., 2021).

Among the organic donors, acetyl phosphate (AcP) is the most frequently used and considered the best in terms of substrate stability, price and reaction equilibria (Chen & Zhang, 2021; Tasnádi et al., 2018). It also being discussed as a possible primordial energy currency prior to the emergence of ATP and acetyl-CoA, due to its plausible formation under prebiotic conditions and relatively high stability (Whicher et al., 2018). Using acetate kinase, ATP can be regenerated from ADP and acetyl phosphate with acetate as side product (Figure 1-4a).

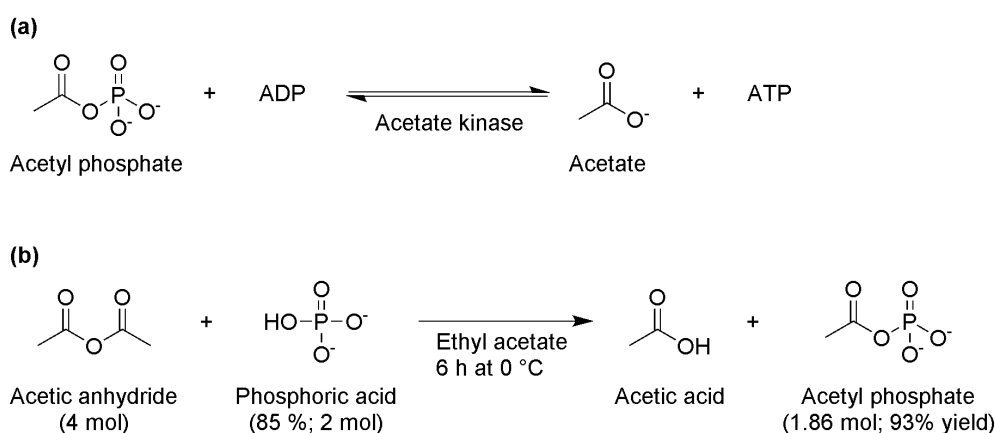


**Figure 1-4.** ATP regeneration from ADP and acetyl phosphate using acetate kinase. (a) Reaction catalyzed by acetate kinase. (b) Synthesis of acetyl phosphate by Crans and Whitesides (1983).

An aqueous solution of acetyl phosphate suitable for regeneration reactions can be synthesized relatively cheaply by acetylation of phosphoric acid with acetic anhydride (Figure 1-4b) followed by extraction of the side product acetic acid with ethyl acetate, which could otherwise shift the reaction equilibrium of the regeneration reaction (Crans & Whitesides, 1983). This resulted in yield of 93%. This method was later successfully reproduced by Alissandratos et al. (2016), who used *E. coli* lysate containing endogenous acetate kinase from *E. coli* (AckA) to regenerate ATP for the generation of nucleoside triphosphates and for cell-free protein synthesis. Other recent examples employing acetate kinase include the production of CDP-choline (Zheng et al., 2021a) and glucose-6-phosphate (Yan et al., 2014). Finally, in the previously mentioned cascade for the production of Islatravir (Chapter 1.1.2), thermostable acetate kinase from *Thermotoga maritima* was responsible for ATP regeneration (Huffman et al., 2019) and was co-immobilized to the ATP-utilizing enzyme pantothenate kinase.

### 1.1.4 Immobilization

Immobilization of enzymes is performed to both improve properties of the biocatalyst (*e.g.* stability, activity or specificity) and to reduce process costs (*e.g.* by enabling recycling of the enzymes and simplified downstream processing) aiming for overall increased economic viability (Bié et al., 2022). Immobilization techniques can be classified depending on whether the enzymes are bound to a carrier/support, entrapped/encapsulated in a carrier and carrier-free methods, in which the enzymes are cross-linked with each other (Figure 1-5).

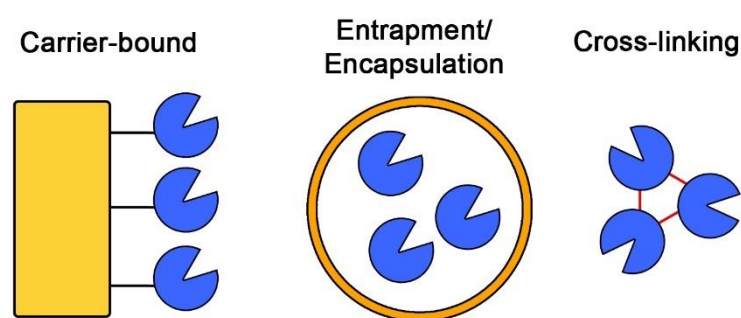


**Figure 1-5.** Classification of immobilization methods. Compiled from Sheldon and van Pelt (2013), Yushkova et al. (2019) and Bié et al. (2022).

The carrier methods can further be classified depending on how the enzyme is bound to the carrier. On one hand, physical adsorption has the weakest interaction and thus least effects on the enzyme (positive or negative), but leaching of the enzyme into the solution can be a significant problem. On the other hand, covalent immobilization displays the lowest leaching and the highest interaction with the enzyme, which can improve properties like the enzyme stability, but also decrease activity (Bié et al., 2022; Sheldon & van Pelt, 2013). Ionic interactions between oppositely charged enzyme and support or affinity immobilization like usage of the interaction of  $\text{Ni}^{2+}$  with hexahistidine-tags are other options (Mohamad et al., 2015). Entrapment and encapsulation work by embedding the enzymes in a gel matrix (entrapment) or surrounding the enzymes with a semi-permeable membrane (encapsulation). However, mass-transfer can be severely limited depending on the ability of the substrates to pass through the used polymer and leaching can also be a factor (Bié et al., 2022). Finally, enzyme cross-linking is a carrier-free method. Usually, cross-linked enzyme aggregates (CLEAs) are prepared by producing enzyme aggregates through precipitation followed by addition of a bifunctional cross-linking agent like glutaraldehyde (Yushkova et al., 2019). In comparison to the other methods, specific activity of the catalyst is not diluted by large additions of a carrier, (Sheldon & van Pelt, 2013), however activity of the enzymes is often reduced by the immobilization procedure (Bié et al., 2022).

Covalent immobilization is the most feasible method for long-term use of an immobilisate, since it has the highest potential for increased stability of the enzyme and the lowest amount of leaching (Bié et al., 2022). The increases in stability are often caused by an induced rigidity of the enzyme, which in turn is also an explanation for the often-witnessed decreases in activity. Other factors include binding of catalytically important residues or binding of the enzyme in an orientation, where mass-transfer to the active site is hindered, or usage of harsh immobilization reagents like sodium borohydride (Naramittanakul et al., 2021; Ruzicka et al., 2006; Sheldon & van Pelt, 2013). A mild method for covalent binding is the usage of *N*-hydroxysuccinimide-esters (NHS-esters), in which primary amino groups of enzymes (*e.g.* lysine side chains) react with the NHS-activated carrier to form a stable amide bond (Figure 1-6)(Lim et al., 2014; ThermoScientific, 2022).

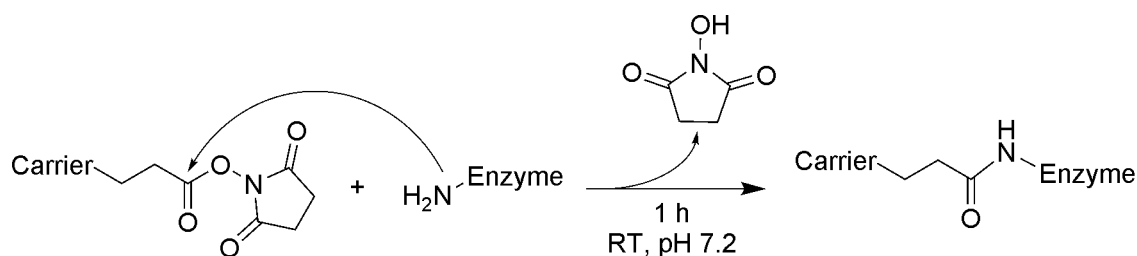


**Figure 1-6.** Covalent immobilization using a carrier activated with NHS-ester groups. RT: room temperature (ThermoScientific, 2022).

## 1.2 Bioactive Dipeptides

### 1.2.1 Properties

L- $\alpha$ -dipeptides (hereinafter abbreviated to dipeptides) are the shortest possible peptides from L-amino acids. They are formed unspecifically during hydrolytic breakdown of proteins and specifically through designated biosynthetic pathways. Despite their apparently simple structure, they encompass a large spectrum of properties. They are often more than the sum of their parts displaying physical or physiological properties different from their constituent amino acids. While alanine and glutamine display solubilities of 89 and 36 g/L in water, respectively, the dipeptide Ala-Gln has a solubility of 586 g/L. Similarly, tyrosine is practically insoluble, but the Ala-Tyr dipeptide is soluble with 14 g/L. Consequently, they are used in infusions in parenteral nutrition, where the solubilities of the single amino acids are not suitable. They were shown to be readily hydrolyzed into the amino acids after intravenous injection (Albers et al., 1988; Fürst et al., 1997) and glutamine dipeptides were shown to improve clinical outcomes as shown in a recent meta study (Stehle et al., 2017). Dipeptides can also have a wide range of bioactivities in living organisms (Table 1-2).



**Table 1-2.** Effects of a selection of bioactive dipeptides. APPA: 2-Amino-5-phosphono-3-*cis*-pentenoic acid; T $\beta$ L: Tabtoxinine  $\beta$ -lactam

Effect	Example	Reference
Analgesic	Tyr-Arg (kyotorphin)	Takagi et al. (1979)
Antibiotic	Ala-Anticapsin (bacilysin)	Özcengiz and Öğülür (2015)
Antifungal	Arg-APPA (rhizocticin A)	Kugler et al. (1990)
Antihypertensive	Arg-Phe	Kagebayashi et al. (2012)
Anxiolytic/antidepressant	Trp-Leu	Mizushige (2021)
Neuroprotective	Leu-Ile	Nitta et al. (2004)
Phytotoxin	T $\beta$ L-Thr (Tabtoxin)	Uchytel and Durbin (1980)
Salt-taste enhancer	Arg-Ala	Schindler et al. (2011)
Sweet taste	Asp-Phe-OMe	Maillet et al. (2015)
Umami-taste enhancer	Gly-Glu	Zhang et al. (2017)

Among the bioactive dipeptides, arginyl dipeptides constitute an interesting object of study, since they can possess analgesic (kyotorphin), antifungal (rhizocticin A), antihypertensive (Arg-Phe) or salt-taste enhancing effects (Arg-Ala).

## 1.2.2 Applications of Arginyl Dipeptides

### 1.2.2.1 Salt-Taste Enhancement

Salt (sodium chloride) is an essential nutrient and an adequate supply is important for electrolyte homeostasis, maintenance of cell plasma volume, absorption of nutrients and overall cell physiology. Sodium contributes to the membrane potential of most cells and is involved in the action potential necessary for the transmission of nerve impulses and muscle contractions (Kaushik et al., 2018; Puri & Lee, 2021). However, modern food products and consumer choices often lead to an excessively high salt intake. The WHO (World Health Organization) recommends a maximum daily intake of five grams salt, which is surpassed in most countries worldwide and even reaches above ten grams in many western countries (Strazzullo et al., 2009; Strohm et al., 2016; WHO, 2012). The foods contributing to the salt intake vary between countries depending on eating habits and cultural aspects (Webster et al., 2014). On one hand, 95% of dietary salt in the United Kingdom comes from processed foods, while these account for only 63 % in Japan. On the other hand, 20 % of the salt intake in Japan is caused by soy sauce alone (Anderson et al., 2010). Foods contributing

significantly to the salt intake in most populations are bread products, cereals and grains, meat and dairy products, and sauces (Bhat et al., 2020; Mattes & Donnelly, 1991).

According to the World Health Organization (WHO), non-communicable diseases (NCDs) like diabetes, cancer and cardiovascular diseases are the primary cause of high mortality and morbidity worldwide (Shen et al., 2022). Their “Global action plan for the prevention and control of NCDs” identifies excessive consumption of nutrients like salt, sugar and fat as important risk factors for NCDs and a reduction of salt intake is considered to be one of the most cost-effective interventions to reduce the impact of NCDs (Santos et al., 2021; Shen et al., 2022; WHO, 2013). An excessively high salt intake is correlated with high blood pressure and other cardiovascular diseases (He & MacGregor, 2009; Trieu et al., 2015). Consequently, a low salt diet was shown to decrease blood pressure both in hypertensive and normotensive patients (Graudal et al., 2020; He & MacGregor, 2002; He et al., 2013). Apart from cardiovascular diseases, a recent meta-study also linked a high salt intake to increased risk for gastric cancer (Wu et al., 2021a) and a low salt diet was also shown to improve chronic kidney disease (Garofalo et al., 2018; Shi et al., 2022)

The WHO plan set a goal of a relative decrease in salt intake of 30 % until 2025 (WHO, 2013). However, decreasing the salt content of food is usually not tolerated well by the consumer. The salty taste has an important function for the overall taste of food and enhances the flavor by suppressing bitterness (Breslin & Beauchamp, 1997; Desmond, 2006; Shen et al., 2022). Salt can be substituted with other salts like potassium chloride, but these produce bitter and metallic off-flavors above a certain threshold (Shen et al., 2022). Similarly, arginine can enhance salt-taste, but has a fishy off-flavor.

In 2011, Schindler et al. (2011) hydrolyzed the fish protein protamine with chymotrypsin and trypsin and identified arginyl dipeptides like Arg-Pro as salt-taste enhancers by activity-guided fractionation using a trained sensory panel. They also conducted sensory analyses using commercial dipeptides in two different matrices (water and model broth with 50 mmol/L NaCl) to quantitate the salt-taste enhancing effects. The largest enhancements were found for Arg-Ser, Arg-Gly, Ala-Arg, Arg-Ala and Arg-Pro, which increased the perceived saltiness by approximately 15 to 21%. The effects differed depending on the matrix and the order of the amino acids in the dipeptide. In some cases, like Arg-Ala and Ala-Arg, both N- and C-terminal arginyl dipeptides showed similar effects, while in others, one had a salt-taste enhancing effect (Arg-Ser) and the other a salt-taste reducing effect (Ser-Arg). Overall, more N- than C-terminal arginyl dipeptides exhibited significant salt-taste enhancing

effects. With some exceptions, most of the salt-taste enhancing dipeptides produced no off-flavors.

The nature and function of the salt taste receptors is still under investigation (Puri & Lee, 2021; Shen et al., 2022; Vandenbeuch & Kinnamon, 2020). At least two different mechanisms are known: The amiloride-sensitive and amiloride-insensitive pathways. Amiloride is a high-affinity blocker of epithelium sodium channels (ENaCs), which are specific for  $\text{Na}^+$  and likely part of salt-taste recognition. In contrast, the amiloride-insensitive pathway is nonselective and  $\text{Na}^+$ ,  $\text{K}^+$  and  $\text{NH}_4^+$  salts are recognized through it. Xu et al. (2017) investigated the mechanism behind the salt-taste enhancement by arginyl dipeptides using cultured human fungiform taste papillae cells and found that Arg-Ala, Arg-Ala and Arg-Pro significantly increased the  $\text{Ca}^{2+}$ -cell responses to sodium chloride, with Ala-Arg being the most consistent. For this dipeptide, it was then shown that the cell responses depended on ENaC $\alpha$  and ENaC $\delta$  subunits and, thus, a salt-taste enhancement through the amiloride-sensitive pathway was plausible. The two amino acids of the dipeptide, Arg and Ala, were similarly examined either alone or in combination, and had no effect on the cell response. This was also the case for the dipeptides Arg-Glu, Glu-Arg, Asp-Asp and Glu-Asp. Results for the former two were in line with Schindler et al. (2011), who found no enhancement for Arg-Glu or Glu-Arg. However, Zheng et al. (2021b) identified both Asp-Asp and Glu-Asp as salt-taste enhancing, which could signify that they work through a different mechanism.

The application of hydrolysates enriched in arginyl dipeptides was examined by Harth et al. (2018), who screened 15 basidiomycete fungi for peptidolytic activity for the hydrolysis of casein and lysozyme leading to formation of arginyl dipeptides. *Trametes versicolor* showed the highest dipeptide formation with lysozyme and the resulting hydrolysate was shown to have salt-taste enhancing effects in a model cheese matrix and curd cheese.

### 1.2.2.2 Antihypertensives

Apart from causing cardiovascular diseases, hypertension is also the most important modifiable risk factor for cerebrovascular and renal diseases and is involved in many other diseases like diabetes, cognitive dysfunction and dementia and obesity (Kearney et al., 2004; Messerli et al., 2007). There are many pharmaceutical targets for the treatment of hypertension. The renin-angiotensin system is the most recognized humoral system for the control of blood pressure and one of the primary targets for pharmaceutical interventions. Renin cleaves angiotensinogen to form angiotensin I. This is then cleaved further by the

angiotensin I-cleaving enzyme (ACE) to form angiotensin II, which is a vasoconstrictor. Additionally, ACE also cleaves the vasodilator bradykinin, resulting in an inactive form and leading to an overall increase in blood pressure (Manzanares et al., 2019). Inhibitors of both renin and ACE are used as pharmaceutical drugs to lower blood pressure.

A number of antihypertensive dipeptides are known such as Val-Tyr (Matsui et al., 2002; Vercruysse et al., 2008), Ala-Ala (Heres et al., 2021), Ile-Trp (Martin et al., 2015) and Arg-Phe (Kagebayashi et al., 2012). For most, the proposed mechanism is inhibition of ACE. However, Arg-Phe had a vasorelaxing effect on isolated mesenteric arteries from spontaneously hypertensive rats (SHRs; an accepted animal model for human hypertension) and also lowered blood pressure when administered orally to these rats (Miralles et al., 2018). It demonstrated no ACE-inhibiting effects, but its antihypertensive effect was blocked by a CCK (cholecystokinin) inhibitor (Kagebayashi et al., 2012). CCK is a peptide hormone involved in regulating satiety, but it has also been shown to have a vasorelaxing effect on the mesenteric artery, and has also been implicated in regulating renal sodium excretion, and improving salt-sensitive hypertension (Jiang et al., 2016; Jiang et al., 2022; Kagebayashi et al., 2012; Ruiz-Gayo et al., 2006). Other peptides apparently working through CCK are Phe-Trp, Phe-Trp-Gly-Lys and the milk-derived Arg-Phe-Trp-Gly-Lys (Koyama et al., 2020).

A possible role for antihypertensive (di)peptides is the creation of functional foods, which have already been approved in Japan (Iwatani & Yamamoto, 2019; Yagasaki & Hashimoto, 2008). Hydrolysates of foods like bonito and wakame contain ACE-inhibitory peptides and were shown to have antihypertensive effects (Sato et al., 2002; Yokoyama et al., 1992). These could be applied to treat pre-hypertensive blood pressure, for which pharmaceutical intervention is usually not indicated due to the associated side effects (Michelke et al., 2018).

### **1.3 Production of Dipeptides**

#### **1.3.1 Strategies**

The chemical synthesis of dipeptides is achieved using methods developed for chemical peptide synthesis, which are performed either in solution or using a solid-phase approach, with the former mostly being used for small peptides up to tetrapeptides (Apostolopoulos et al., 2021). In general, all peptide synthesis methods follow the same principles (Yagasaki & Hashimoto, 2008). First, to ensure a specific reaction, all functional groups – both main and side chain – with the exception of the amino and carboxy groups that will form the peptide bond – need protection groups. Common protection groups are Boc/Bzl

(*tert*-butyloxycarbonyl/benzyl) and Fmoc/*t*-Bu (fluorenylmethyloxycarbonyl/*tert*-butyl) (Apostolopoulos et al., 2021). Second, the free carboxy group needs to be activated with compounds like carbodiimides followed by a nucleophilic attack of the free amino group to form the peptide bond. Last, all protection groups need to be removed. The advantages of the chemical synthesis are its high flexibility and often high yields. However, the need for multiple reaction steps and protection groups increases the costs and along with the reliance on toxic chemicals the ecological impact (Guzmán et al., 2007; Yagasaki & Hashimoto, 2008).

A wide variety of biocatalytic approaches for the production of dipeptides have been developed (Table 1-3).

**Table 1-3.** Overview of biocatalytic methods to produce dipeptides. Cbz: carboxybenzyl

Reaction	Substrates	Enzyme	Product	Reference
Reverse hydrolysis	Cbz-Asp + PheOMe	Thermolysin	Cbz-Asp-PheOMe (Aspartame precursor)	Isowa et al. (1979)
Hydrolysis of natural substrates	Casein, lysozyme	Peptidases from basidiomycetes	Hydrolysate with arginyl dipeptides	Harth et al. (2018)
Hydrolysis of unnatural substrates	...(Ile-Trp) <sub>2</sub> ...	Chymotrypsin	Ile-Trp	Michelke et al. (2018)
Condensation with activated amino acid	Ala-OMe + Gln	Amino acid methylester acyltransferase	Ala-Gln	Yokozeki and Hara (2005) and Hirao et al. (2013)
L-Amino acid ligases	Arg + Ser	RizA	Arg-Ser	Kino et al. (2009)

The economically most significant one is the production of aspartame, which is produced through reverse hydrolysis using the peptidase thermolysin. The condensation of the *N*-protected aspartate and the phenylalanine methylester is thermodynamically driven by the precipitation of the product dipeptide, which can then be deprotected to yield aspartame (Bornscheuer & Buchholz, 2005). Because of the usage of protection groups, this is usually characterized as a chemoenzymatic method, due to the combination of principles of chemical and biocatalytic synthesis. Another chemoenzymatic method is the usage of a weakly activated amino acid methylester and an amino acid methylester acyltransferase, which was used to synthesize Ala-Gln by Yokozeki and Hara (2005) and Hirao et al. (2013). The ethyl ester of arginine was used to produce Arg-Arg with trypsin (Aso et al., 1992).

Biocatalytic methods can be divided into those with a top-down approach, producing dipeptides out of a larger peptide (hydrolytic methods), or a bottom-up approach, where the dipeptide is synthesized from its respective amino acids. Both Schindler et al. (2011) and Harth et al. (2018) showed that arginyl dipeptides were formed through the hydrolysis of natural proteins using peptidases. In order to improve yields and enrich the desired dipeptides in these approaches, more specific peptidases are needed. A possible candidate are dipeptidyl peptidases, which are exopeptidases specifically cleaving dipeptides from the N-terminus of peptides (Vorwerk, 2022).

Apart from the hydrolysis of natural substrates, unnatural substrates have been employed as well. Doel et al. (1980) and Murata et al. (1993) created synthetic DNA sequences to heterologously produce a Poly-(Asp-Phe) peptide in *E. coli* for hydrolytic production of the aspartame precursor. Michelke et al. (2018) created a construct with a synthetic gene coding for a total of 16 Iso-Trp (IW) dipeptide units, with four “IWIWIWIW” blocks separated by heptapeptide spacers. The gene was then fused with the sequence coding for maltose-binding protein for soluble production and purification. After hydrolysis of the resulting peptide, Ile-Trp, an antihypertensive dipeptide, was successfully isolated and characterized, although with a relatively low overall yield due to the non-functional peptides from the tag-sequence and spacer peptides constituting a large part of the produced protein.

Finally, bottom-up biocatalytic synthesis from two unprotected, non-activated amino acids can be achieved by using L-amino acid ligases.

### 1.3.2 L-Amino Acid Ligases

L-amino acid ligases (LALs; EC 6.3.2.28) are a class of enzymes catalyzing the condensation of two L-amino acids to their respective dipeptides under the hydrolysis of ATP to ADP and  $P_i$ . They belong to the ATP-dependent carboxylate-amine/ammonia ligase family and contain an ATP-grasp domain consisting of two  $\alpha/\beta$  subdomains for binding ATP (Galperin & Koonin, 1997; Pitzer & Steiner, 2016). The bound cofactor is used to activate the carboxy group of the N-terminal amino acid substrate by formation of an acyl phosphate, which can then be attacked by the amino group of the C-terminal amino acid substrate to form a tetrahedral intermediate. Finally, phosphate is released from the intermediate to yield the dipeptide product (Figure 1-7).

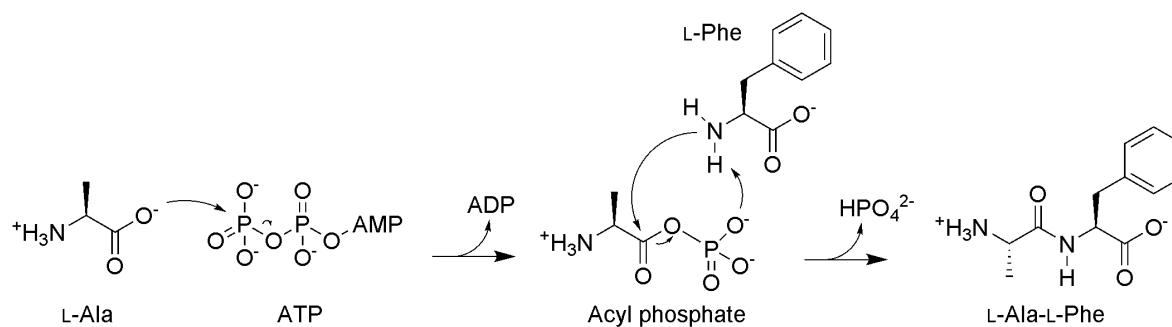


**Figure 1-7.** Proposed mechanism for LALs. The second reaction proceeds *via* a tetrahedral intermediate (not shown). Adapted from Shomura et al. (2012).

The first LAL YwfE (also referred to as BacD) was identified in *B. subtilis* 168 as responsible for the synthesis of the antibiotic dipeptide bacilysin from L-Ala and the non-proteinogenic L-amino acid anticapsin. The analysis of its substrate spectrum showed that it produced 111 out of 231 possible dipeptide products with a preference for non-bulky, neutral amino acids like Ala, Ser and Gly as N-terminal amino acid and bulky, neutral amino acids like Phe, Met, Leu as C-terminal substrate and was suitable for the production of Ala-Gln. *In silico* screenings based on the ywfE gene enabled the discovery of new LALs such as Rsp1486a and BL00235 (Table 1-4), as well as PSPPH\_4299 from *Pseudomonas syringae* pv. *phaseolicola* 1448A and Plu1440 from *Photobacterium luminescens* subsp. *laumondii* TT01 (Arai & Kino, 2008; Kino et al., 2010).

RizA was identified during work on the elucidation of the biosynthesis of the antifungal rhizocticins produced by *B. subtilis* NBRC3134 (Kino et al., 2009). Rhizocticin A is the dipeptide L-arginyl-L-2-amino-5-phosphono-3-*cis*-pentenoic acid (Arg-APPA) and the authors assumed that an LAL was responsible for its formation similar to the biosynthesis of bacilysin (Kugler et al., 1990). They constructed an assay with arginine as a substrate, and used Fe(III) and hydroxylamine to detect the acyl phosphate intermediate (in this case arginyl phosphate) by formation of arginyl hydroxamate, which could then be measured photometrically. RizA was purified from the cell extract after detection of its activity, and the full gene sequence was constructed from its N-terminal peptide sequence by cassette PCR. It was then recombinantly produced in *E. coli* with an N-terminal his-tag. Characterization showed a dependence on Mg<sup>2+</sup> as a cofactor and an optimal reaction temperature of 37 °C and pH of 9.5. It showed an absolute specificity for Arg as N-terminal amino acid and a broad specificity for the C-terminal amino acid as all amino acids, but proline were accepted. Similarly, BL00235 only accepted Met and Gly as N-terminal substrates, but only small amino acids at the C-terminal position. Conversely, YwfE and

RSp1486a had a much broader specificity with the latter showing approximately the opposite specificity of YwfE (Table 1-4). Another significant LAL with a distinct substrate specificity was TabS (Table 1-4), which was shown to be able to produce the bioactive dipeptides Arg-Phe (antihypertensive), Leu-Ile (neuroprotective) and Leu-Ser (salt-taste enhancer).

**Table 1-4.** Overview of characterized LALs. n. i.: not identified

	<b>YwfE</b>	<b>RSp1486a</b>	<b>BL00235</b>	<b>RizA</b>	<b>TabS</b>	<b>BILal</b>
<b>Discovered</b>	Tabata et al. (2005)	Kino et al. (2008a)	Kino et al. (2008b)	Kino et al. (2009)	Arai et al. (2013)	(Liu et al., 2021)
<b>From</b>	<i>Bacillus subtilis</i> 168	<i>Ralstonia solanacearum</i>	<i>Bacillus licheniformis</i> NBRC12200	<i>Bacillus subtilis</i> NBRC3134	<i>Pseudomonas syringae</i> NBRC14081	<i>Bacillus amyloliquefaciens</i>
<b>Natural product</b>	Bacilysin	n. i.	n. i.	Rhizocitcin A	Tabtoxin	n. i.
<b>N-terminal specificity</b>	Non-bulky, neutral	Bulky	Met, Gly	Arg	Gln, Arg, Lys, Tyr, Asn, Pro, Phe, His, Met, or Leu	n. i.
<b>C-terminal specificity</b>	bulky neutral	Non-bulky	Small	All except Pro	Thr, Val, Ile, Ser, Ala, Cys, Trp, or Gly	n. i.
<b>Possible application</b>	Ala-Gln	-	Met-Gly	Arg-X	Arg-Phe, Leu-Ile, Leu-Ser	Ala-Gln
<b>Structures (PDB ID)</b>	3vmm, 3wnz, 3wo0, 3wo1,	No	3vot	4wd3	No	No
<b>Engineering studies</b>	Yes (Tsuda et al., 2014)	No	Yes (Kino & Kino, 2015)	No	Yes (Kino et al., 2016)	Yes (Liu et al., 2021)

YwfE was also the first LAL, for which an x-ray structure was published in 2012, which contained an Ala-Phe substrate analogue (Shomura et al., 2012). Three additional structures were published in 2014 containing different substrates and cofactors (Tsuda et al., 2014). For BL00235, a crystal structure was also published in 2012, which became the basis for engineering it for reduced production of the side product Met-Met in favor of the salt-taste enhancer Met-Gly (Kino & Kino, 2015; Suzuki et al., 2012). Another salt-taste enhancer, Pro-Gly, was produced in low quantities by TabS, which was addressed by performing saturation mutagenesis on two residues leading to an improved variant (Kino et al., 2016). BILAL was engineered for the improved production of Ala-Gln (Liu et al., 2021). The latest published LAL structure has been for RizA (Kagawa et al., 2015).



## 2 Aim of This Thesis

A recent review on LALs identified both the establishment of ATP regeneration and immobilization of these enzymes as important endeavors, but noted that these have not been explored in the scientific literature so far (Wang et al., 2020). The only exceptions were a small number of patents describing the combination of PPKs with LALs (Hashimoto et al., 2006; Yu et al., 2021; Zhu et al., 2019) and one patent on immobilization of an LAL (Yu et al., 2020). Therefore, there was still a great need for scientific exploration of these topics with an LAL.

RizA from *B. subtilis* showed an absolute specificity for arginine as N-terminal substrate and was therefore a perfect candidate for the production of both the antihypertensive Arg-Phe and a range of salt-taste enhancing dipeptides like Arg-Ser, Arg-Gly and Arg-Ala. While the ability of RizA to form Arg-X dipeptides had already been published, product concentrations were only reported for Arg-Ser and Arg-Ala and were too low for industrial application (Kino et al., 2009). Additional barriers were the potentially high costs of enzymes and the cofactor ATP. Despite the availability of an x-ray structure for RizA, no engineering studies had been performed on it so far (Table 1-4). The aims of this thesis were to examine the application of biocatalytic engineering strategies (Chapter 1.1.2) to improve the economic viability of RizA for the production of arginyl dipeptides, expand the knowledge about engineering the substrate specificity of LALs and provide the first scientific investigations into establishing ATP regeneration and performing (co-)immobilization for LALs.

First, ATP regeneration had to be established by coupling the ATP-dependent dipeptide formation by RizA with acetate kinase from *E. coli* (AckA), which catalyzes the formation of ATP from acetyl phosphate. Reaction conditions of this system had to be optimized and applied for the production of Arg-Ser, Ala and Arg-Gly. Second, mutagenesis on RizA had to be performed and the resulting variants examined for their substrate specificity using different amino acid combinations consisting of arginine and four amino acids differing in size and polarity (aspartic acid, serine, alanine, phenylalanine). Both formation of the heterodipeptide product (Arg-X) and homodipeptide side product (Arg-Arg) were to be analyzed. At last, the biocatalytic system comprised of engineered RizA variants and AckA for ATP regeneration had to be co-immobilized to enable reusability of the enzymes and provide easier separation from the reaction in an effort to pave the way towards a future industrial bioprocess.

### **3 Preamble to the Publication “Recombinant Production of Arginyl Dipeptides by L-Amino Acid Ligase RizA Coupled with ATP Regeneration”**

The dependency on ATP is a critical drawback not only for RizA, but for the whole enzyme class of L-amino acid ligases in general. Despite the obvious need for ATP regeneration, coupling an LAL to an ATP-regenerating enzyme had not been examined in the scientific literature yet (Chapter 2).

As described in the introduction (Chapter 1.1.3), application of acetate kinase and acetyl phosphate is one of the most widely used strategies. Since the ability of acetate kinase from *E. coli* to provide ATP regeneration was demonstrated in a recent study, it was chosen and recombinantly produced in *E. coli* for coupling with RizA (Alissandratos et al., 2016). After optimization of the reaction conditions, a low ATP concentration of 0.5 mM was sufficient for a reaction containing 50 mM of each substrate. In addition to supplying enough of the cofactor, it was discovered that ATP had an inhibiting effect on RizA and that the low concentration of ATP thus improved product formation. The formation of the side product Arg-Arg was an unexpected result, since Arg-Arg formation was previously only described for reactions containing only arginine (Kino et al., 2009). Therefore, increasing the specificity of the reaction became another engineering goal for this system (Chapter 6). Overall, using AckA with acetyl phosphate proved to be a very effective strategy for ATP regeneration and became the basis for all further experiments.

I conceptualized the study and all published data was generated and interpreted by me. Tim A. Mast worked during his bachelor thesis on the recombinant production of AckA and its combination with RizA for ATP regeneration (Mast, 2020) under my supervision and further assisted in enzyme purifications as a student assistant. Prof. Berger was involved in conceptualization, supervision and administration of the project and funding acquisition. Dr. Ersoy was also involved in supervision and administration of the project. The work was published in the peer-reviewed journal *Catalysts* on 25<sup>th</sup> of October 2021 as part of the Special issue “Enzyme Catalysis, Biotransformation and Bioeconomy”. It was featured on the front page of the journal’s website from 25<sup>th</sup> of January 2022 until end of March 2022.

DOI: 10.3390/catal11111290

## 4 Recombinant Production of Arginyl Dipeptides by L-Amino Acid Ligase RizA Coupled with ATP Regeneration

### 4.1 Abstract

Arginyl dipeptides like Arg-Ser, Arg-Ala, and Arg-Gly are salt-taste enhancers and can potentially be used to reduce the salt content of food. The L-amino acid ligase RizA from *B. subtilis* selectively synthesizes arginyl dipeptides. However, industrial application is prevented by the high cost of the cofactor adenosine triphosphate (ATP). Thus, a coupled reaction system was created consisting of RizA and acetate kinase (AckA) from *E. coli* providing ATP regeneration from acetyl phosphate. Both enzymes were recombinantly produced in *E. coli* and purified by affinity chromatography. Biocatalytic reactions were varied and analyzed by RP-HPLC with fluorescence detection. Under optimal conditions the system produced up to 5.9 g/L Arg-Ser corresponding to an ATP efficiency of 23 g Arg-Ser per gram ATP. Using similar conditions with alanine or glycine as second amino acid, 2.6 g/L Arg-Ala or 2.4 g/L Arg-Gly were produced. The RizA/AckA system selectively produced substantial amounts of arginyl dipeptides while minimizing the usage of the expensive ATP.

**Keywords:** L-amino acid ligase; acetate kinase; coupled catalysis; arginyl dipeptides; salt taste; ATP regeneration

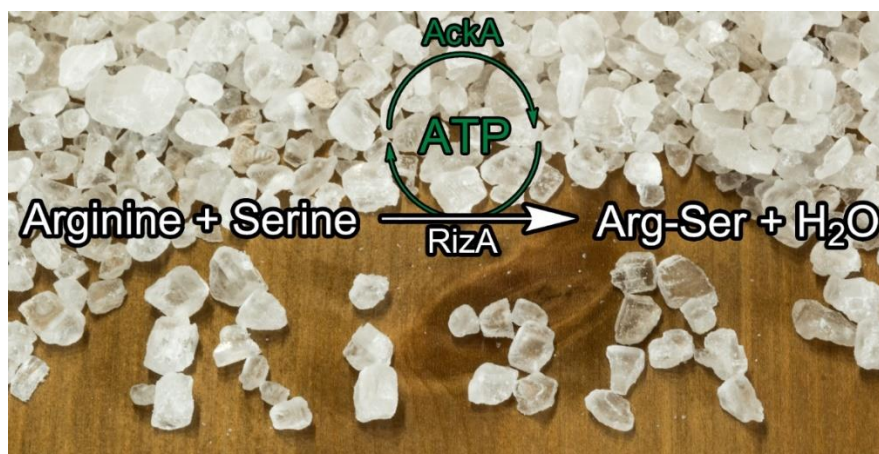


**Figure 4-1.** Graphical abstract of the publication (Bordewick et al., 2021b).

## 4.2 Introduction

The reduction of salt intake is one of the most prevalent public health initiatives, as an excessively high salt intake is correlated with high blood pressure and other cardiovascular diseases (He & MacGregor, 2009; Trieu et al., 2015). But success is limited as the recommended amount of five grams by the WHO is far exceeded by the actual salt intake in most Western countries surpassing ten grams (Strazzullo et al., 2009; WHO, 2012). It was shown that reduction of salt intake can substantially lower the blood pressure of both hypertensive and healthy people (He & MacGregor, 2002). However, reductions in salt-content of food are usually not well tolerated, as salt has an important function for the taste of food (Desmond, 2006). Apart from saltiness being one of five tastes, it also enhances the flavor by suppressing bitterness (Breslin & Beauchamp, 1997). In 2011, arginyl dipeptides formed by hydrolysis of fish protein were identified as salt-taste enhancers (Schindler et al., 2011). The strongest effects were found for Arg-Pro, Arg-Ala, Arg-Gly and Arg-Ser which increased the perceived salt-taste intensity by 10 to 20% without any off-flavors and are thus suitable candidates to reduce the salt content of food.

Chemical synthesis of dipeptides requires the use of protecting groups to direct the specificity of the reaction which increases costs and produces additional waste (Yagasaki & Hashimoto, 2008). In a biocatalytic approach, peptidases from basidiomycetes were used to produce protein hydrolysates enriched in salt-taste enhancing dipeptides (Harth et al., 2018). A relatively novel enzyme class in the biocatalytic toolkit are L-amino acid ligases (LALs; EC 6.3.2.28) which condense two amino acids to their corresponding dipeptide under hydrolysis of ATP to ADP (adenosine diphosphate) (Wang et al., 2020). The LAL RizA from *Bacillus subtilis* NBRC3134 has a high specificity for producing dipeptides with an N-terminal arginine and is an ideal candidate for the synthesis of salt-taste enhancing dipeptides (Kino et al., 2009). However, the need for stoichiometric amounts of ATP presents an enormous hurdle for the industrial application due to its high price. Many strategies were developed to regenerate ATP either by using endogenous enzymes of whole cells (Alissandratos et al., 2016; Huang & Yin, 2020) or isolated enzymes (Andexer & Richter, 2015; Li et al., 2020b; Yan et al., 2014). One very prominent strategy is the use of acetate kinase which regenerates ATP from ADP and acetyl phosphate (AcP) (Chen & Zhang, 2021). The necessary acetyl phosphate can be synthesized reasonably cheap by acetylation of phosphoric acid with acetic anhydride (Alissandratos et al., 2016; Crans & Whitesides, 1983) or through biocatalytic strategies such as the synthesis from pyruvate and phosphate by pyruvate oxidase from

*Pediococcus* sp. (Kim & Swartz, 1999). Recently, acetate kinase has been used in a multistep biocatalytic cascade to produce the potential HIV drug Islatravir (Huffman et al., 2019).

In the present work, a reaction system comprised of RizA and AckA was constructed for the production of the salt-taste enhancing dipeptides Arg-Ser, Arg-Ala and Arg-Gly with minimal need for ATP (Figure 4-2).

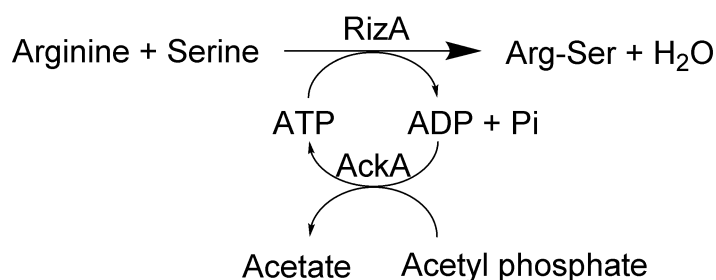


**Figure 4-2.** Reaction scheme for the RizA/AckA system for regeneration of ATP from acetyl phosphate for synthesis of Arg-Ser from arginine and serine.

### 4.3 Results and Discussion

#### 4.3.1 Influence of Substrate Concentrations

RizA and AckA were recombinantly produced in *E. coli* BL21 (DE3) and purified by affinity chromatography. The yields were 14 mg RizA per 100 mL culture and 53 mg AckA per 100 mL culture. Biocatalytic reactions were set up with the purified enzymes to optimize the reaction conditions. The production of Arg-Ser was chosen as the optimization target, since Arg-Ser is among the strongest salt-taste enhancers, and initial experiments showed that RizA had the highest activity for this dipeptide.

Firstly, the substrate concentrations were examined. Reactions were set up with different concentrations of arginine and serine with equimolar amounts acetyl phosphate for 20 and 40 h reaction time. (Figure 4-3a and b). Another set of reactions with different ratios of amino acids to acetyl phosphate was also set up (Figure 4-3c).

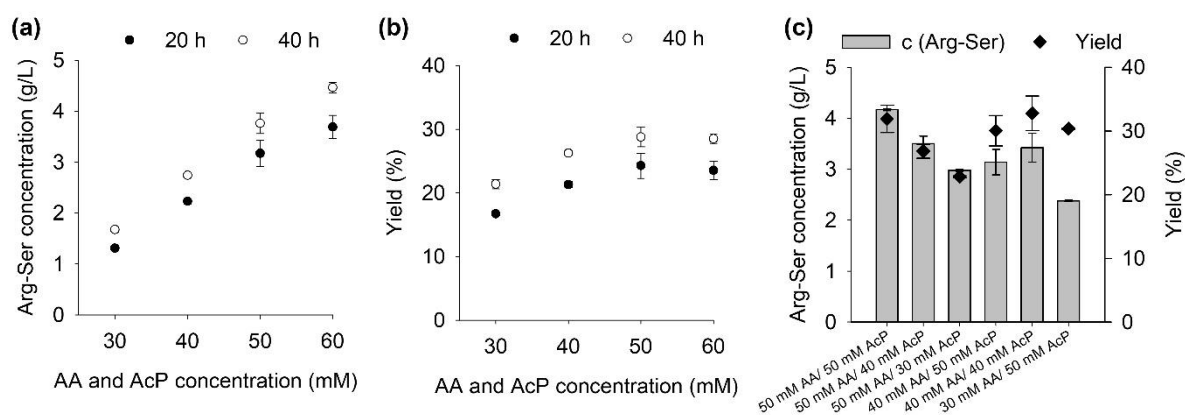


**Figure 4-3.** Effect of substrate amino acids (AA) and acetyl phosphate on the Arg-Ser production. All reactions were performed at 25°C. **(a)** Equimolar concentrations of amino acids and acetyl phosphate with 5 mM  $Mg^{2+}$ . **(b)** Yields for data presented in (a). **(c)** Different ratios of amino acids to acetyl phosphate with 7.5 mM  $Mg^{2+}$  and 20 h reaction time. Reactions were set up in duplicate; data are presented as mean with error bars representing range.

In all samples, most of the product (>80%) was already present in the 20 h samples with only a small increase from 20 to 40 h reaction time. Increasing amino acid alongside acetyl phosphate concentrations led to an approximately linear increase in product concentration up to 60 mM with no signs of substrate inhibition (Figure 4-3a). This is similar to the results reported for the LAL from *Bacillus licheniformis*, where up to 40 mM increased the reaction velocity (Kino & Kino, 2015) while for YwfE up to 100 mM worked (Tsuda et al., 2014). The highest yields were achieved with 50 mM AA and AcP reaching 24% after 20 h and 29% after 40 h (Figure 4-3b).

An equimolar ratio of amino acids to acetyl phosphate was found to be optimal at 50 mM with a yield of 32% (Figure 4-3a). For RizA without ATP regeneration, a lower yield of 25% was achieved with 12.5 mM AA and 12.5 mM ATP, which was the highest yield reported for RizA (Kino et al., 2009).

#### 4.3.2 Influence of Cofactor Concentrations

Both RizA and AckA require ATP and  $Mg^{2+}$  as cofactors. In the literature, LAL reactions without ATP regeneration are often set up with both cofactor concentrations equimolar to the amino acids and ATP (Kino et al., 2008a; Kino et al., 2008b; Kino et al., 2009). Due to the presence of another enzyme and the objective to reduce the ATP usage, both cofactors were analyzed for their effect on the RizA/AckA system. Reactions were set up with ATP and  $Mg^{2+}$  with concentrations from 0.1 to 20 mM with 40 mM amino acids and 24 h reaction time (Figure 4-4a). Additionally, reactions were set up with 50 mM amino acids, 20 and 40 h

reaction time and different concentration ranges to pinpoint the optimum concentration for both cofactors (Figure 4-4b and c).

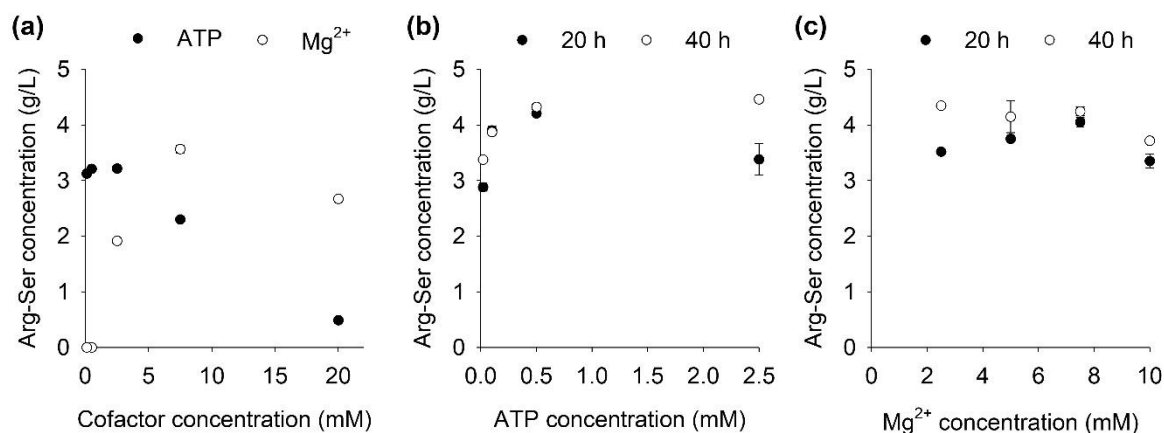


**Figure 4-4.** Effect of the two cofactors ATP and Mg<sup>2+</sup> on Arg-Ser production. (a) ATP and Mg<sup>2+</sup> with 40 mM AA and AcP. (b) ATP with 50 mM AA and AcP at 20/40 h reaction time. (c) Mg<sup>2+</sup> with 50 mM AA and AcP at 20/40 h reaction time. Reactions were set up in duplicate; data are presented as mean with error bars representing range.

The optimum concentrations for ATP were 0.5 mM (Figure 4-4a and b) and for Mg<sup>2+</sup> 7.5 mM (Figure 4-4a and c) at 20 h reaction time. Lower or higher concentrations limited the reaction for both cofactors, although to different degrees. At 0.5 and 0.1 mM Mg<sup>2+</sup>, no product formation was detected, while reducing the ATP concentration to 0.02 mM only reduced the final product concentration by 33% (Figure 4-4a). Conversely, higher ATP concentrations had a strong inhibiting effect on the reaction system as displayed by the 75% reduction in product formation with 20 mM ATP. Inhibition by ATP was also witnessed during experiments without cofactor regeneration in which 30 mM ATP completely inhibited the reaction (Supporting Figure 4-1). Besides the need to minimize ATP due to its cost, the usage of an ATP-regenerating system also alleviated this apparent substrate inhibition imposed on the RizA enzyme by ATP.

### 4.3.3 Influence of Enzyme Concentrations

Reactions with different ratios of RizA to AckA were set up (Figure 4-5a). Additional reactions with varying concentrations of one enzyme were created as well (Figure 4-5b and 4c).

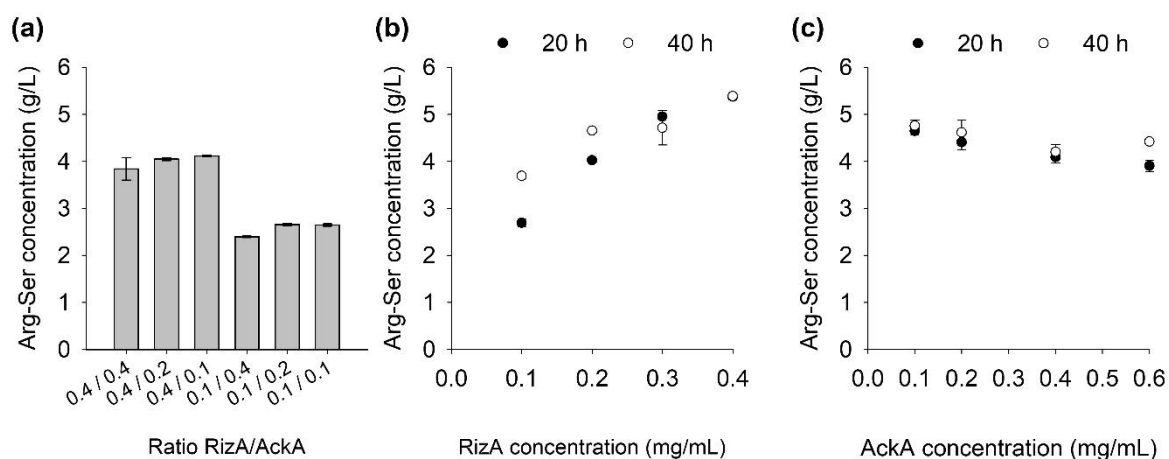


**Figure 4-5.** Effect of two enzymes RizA and AckA on Arg-Ser production. **(a)** Ratios of RizA to AckA (both in mg/mL) with 40 mM AA and AcP. **(b)** RizA with 0.2 mg/mL AckA, 50 mM AA and AcP at 20/40 h reaction time. **(c)** AckA with 0.2 mg/mL RizA, 50 mM AA and AcP at 20/40 h reaction time. Reactions were set up in duplicate; data are presented as mean with error bars representing range.

In the 20 h RizA samples (Figure 4-5b), a fourfold increase from 0.1 to 0.4 mg/mL doubled the final product concentration. The size of the product increase from the 20 to the 40 h samples was inversely correlated with the RizA concentration, as the 0.1 mg/mL sample increased from 2.7 to 3.7 g/L and the 0.4 mg/mL showed no increase. These findings imply that the enzymes in the 0.4 mg/mL reactions were still active, but that the product concentration had reached a ceiling. In the reactions with lower RizA concentrations, this ceiling had not been reached yet and the reaction progress continued. The apparent concentration ceiling is further discussed in Chapter 4.3.5.

In contrast to RizA, higher concentrations of AckA seemed to decrease the product formation, although the effect of the concentration of this enzyme was far less pronounced than with RizA. Addition of 0.1 mg/mL AckA was still sufficient for the reaction. The reactions with different ratios of RizA to AckA (Figure 4-5a) confirmed these results as the 0.4 mg/mL RizA and 0.1 mg/mL AckA reactions contained the highest product concentration.

#### 4.3.4 Influence of Temperature and pH

The optimum temperature and pH for isolated RizA were determined to be 37 °C and pH 9.5 with sharp declines towards lower temperatures/pH values (Kino et al., 2009). In contrast, the pH optimum of AckA was at 7.3, but with a broader spectrum, still possessing 50% activity at pH 9.0 (Nakajima et al., 1978). In order to analyze the optimum of the combined system, reactions were set up with combinations of the three reaction temperatures of 25, 30 and 37 °C and three buffers with pH values of 8.0, 8.5 and 9.0 (Figure 4-6).



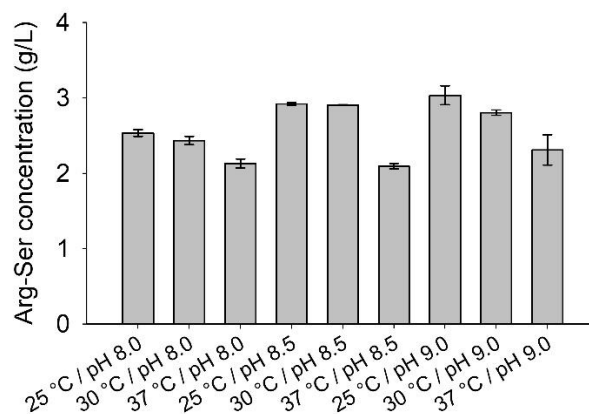


**Figure 4-6.** Effect of the temperature and buffer pH on Arg-Ser production. Reactions were set up in duplicate; data are presented as mean with error bars representing range.

At all pH values, 37 °C reaction temperatures led to the lowest product concentrations while the 30 and 25 °C showed similar results. At constant temperature, the reactions with pH 8.0 contained the lowest product concentrations while pH 8.5 and 9.0 performed similarly. The reaction at 25 °C and pH 9.0 contained the highest product concentration, but the difference was not significantly different from the results at 30 °C or pH 8.5. Overall, the system possessed a broader spectrum with temperatures between 25 and 30 °C and pH 8.5 to pH 9.0 being viable.

#### 4.3.5 Time Course of Formation of Arg-Ser, Arg-Ala, Arg-Gly and Arg-Arg

Reactions were set up with the best observed conditions from the above experiments to optimize the product formation. In addition to arginine and serine, reactions with arginine and either alanine or glycine were also included for the formation of the strong salt-taste enhancers Arg-Ala and Arg-Gly (Kino et al., 2009), respectively (Figure 4-7a and b). Apart from these heterodipeptides, formation of the homodipeptide Arg-Arg was also detected as a side product in the reaction. In order to quantitate the specificity between main product and side product, the ratio Arg-X/Arg-Arg was calculated (Figure 4-7c).

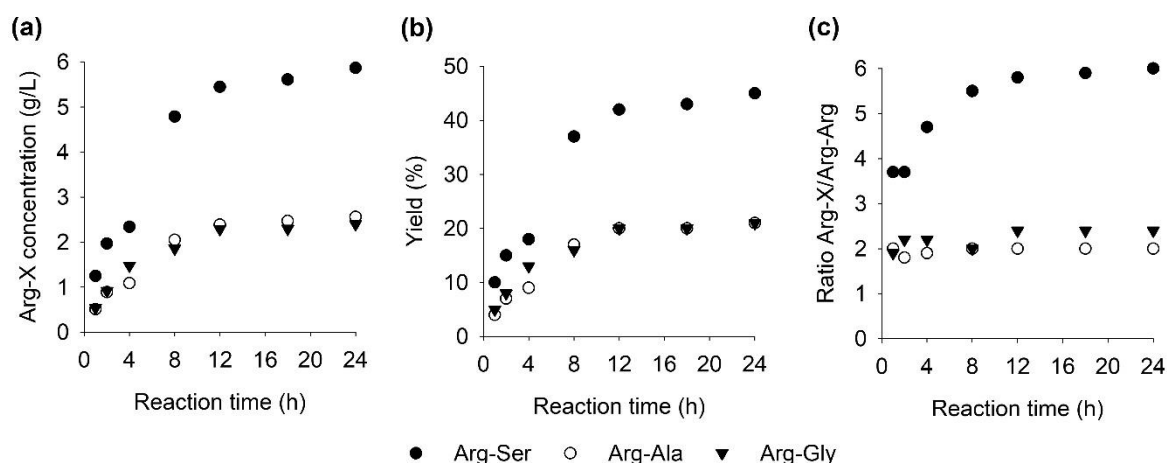


**Figure 4-7.** Time course of dipeptide formation with optimized reaction conditions. 50 mM amino acids and AcP; 0.5 mM ATP; 7.5 mM  $Mg^{2+}$ ; 0.4 mg/mL RizA; 0.1 mg/mL AckA; 25°C; pH 9.0 (a) Product concentrations of Arg-Ser, Arg-Ala and Arg-Gly. (b) Yields of respective Arg-X dipeptides. (c) Ratio of main product Arg-X to side product Arg-Arg.

In general, Arg-Ala and Arg-Gly were formed at similar rates with final product concentrations of 2.4 and 2.6 g/L corresponding to yields of 21% each. Formation of Arg-Ser was significantly higher with a final concentration of 5.9 g/L and a yield of 41%. Similarly, the Arg-Ser reactions contained a higher ratio of Arg-Ser to Arg-Arg over five, while the reactions of Arg-Ala and Arg-Gly had ratios around two. In all cases, over 90% of the product was formed during the first 12 h with only small increases in product concentration after that. The ratio Arg-X/Arg-Arg increased for all reactions with reaction time.

In the original publication on the discovery and recombinant production of RizA, Arg-Arg was only detected in reactions containing only arginine but not in the arginine and serine reaction (Kino et al., 2009). It is possible that Arg-Arg was formed but not detected due to the lower substrate concentrations used. Another explanation might be an effect of the his-tag on the reactivity on the enzyme. An N-terminal his<sub>6</sub>-tag was used in both cases, but the exact placement/linker sequence between tag and RizA could be different and have an effect, although unlikely. Since Arg-Arg is a weak salt-taste enhancer, it does not negatively affect the intended application. To reduce or prevent the formation of Arg-Arg, the substrate specificity of RizA could be engineered by mutagenesis. This was achieved for the production of Met-Gly with the LAL from *Bacillus licheniformis*, in which the production of the side product Met-Met was successfully prevented by a single mutation of Pro85 (Kino & Kino, 2015). Another target for engineering is the yield of the reaction. As shown, the production of dipeptides slowed considerably after 12 h reaching final yields of around 21%

for Arg-Ala and Arg-Gly and 41% for Arg-Ser. Possible reasons for this could be inhibition by phosphate (Dean, 2002) or acetate (Crans & Whitesides, 1983) accumulating during the reaction (Figure 4-2). In the case of the cascade for the production of Islatravir using acetate kinase, the accumulation of phosphate was reduced by the addition of sucrose and sucrose phosphorylase (Chen & Zhang, 2021; Huffman et al., 2019). A ceiling to the final product concentration could also be imposed by the RizA enzyme itself and thus be addressed by protein engineering. This was done for the LAL TabS in which the double mutant S85T/H294D reached a 1.6-fold higher Pro-Gly concentration after 20 h than the wild type (Kino et al., 2016).

The ATP regeneration in this work increased both the efficiency of ATP usage and enabled the highest reported product concentrations for Arg-Ser by a biocatalytic process. For RizA without ATP regeneration, a product concentration of 3.1 mM or 0.8 g/L Arg-Ser was reported with 12.5 mM of amino acids,  $Mg^{2+}$  and ATP (Kino et al., 2009). In terms of ATP efficiency, this corresponds to 0.0064 Arg-Ser per mmole of ATP or 0.13 g Arg-Ser per gram ATP. The optimized system of RizA/AckA used only 0.5 mM ATP to produce 5.9 g/L or 23 g Arg-Ser per gram of ATP corresponding to a 176-fold increase in efficiency. The combination of RizA with AckA presents a large step towards an integrated biocatalytic process (Burgener et al., 2020) for the production of salt-taste enhancers and possibly other bioactive dipeptides like arginyl-phenylalanine, which was found to have antihypertensive properties (Kagebayashi et al., 2012). As a result, the present work may not only pave the way to a better nutritional value of food, but open access to dipeptides with desired functions in human physiology. It improved the economic viability of RizA by dramatically reducing ATP as a cost factor. On the road towards an industrial process, the next step will be immobilization of the reaction system to increase its stability and reusability for a larger-scale bioprocess (Yushkova et al., 2019).

## 4.4 Materials and Methods

### 4.4.1 Chemicals, Reagents and Strains

All chemicals were purchased from Carl Roth (Karlsruhe, Germany) or Sigma Aldrich (Taufkirchen, Germany) if not otherwise indicated. Enzymes for molecular biology were purchased from Thermo Fisher Scientific (St. Leon-Roth, Germany). The pET28a vector was purchased from Merck KGaA (Darmstadt, Germany). The *E. coli* strains BL21 (DE3) and TOP10 were maintained in our laboratory. Oligonucleotides were synthesized by Microsynth Seqlab GmbH (Goettingen, Germany).

#### 4.4.2 Construction of pET28a\_his6-rizA and pET28a\_his6-ackA Constructs

The sequence of *rizA* (UniProt accession B5UAT8) was codon-optimized with the software SnapGene version 5.1.7 (2020) from GSL Biotech LLC (Chicago, USA) and an N-terminal 6his-tag sequence was added. The *his6-rizA* (Supporting Sequence 4-1) gene was produced as a synthetic gene by Thermo Fisher Scientific (St. Leon-Roth, Germany) with restriction sites for NcoI and NotI. The delivered pMA-T-*his6-rizA* vector and the pET28a vector were digested with FastDigest NcoI and NotI followed by ligation of the *his6-rizA* fragment into the pET28a vector with T4 DNA ligase. The product was transformed into chemocompetent *E. coli* TOP10 cells by heat-shock transformation. After overnight incubation at 37 °C, clones were selected for overnight incubation, plasmids were isolated with the innuPREP Plasmid Mini Kit 2.0 from Analytik Jena (Jena, Germany) and the correct sequence confirmed by sequencing by Microsynth Seqlab GmbH (Goettingen, Germany). For the pET28a\_ackA construct, genomic DNA of *E. coli* was isolated by the method of El-Ashram et al. (2016) and the *ackA* gene was amplified with Phusion High Fidelity Polymerase using the primers “CATCATATGATGTCGAGTAAGTTAGTACTGGTTCTG” and “GTAGCGGCCGCTCAGGCAGTCAGGCGGC” containing NdeI and NotI restriction sites. The amplificate was inserted into the pET28a vector analogously to *rizA* above with the respective digestion enzymes resulting in an open reading frame coding for *his6-ackA* (Supporting Sequence 4-2). Both constructs were transformed into *E. coli* BL21 (DE3) for expression and glycerol stocks were created for storage at -80 °C.

#### 4.4.3 Cultivation and Expression

Precultures were inoculated from glycerol stocks in 5 mL LB medium with 50 µg/mL kanamycin and incubated overnight at 37 °C, 200 rpm. For cultivation, 400 mL TB medium with 50 µg/mL kanamycin in a shaking flask with baffles were inoculated with 4 mL preculture and incubated at 37 °C and 160 rpm until an OD<sub>600</sub> of 0.6 – 0.8 was reached. Expression was induced by addition of 10 µM IPTG and performed at 20°C and 160 rpm for 20 h. After harvesting the cells by centrifugation at 5000× g at 4 °C for 15 min, the cell pellets were frozen and stored at -20 °C until purification.

#### 4.4.4 Purification

A cell pellet from 100 mL culture was resuspended in 10 mL disruption buffer (100 mM tricine pH 8.0, 10 mM imidazole) and sonicated for 7.5 min (50% amplitude; 0.5 cycle) with a UP50H sonicator from Hielscher Ultrasonics GmbH (Teltow, Germany). After centrifugation at 5000 x g at 4 °C for 40 min, the supernatant was purified by affinity

chromatography with a gravity-flow column containing 2 mL Protino Ni-NTA Agarose (Macherey-Nagel, Dueren, Germany) according to the manufacturer's instructions. The eluted protein was desalted by PD10 columns from Cytiva (Washington, USA) according to the manufacturer's instructions. The desalted eluate was frozen in liquid nitrogen and aliquots were stored at -80 °C. Protein concentrations were determined with Bradford solution from Sigma-Aldrich (Taufkirchen, Germany).

#### 4.4.5 Biocatalysis

Biocatalytic reactions were set up in 0.2 mL PCR tubes with 50 µL reaction volume. If not otherwise stated, reactions contained 40 mM arginine and serine, 40 mM AcP, 0.5 mM ATP, 7.5 mM MgSO<sub>4</sub>, 0.2 mg/mL RizA, 0.2 mg/mL AckA and 25 mM tricine buffer pH 8.5. Reactions were set up in duplicates and incubated at 25 °C for 20 h in a Biometra thermal cycler from Analytik Jena (Jena, Germany) and inactivated by heating to 70 °C. Samples were stored at -20 °C until analysis.

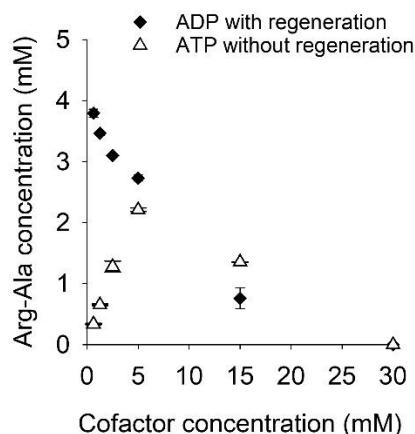
#### 4.4.6 Analysis

The amino groups of dipeptides were derivatized with *o*-phthalaldehyde and analyzed by RP-HPLC with fluorescence detection as previously described by Rottmann et al. (2021) for the analysis of single amino acids. The gradient was modified as follows: 0 min: 90% A, 5 min: 90% A, 25 min: 60% A, 30 min: 0% A, 35 min: 0% A, 40 min: 90% A, 45 min: 90% A. Analytical standards of the dipeptides Arg-Ser, Arg-Ala, Arg-Gly and Arg-Arg were purchased from Bachem (Bubendorf BL, Switzerland) and used for external calibration. Standards were set up in duplicate. Data was visualized with SigmaPlot version 14.5 (2020) from Systat Software GmbH (Erkrath, Germany).

#### 4.5 Conclusions

ATP regeneration by acetate kinase increased both the yield and economic viability of dipeptide synthesis by RizA. The coupled reaction system provides a foundation for the development of an industrial process for the specific production of salt-taste enhancing arginyl dipeptides.

#### 4.6 Supplementary Materials



**Supporting Figure 4-1.** Comparison of reaction with or without regeneration. Reaction conditions were not yet optimized and were 30 mM arginine and alanine, 30 mM  $Mg^{2+}$ , 0.2 mg/mL RizA, 20 mM tricine buffer pH 8.0, 25 °C, 20 h reaction time, 200  $\mu$ L reaction volume. Reactions without regeneration contained ATP with concentrations between 0.625 and 30 mM. Reactions with regeneration contained 0.25 mg/mL AckA and ADP with concentrations between 0.625 and 30 mM. Both cofactors inhibit the reaction at higher concentrations and 30 mM of each led to no detectable product.

>his6-rizA

```

ATGGGTAGCAGCCATCACCATCATCATCATAGCAGCGGTATGCTGCGTATTCTGCTGATTA
ATAGCGATAAACCGGAACCGATTTCAGTTCTTCCAGAAAGATAAAGAAACCAACGACAGCAT
TAACATCAGCGTTATTACCCGTAGCTGTTATGCACCGCTGTATAGCCATTGGGCAGATCAT
GTTTATATTGTGGATGATGTTACCGATCTGACCGTTATGAAAAGCCTGATGCTGGAAATTC
TGAAAGTTGGTCCGTTTGATCATATTGTTAGCACCACCGAAAAAGCATTCTGACCGGTGG
TTTTCTGCGTAGCTATTTCCGGTATTGCAGGTCCGGTTTTGAAACCGCACTGTATATGACC
AATAAACTGGCCATGAAAACCAAATGAAAATGGAAGGTATTCCGGTTGCAGATTTTCTGT
GTGTTAGCCAGGTTGAAGATATTCCGGCAGCCGGTGAAAACTTGGTTGGCCGATTATTGT
TAAACCGGCATTAGGTAGCGGTGCACTGAATACCTTTATTATCCATAGCCTGGATCACTAT
GAGGATCTGTATAGCACCAGCGGTGGTCTGGGTGAACTGAAAAAACAATAGCCTGATGA
TCGCCGAAAAGTGCATTGAAATGGAAGAATTTTCATTGCGATAACCCTGTATGCCGATGGTGA
AATTCTGTTTTGTGAGCATCAGCAAATATACCGTTCCGCTGCTGAAAGGTATGGCAAAAATT
CAGGGTAGCTTTATTCTGAGCCAGAATGATCCGGTGTATGCAGAAATTCTGGAACTGCAGA
AAAGCGTTGCACAGGCATTTTCGTATTACCGATGGTCCGGGTCATCTGGAAATCTATCGTAC
CCATAGTGGCGAACTGATTGTGGGTGAAATTGCAATGCGTATTGGTGGTGGTGGCATTAGC
CGTATGATTGAGAAAAAATTCAACATCAGCCTGTGGGAAAGCAGCCTGAATATTAGCGTTT
ATCGTGATCCGAATCTGACGGTTAATCCGATTGAAGGCACCGTTGGTTATTTTAGCCTGCC
GTGTCGTAATGGCACCATTAAAGAATTTACCCCGATCGAAGAATGGGAAAACTGGCAGGT
ATTCTGGAAGTTGAACTGCTGTATCAAGAGGGTGTATGTGGTTGATGAAAAACAGAGCAGCT

```

CATTTGATCTGGCACGTCTGTATTTTTGCCTGGAAAATGAAAATGAAGTGCAGCATCTGCT  
GGCACTGGTTAAACAGACCTATTATCTGCATCTGACCGAAGATCACATGATGAACCAGTAA

**Supporting Sequence 4-1.** DNA sequence of his6-rizA

>his6-ackA

ATGGGCAGCAGCCATCATCATCATCACAGCAGCGGCCTGGTGCCGCGCGGCAGCCATA  
TGATGTGCGAGTAAGTTAGTACTGGTTCTGAACTGCGGTAGTTCTTCACTGAAATTTGCCAT  
CATCGATGCAGTAAATGGTGAAGAGTACCTTTCTGGTTTAGCCGAATGTTTCCACCTGCC  
GAAGCACGTATCAAATGGAAAATGGACGGCAATAAACAGGAAGCGGCTTTAGGTGCAGGCG  
CCGCTCACAGCGAAGCGCTCAACTTTATCGTTAATACTATTCTGGCACAAAACAGAACT  
GTCTGCGCAGCTGACTGCTATCGGTACCGTATCGTACACGGCGGCGAAAAGTATAACCAGC  
TCCGTAGTGATCGATGAGTCTGTTATTCAGGGTATCAAAGATGCAGCTTCTTTTGCACCGC  
TGCACAACCCGGCTCACCTGATCGGTATCGAAGAAGCTCTGAAATCTTTCCACAGCTGAA  
AGACAAAACGTTGCTGTATTTGACACCGCGTTCCACCAGACTATGCCGGAAGAGTCTTAC  
CTCTACGCCCTGCCTTACAACCTGTACAAAGAGCACGGCATCCGTCGTTACGGCGCGCACG  
GCACCAGCCACTTCTATGTAACCCAGGAAGCGGCAAAAATGCTGAACAAACCGGTAGAAGA  
ACTGAACATCATCACCTGCCACCTGGGCAACGGTGGTTCCGTTTCTGCTATCCGCAACGGT  
AAATGCGTTGACACCTCTATGGGCCTGACCCCGCTGGAAGGTCTGGTCATGGGTACCCGTT  
CTGGTGATATCGATCCGGCGATCATCTTCCACCTGCACGACACCCTGGGCATGAGCGTTGA  
CGCAATCAACAACTGCTGACCAAAGAGTCTGGCCTGCTGGGTCTGACCGAAGTGACCAGC  
GACTGCCGCTATGTTGAAGACAACCTACGCGACGAAAGAAGACGCGAAGCGCGCAATGGACG  
TTTACTGCCACCGCCTGGCGAAATACATCGGTGCCCTACACTGCGCTGATGGATGGTTCGTCT  
GGACGCTGTTGTATTCCTGCTGGTGGTATCGGTGAAAATGCCGCAATGGTTCGTGAACTGTCT  
CTGGGCAAACTGGGCGTGCTGGGCTTTGAAGTTGATCATGAACGCAACCTGGCTGCACGTT  
TCGGCAAATCTGGTTTCATCAACAAAGAAGGTACCCGTCCTGCGGTGGTTATCCCAACCAA  
CGAAGAACTGGTTATCGCGCAAGACGCGAGCCGCCTGACTGCCTGA

**Supporting Sequence 4-2.** DNA sequence of his6-ackA

**4.7 Disclosures**

**Author Contributions:** Conceptualization, S.B. and R.G.B.; methodology, S.B. and T.A.M.; validation, S.B.; formal analysis, S.B.; investigation, S.B. and T.A.M.; writing—original draft preparation, S.B.; writing—review and editing, R.G.B. and F.E.; visualization, S.B.; supervision, R.G.B. and F.E.; project administration, R.G.B. and F.E.; funding acquisition, R.G.B. All authors have read and agreed to the published version of the manuscript.

**Funding:** The project was supported by funds of the Federal Ministry of Food and Agriculture (BMEL) based on a decision of the Parliament of the Federal Republic of Germany via the Federal Office for Agriculture and Food (BLE) under the innovation support programme. The publication of this article was funded by the Open Access Fund of Leibniz Universität Hannover.

**Data Availability Statement:** Data are contained within the article and supplementary materials.

**Conflicts of Interest:** The authors declare no conflict of interest.



## **5 Preamble to the Publication “Mutagenesis of the L-Amino Acid Ligase RizA Increased the Production of Bioactive Dipeptides”**

The first study on the RizA and AckA system (Chapter 4) uncovered two challenges for engineering: Further improving the yield of the desired dipeptides and the specificity by decreasing formation of the side product Arg-Arg. In addition, the focus on only salt-taste enhancing dipeptides was widened to include the antihypertensive Arg-Phe; however, preliminary experiments showed very low product formation for this dipeptide with wild type RizA. The few protein engineering studies that had been performed on other LALs (Chapter 1.3.2) showed that changing the substrate specificity was possible, but despite the availability of an x-ray structure for RizA, no such study had been conducted on it so far. Therefore, a mutagenesis study of RizA was conceived to both investigate positions that were already known to govern substrate specificity in other LALs and to use the structure of RizA to select new positions for engineering.

A total of 21 variants were created based on substitutions to eight positions, of which four positions (S84, S156, A158 and D376E) had never been implicated to affect activity and substrate specificity in LALs before this study. Five different amino acid combinations were examined as substrates and improved variants both in terms of activity and specificity were identified for the production of all of the resulting dipeptides. All four new and two of the known positions (T81 and K83) were found to be important for activity and specificity. Mutations at the remaining two positions (G289 and I291) had only detrimental effects.

I conceptualized the study and all published data was generated and interpreted by me. Prof. Berger was involved in conceptualization, supervision and administration of the project and funding acquisition. Dr. Ersoy was also involved in supervision and administration of the project. Both Selina Quehl and Lara Mahnke worked during their bachelor theses on the mutagenesis of RizA (Mahnke, 2021; Quehl, 2021) under my supervision and were involved in the creation of some of the used variants. Tim A. Mast was involved in purifications as a student assistant. The work was published in the peer-reviewed journal *Catalysts* on 17<sup>th</sup> of November 2021 as part of the Special issue “Enzyme Catalysis, Biotransformation and Bioeconomy”.

DOI: 10.3390/catal11111385

## 6 Mutagenesis of the L-Amino Acid Ligase RizA Increased the Production of Bioactive Dipeptides

### 6.1 Abstract

The L-amino acid ligase RizA from *B. subtilis* selectively synthesizes dipeptides containing an N-terminal arginine. Many arginyl dipeptides have salt-taste enhancing properties while Arg-Phe has been found to have an antihypertensive effect. A total of 21 RizA variants were created by site-directed mutagenesis of eight amino acids in the substrate binding pocket. The variants were recombinantly produced in *E. coli* and purified by affinity chromatography. Biocatalytic reactions were set up with arginine and four amino acids differing in size and polarity (aspartic acid, serine, alanine and phenylalanine) and were analyzed by RP-HPLC with fluorescence detection. Variant T81F significantly improved the yield in comparison to wild type RizA for aspartic acid (7 to 17%), serine (33 to 47%) and alanine (12 to 17%). S84F increased product yield similarly for aspartic acid (7 to 17%) and serine (33 to 42%). D376E increased the yield with alanine (12 to 19%) and phenylalanine (11 to 26%). The largest change was observed for S156A, which showed a yield for Arg-Phe of 40% corresponding to a 270% increase in product concentration. This study expands the knowledge about positions governing the substrate specificity of RizA and may help to inform future protein engineering endeavors.

**Keywords:** L-amino acid ligase; biocatalysis; mutagenesis; coupled catalysis; arginyl dipeptides; salt taste; protein engineering; substrate specificity

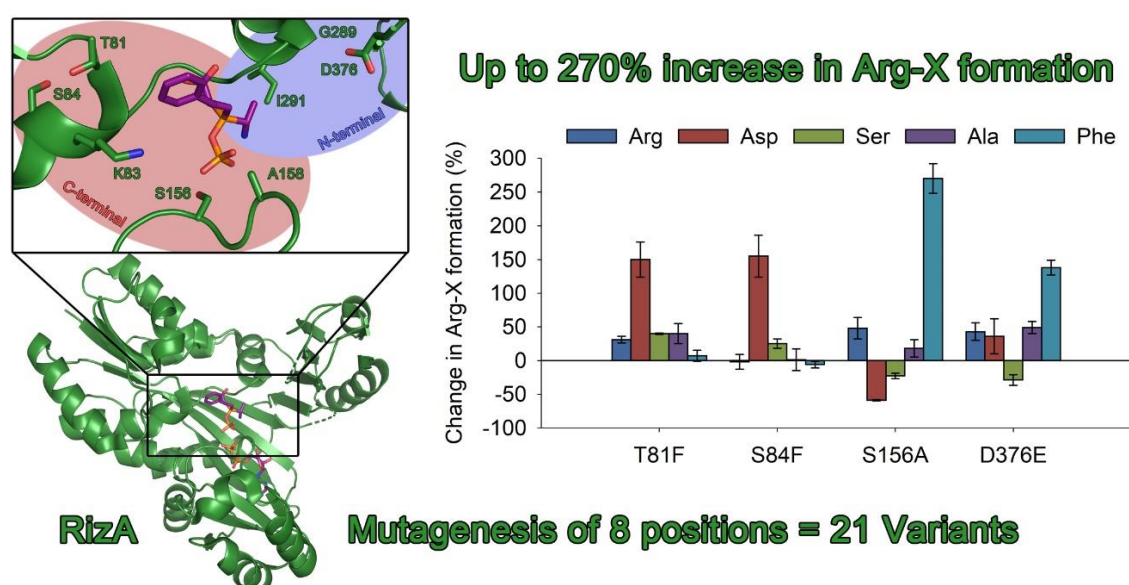


**Figure 6-1.** Graphical abstract of the publication (Bordewick et al., 2021a).

## 6.2 Introduction

Dipeptides constitute a promising substance class and are often more than the sum of their parts. They have physical properties different from their corresponding amino acids like improved heat stability or solubility (Fürst, 2001) and may induce pharmacological or other bioactive effects (Yagasaki & Hashimoto, 2008). Several dipeptides have been described as antihypertensives (Kagebayashi et al., 2012; Martin et al., 2015), while others have been implicated in possible medical applications due to their anticancer (Prakash et al., 2021) or neuroprotective properties (Ano et al., 2019a; Ano et al., 2019b; Ano et al., 2019c; Santos et al., 2012). The greatest industrial importance belongs to the low-calorie sweetener aspartame, the methyl ester of Asp-Phe, which currently has an estimated global market of 25,000 tons per year (Yagasaki & Hashimoto, 2008; Yokozeki & Abe, 2020). Additionally, dipeptides often have effects on other tastes and can possess salt-taste (Harth et al., 2018; Kino & Kino, 2015; Schindler et al., 2011) or umami-enhancing (Yan et al., 2021; Zhang et al., 2017) properties.

The chemical synthesis of dipeptides is a multi-step process necessitating the use of protecting groups, which increases waste and complicates purification (Gill et al., 1996; Yagasaki & Hashimoto, 2008). Biocatalysis has emerged as a more sustainable route for performing highly specific reactions without the need for protecting groups or harmful reagents (Behrens et al., 2011; Sheldon & Woodley, 2018). In the past, identifying an enzyme with the fitting natural activity for the desired purpose was a laborious task; today an abundance of bioinformatic tools exists to both facilitate the discovery of new enzymes and to adapt existing ones to the desired bioprocess by protein engineering (Bornscheuer et al., 2012). A recent development in biocatalytic dipeptide synthesis was the discovery of L-amino acid ligases (LALs; EC 6.3.2.28), which synthesize dipeptides from their respective amino acids using ATP (adenosine triphosphate). The discovery of the first LAL YwfE (also called BacD) from *Bacillus subtilis* was published in 2005 (Tabata et al., 2005). It synthesized a large variety of different dipeptides and generally preferred smaller amino acids like alanine as the N-terminal and larger amino acids like phenylalanine as its C-terminal substrate. It was also the first LAL, for which a structure was published (Suzuki et al., 2012). Another LAL was identified in *Ralstonia solanacearum* (RsLAL) with substrate specificities for N- and C-terminal substrates roughly opposite to those of BacD (Kino et al., 2008a). The structure for the LAL from *Bacillus licheniformis* NBRC12200 (Bl-LAL) enabled the structural comparison between LALs with different substrate specificities and thus gave insight into

how these differences relate to the structural level (Kino et al., 2008b; Suzuki et al., 2012). Later, this was used in the engineering of Bl-LAL for the production of Met-Gly (Kino & Kino, 2015). Another recent engineering study improved the production of Pro-Gly by the LAL TabS from *Pseudomonas syringae* NBRC14081 (Kino et al., 2016). Among these enzymes with different substrate specificities, RizA from *Bacillus subtilis* NBRC3134 stands out due to its high N-terminal specificity accepting only arginine, but relaxed C-terminal specificity accepting every amino acid except proline (Kino et al., 2009).

We previously worked on the production of the salt-taste enhancing dipeptides Arg-Ser, Arg-Ala and Arg-Gly with RizA coupled to acetate kinase for ATP regeneration to remove the cost of ATP as the major economic obstacle of this reaction (Bordewick et al., 2021b). Apart from these salt-taste enhancing dipeptides, RizA should also be capable of producing Arg-Phe, which has been described as antihypertensive (Arai et al., 2013; Kagebayashi et al., 2012). However, preliminary tests showed very low yields. Since a crystallographic structure of RizA has been published (Kagawa et al., 2015), a mutagenesis study of the substrate binding pocket of RizA was conceived to increase the production of several bioactive dipeptides and to gain knowledge about the substrate specificity of LALs for future engineering endeavors.

## 6.3 Results and Discussion

### 6.3.1 Selection of Mutations

The selection of important positions for substrate specificity was based on the structure of RizA, a sequence alignment of RizA with BacD, Bl-LAL (Kino et al., 2008b), RsLAL (Kino et al., 2008a), and TabS (Arai et al., 2013), and data from the literature on the substrate specificity and engineering of these LALs. Since the published structure of RizA (pdb: 4wd3) does not contain a substrate, a structural alignment with BacD containing a substrate analog of the Ala-Phe dipeptide (pdb: 3vmm) was used to approximate substrate binding as has been previously done in the original publication on the RizA structure (Kagawa et al., 2015) and also for the engineering of Bl-LAL (Kino & Kino, 2015).

To gain insight into the substrate specificity of RizA, eight different amino acids in the substrate binding pocket were chosen (Figure 6-2). Threonine 81 (T81), lysine 83 (K83), serine 84 (S84), serine 156 (S156) and alanine 158 (A158) were selected in the C-terminal binding pocket. Additionally, glycine 289 (G289), isoleucine 291 (I291) and aspartic acid 376 (D376) were chosen in the N-terminal binding pocket.

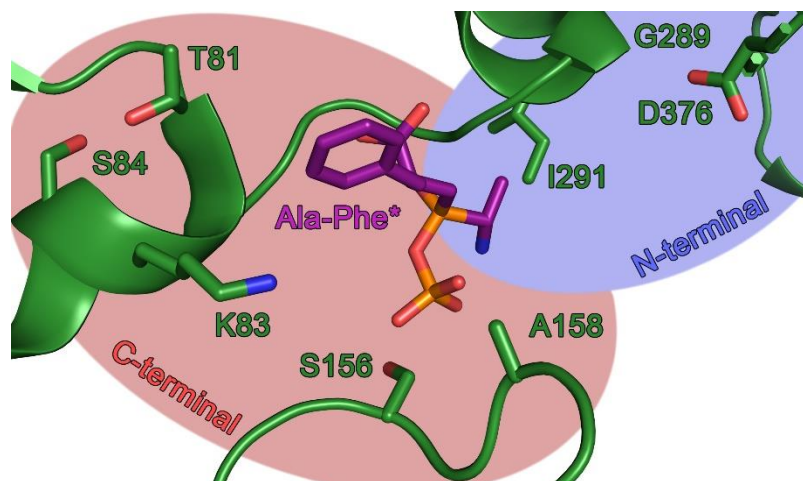


**Figure 6-2.** Mutated residues of RizA (green) in the C- (red) and N-terminal (blue) binding pocket (PDB ID: 4wd3). The structure contains the phosphorylated phosphino-analog of L-Ala-L-Phe (purple) from the structural alignment with BacD (PDB ID: 3vmm). Structures were displayed using PyMOL (Schrödinger, 2020). T81, K83 and S84 are located on an  $\alpha$ -helix very close to the C-terminal substrate (Figure 6-3a). In between them is E82, which is strictly conserved among LALs (Figure 6-3b) and has been implicated as an essential residue for the catalytic cycle (Shomura et al., 2012; Suzuki et al., 2012). Mutation of the homologous E109 to alanine in BacD resulted in a nearly total loss of activity. In contrast, the neighboring residues differ greatly depending on the LAL, and their close proximity to the substrate suggests a role in substrate specificity. K83 has already been recognized for this function and mutations of the homologous P85 in B1-LAL (Kino & Kino, 2015), S85 in TabS (Kino et al., 2016) and L110 in BaLAL (Liu et al., 2021) were used for successfully tuning the substrate specificity. Because of its apparent importance, six variants were constructed. K83L/P/S/F were chosen because of their presence in the other LALs (Figure 6-2b). Additionally, K83R was chosen because of the similar charge to lysine but larger size, and K85T since S85T improved activity in TabS (Kino et al., 2016). Position 81 has been implicated as N108 in BacD in substrate binding, but the only engineering attempt was made in BaLAL, where N108F improved product formation (Liu et al., 2021). Here, the homologous amino acids in other LALs were chosen for position 81 with the addition of alanine. S84 has – to our knowledge – never been targeted for its effect on substrate specificity, perhaps because of its greater distance from the substrate. However, due to its position and likely interaction with T81 (Figure 6-3a), an influence would still be plausible and S84F/L were created.

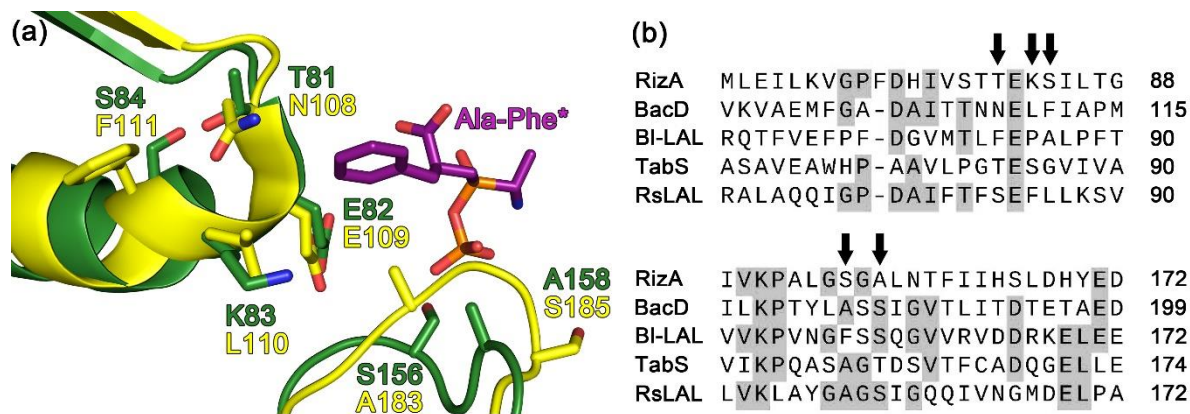


**Figure 6-3.** Residues in the C-terminal binding pocket. (a) Structural alignment of RizA (green; PDB ID: 4wd3) with BacD (yellow; PDB ID 3vmm) containing Ala-Phe analog (purple). The structures were displayed using PyMOL (Schrödinger, 2020). (b) Sequence alignment of RizA with other LALs. Arrows indicate positions that were mutated in RizA. Grey highlighting indicates conservation above 50%.

S156 and A158 are located on a different loop at the side of the phosphorylated substrate (Figure 6-3a). In contrast to positions 81 to 84, the structural alignment with the homologous loop in BacD showed large differences in this part of the enzymes. While A158 in RizA is oriented towards the C-terminal binding pocket, S185 of BacD is oriented further towards the N-terminal binding pocket. Besides their proximity to the substrate, both positions were also noticeable on the sequence level. Position S156 was relatively conserved and contained an alanine in all other LALs except BI-LAL, while at A158 all LALs contained a serine or the similar threonine. As a result, S156A/F and A158S/T were chosen for mutagenesis.

In the N-terminal binding pocket, G289 and I291 are located at the beginning of an  $\alpha$ -helix (Figure 6-4). The loop before the  $\alpha$ -helix is located directly at the N-terminal substrate and is highly conserved (Figure 6-4a and b) containing, among others, R285, whose homologous R328 in BacD has been identified as an essential residue for catalysis involved in forming an oxyanion-hole for the phosphorylated intermediate (Tsuda et al., 2014). In the same enzyme, both W332 and M334 corresponding to G289 and I291 in RizA (Figure 6-4a and b) have been strongly associated with N-terminal substrate specificity and the role of W332 was corroborated both by mutagenesis analysis and crystallographic study of W332A. The position equivalent to I291V was targeted in TabS by saturation mutagenesis, and H294D was part of a double mutant with increased production of Pro-Gly (Kino et al., 2016). D376 was proposed as important for binding arginine as the N-terminal substrate and an explanation for the high specificity of RizA for this amino acid (Kagawa et al., 2015). Because of their main role in N-terminal specificity, only few mutations of these residues were examined for their role: G289S, I291V and D376E.



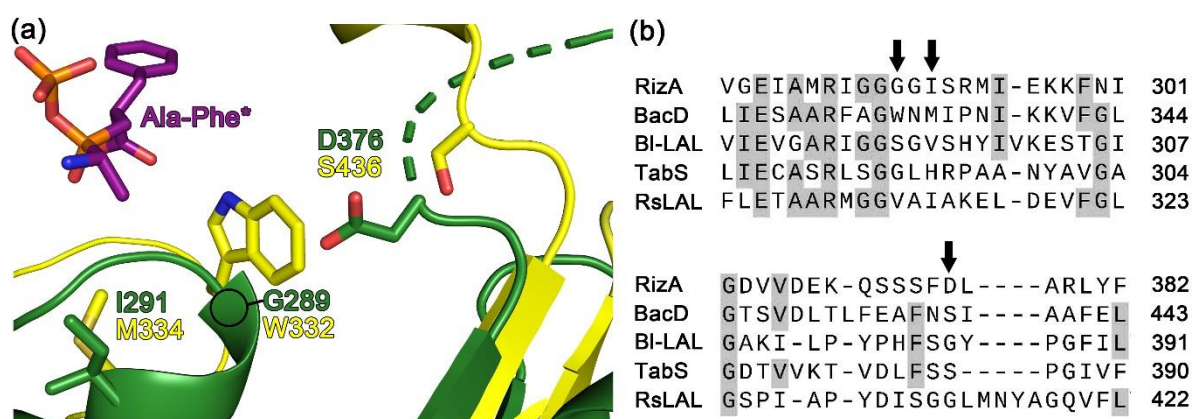


**Figure 6-4.** Residues in the N-terminal binding pocket. (a) Structural alignment of RizA (green; PDB ID 4wd3) with BacD (yellow; PDB ID 3vmm) containing Ala-Phe analog (purple). The structures were displayed using PyMOL (Schrödinger, 2020). (b) Sequence alignment of RizA with other LALs. Arrows indicate positions that were mutated in RizA. Grey highlighting indicates conservation above 50%.

### 6.3.2 Biocatalytic Performance of RizA Variants With Different Substrates

#### 6.3.2.1 Recombinant Production of RizA Variants and Biocatalysis Setup

The desired mutations were introduced by site-directed mutagenesis. The variants were recombinantly produced in *E. coli* BL21 (DE3) and purified by affinity chromatography. A panel of five amino acids was chosen representing a spectrum of different sizes, polarities and properties of the resulting dipeptides. All reactions contained arginine as the N-terminal amino acid, and reactions containing only arginine were performed to compare the formation of Arg-Arg in these reactions with those containing a second amino acid and Arg-Arg as a side product. Moreover, it represented a large, basic amino acid. In contrast, aspartic acid is a small, acidic amino acid and the resulting Arg-Asp a moderate salt-taste enhancer. Serine and alanine are both small amino acids differing in polarity and were also chosen, since both resulting heterodipeptides are strong salt-taste enhancers (Kino et al., 2009). Finally, phenylalanine was included as a large, non-polar amino acid and since Arg-Phe has been described as antihypertensive (Kagebayashi et al., 2012). Biocatalysis was performed using ATP regeneration and dipeptide monitoring by RP-HPLC with fluorescence detection as previously described (Bordewick et al., 2021b). Based on these results, a reaction time of 20 h was chosen because the yield with wild type RizA approached an equilibrium at that time. The data was first evaluated separately for each amino acid combination in terms of main product (Arg-X) formation and the specificity regarding the formation of the side product (Arg-Arg). At last, the effect of the mutations on the biocatalytic performance was analyzed to increase the understanding of the substrate specificity of LALs and provide possible targets for engineering.

### 6.3.2.2 Arginine Only

With arginine being the only substrate, wild type RizA produced 5.6 mM Arg-Arg corresponding to a yield of 19% (Figure 6-5). The highest concentrations were found in the samples from K83F and S156F containing 10.2 and 10.5 mM Arg-Arg, respectively. Many mutations in the C-terminal binding pocket increased the formation of Arg-Arg, while mutations in the N-terminal binding decreased it with the exception of D376E. S84F performed similarly to the wild type, while S84L was among the variants containing the least Arg-Arg and constituted the only mutation in the C-terminal binding pocket that reduced Arg-Arg formation.

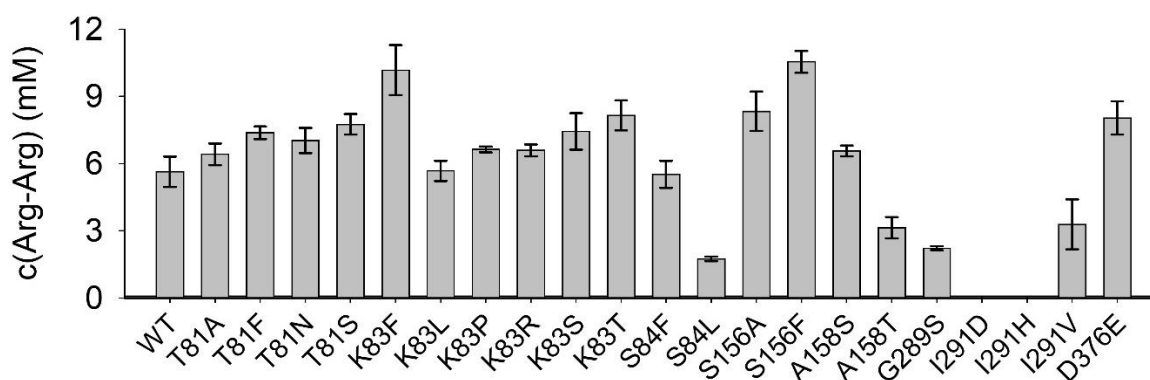


**Figure 6-5.** Formation of Arg-Arg by the RizA variants. 60 mM arginine and 20 h reaction time at 25°C. Reactions were set up in triplicates and data is presented as mean  $\pm$  standard deviation.

### 6.3.2.3 Arginine + Aspartic acid

With aspartic acid, the wild type enzyme produced only 2,0 mM Arg-Asp (7% yield), which was the lowest yield among the examined heterodipeptides (Figure 6-6). In comparison, both T81F and S84F increased Arg-Asp formation to 5 mM. Most of the mutations in the C-terminal binding pocket led to product concentrations comparable to the wild type or above while both S156A/F alongside the C-terminal binding pocket mutations decreased the Arg-Asp concentration below 1 mM. To evaluate the formation of the side product Arg-Arg versus the main product Arg-Asp, the specificity ratio Arg-Asp/Arg-Arg was calculated. (Figure 6-6). Most variants showed ratios between 2.0 and 1.0. In general, the change in ratio correlated with the increase in Arg-Asp formation and increased from 1.3 in the wild type reaction to 2.8 and 2.4 in the variants with the highest heterodipeptide increase, T81F and S84F. In line with this, the variants with the lowest Arg-Asp formation also showed the lowest ratios. In contrast, the specificity in the K83 variants remained on the wild type level or decreased despite most of these variants increasing Arg-Asp formation. The most



significant outlier was S84L in that it increased specificity to a ratio of 2.4 like S84F, but severely reduced main product formation as well.

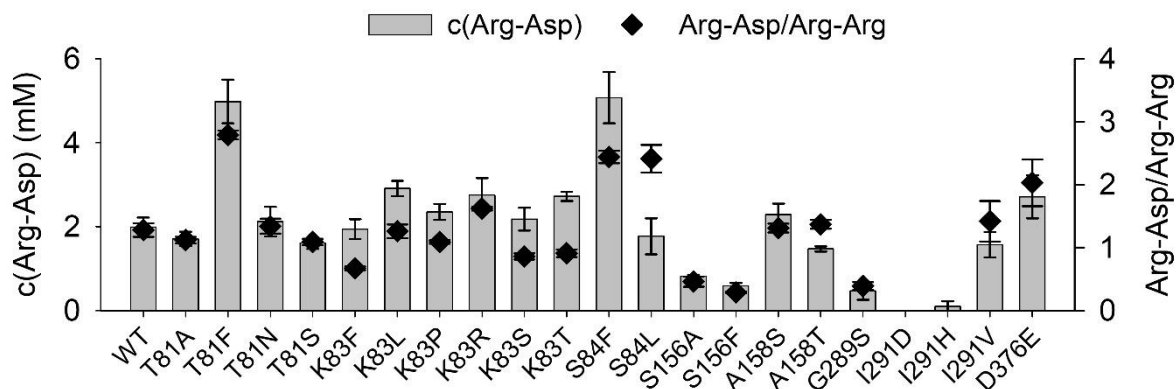


**Figure 6-6.** Formation of Arg-Asp and Arg-Arg by the RizA variants. 30 mM of both arginine and aspartic acid and 20 h reaction time at 25°C. Reactions were set up in triplicates and data is presented as mean  $\pm$  standard deviation.

#### 6.3.2.4 Arginine + Serine

Wild type RizA displayed the highest observed product formation with serine producing 10.0 mM Arg-Ser and a yield of 33 % (Figure 6-7). Like for aspartic acid, T81F and S84F showed the highest increases in product formation to 14.1 mM and 12.5 mM, respectively. With the exception of S84L, S156A/F and A158T, all mutations in the C-terminal binding pocket retained most of the activity of the wild type enzyme or increased it. All mutations in the N-terminal binding pocket decreased product formation or prevented it, as was the case for I291D and I291H. Regarding side product formation, wild type RizA displayed the highest specificity for Arg-Ser versus Arg-Arg among the examined amino acids, producing Arg-Ser at a ratio of 7.8 to Arg-Arg (Figure 6-7). In the variants, these ratios varied between 3.2 in G289S and 11.6 in S84F, which were also the variants with the lowest/highest detected Arg-Arg concentrations, respectively (Figure 6-5). S84L also increased the ratio to 10.9, again in combination with reduced activity. Similarly, I291V lowered the activity but increased specificity to 9.3. Similar to the reactions with aspartic acid, K83F/S/T increased product formation but lowered specificity. While T81F showed the largest increase in main product formation, it only displayed a small increase to 8.3.

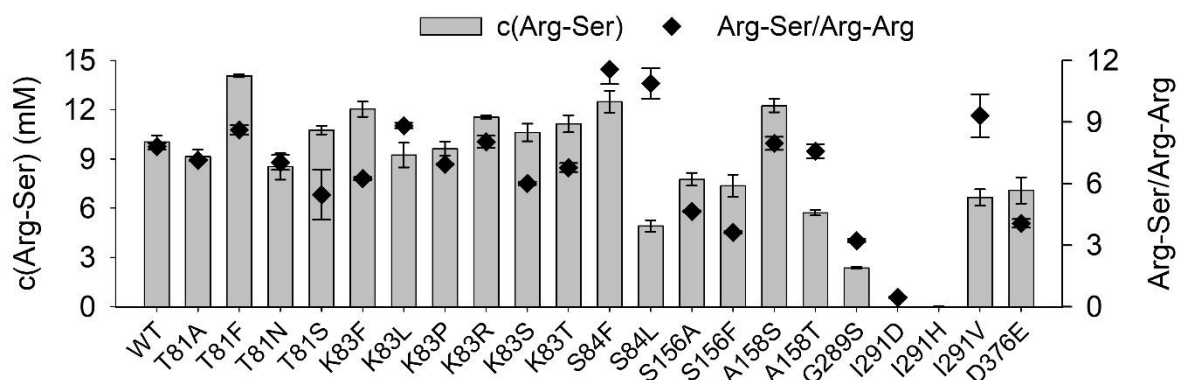


**Figure 6-7.** Formation of Arg-Ser and Arg-Arg by the RizA variants. 30 mM of both arginine and serine and 20 h reaction time at 25°C. Reactions were set up in triplicates and data is presented as mean  $\pm$  standard deviation.

### 6.3.2.5 Arginine + Alanine

Arg-Ala was produced by the wild type at a concentration of 3.8 mM (13 % yield) and the variants ranged from 1.2 mM in G289S to 5.6 mM in D376E (Figure 6-8). Apart from D376E, T81F and S156F also increased product concentration. Most mutations in the C-terminal binding pocket retained activity comparable to the wild type enzyme with the exception of S84L, which only produced 1.7 mM Arg-Ala. In contrast to D376E, all other mutations in the N-terminal binding pocket were detrimental to the formation of Arg-Ala. Most variants retained an Arg-Ala/Arg-Arg ratio comparable to the wild type (1.8) or below with K83F showing the lowest detected specificity of 1.2 (Figure 6-8). S84L and I291V had the highest specificity of 2.7, but at the expense of overall activity.

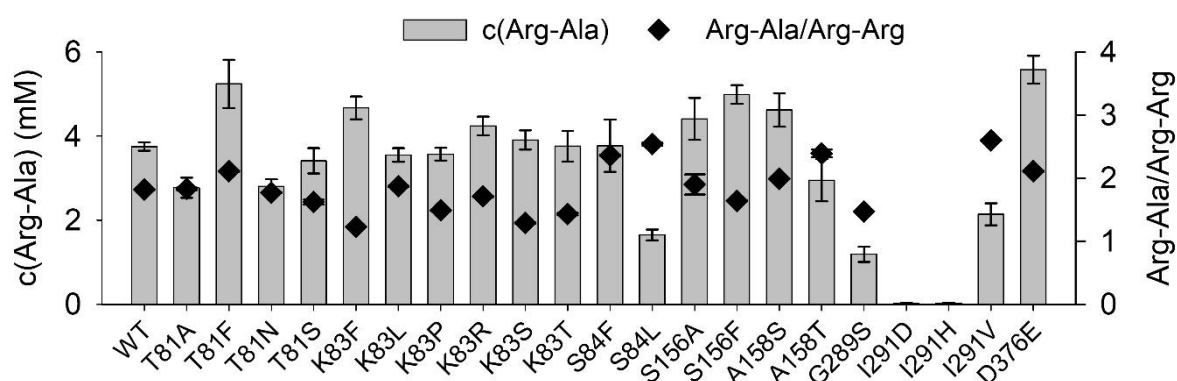


**Figure 6-8.** Formation of Arg-Ala and Arg-Arg by the RizA variants. 30 mM of both arginine and alanine and 20 h reaction time at 25°C. Reactions were set up in triplicates and data is presented as mean  $\pm$  standard deviation.

### 6.3.2.6 Arginine + Phenylalanine

Among the examined amino acids, phenylalanine showed the second lowest product concentration with 3.3 mM Arg-Phe and a yield of 11% using the wild type enzyme (Figure 6-9). In contrast, the variant S156A produced the highest heterodipeptide concentration in this study, with the exception of the serine reactions. In total, 12.1 mM Arg-Phe were produced corresponding to a yield of 40%. Other variants with significant increases were D376E, S156F and K83F. Most other variants performed on the wild type level or below. S156A displayed the highest increase in specificity observed in this study from a ratio of 1.4 with wild type RizA to 9.7 in this variant (Figure 6-9). D376E and S156F showed increased ratios, but K83F did not display a significant difference in ratio despite increased formation of Arg-X indicating a higher production of Arg-Arg as well.

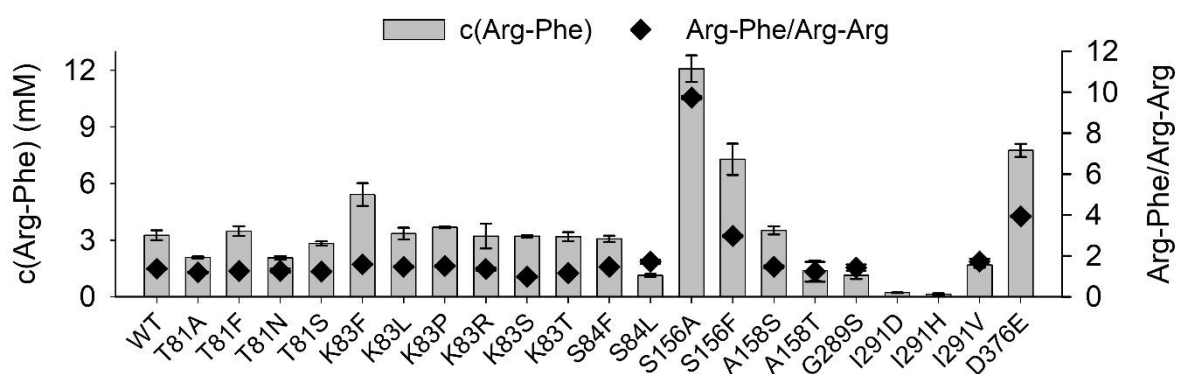


**Figure 6-9.** Formation of Arg-Phe and Arg-Arg by the RizA variants. 30 mM of both arginine and phenylalanine and 20 h reaction time at 25°C. Reactions were set up in triplicates and data is presented as mean  $\pm$  standard deviation.

### 6.3.3 Effects of Mutations on the Substrate Specificity and Biocatalytic Productivity of RizA

To analyze the effect of the mutations on the substrate specificity and biocatalytic performance, the percentage change of Arg-X product formation was calculated for each substrate and variant in comparison to the wild type enzyme (Figure 6-10). Additionally, a 3D bar chart summarizing dipeptide formation for all amino acid combinations is available in Supporting Figure 6-1.

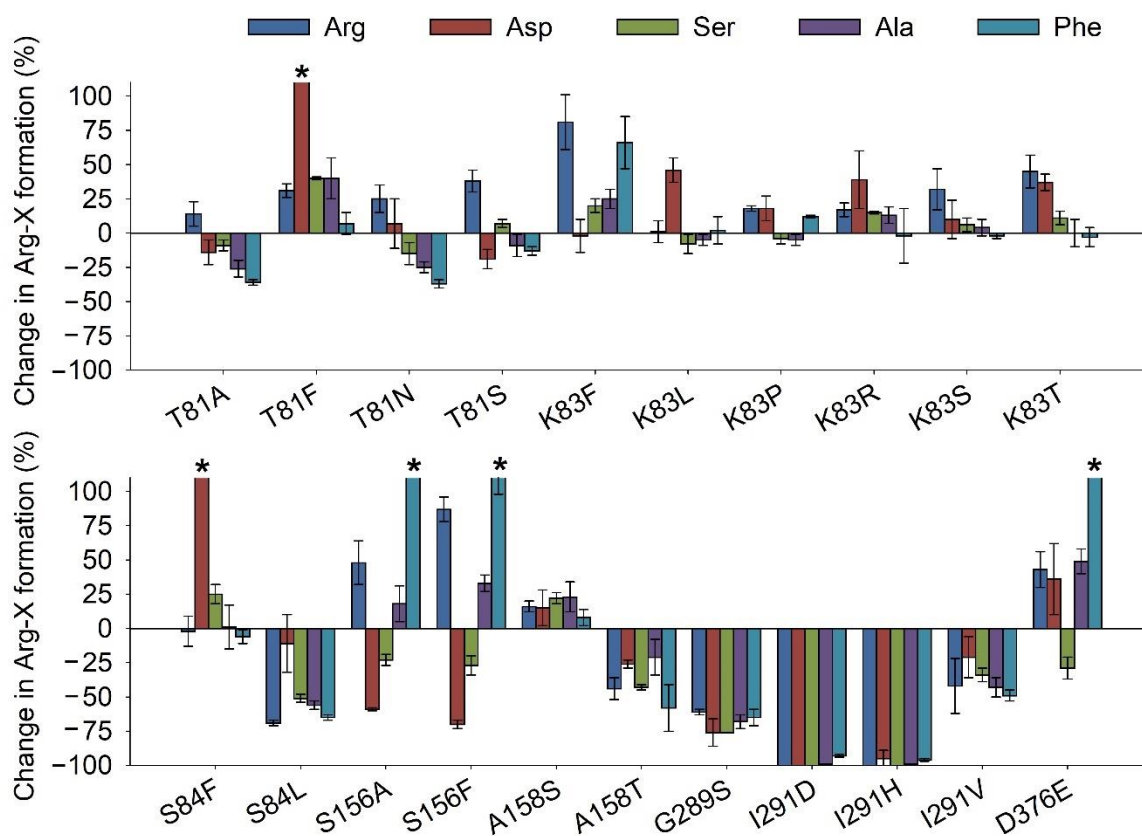


**Figure 6-10.** Change in product formation with RizA variants compared to the wild type with each substrate. \*Values over 100% were truncated: T81F with Asp:  $150 \pm 26\%$ ; S84F with Asp:  $155 \pm 31\%$ ; S156A with Phe:  $270 \pm 22\%$ ; S156F with Phe:  $123 \pm 25\%$ ; D376E with Phe:  $138 \pm 11\%$  (see Supporting Figure 6-2 for graph without truncation).

T81A/N/S had similar effects and generally increased Arg-Arg production, but decreased the other dipeptide concentrations by up to 37%. In contrast, T81F increased product formation for all amino acids except phenylalanine significantly up to 150% for aspartic acid. Bl-LAL also contains a phenylalanine at the respective position (Figure 6-3) and was found to prefer small amino acids like serine or alanine as its C-terminal substrate (Kino et al., 2008b). TabS has been shown to accept serine as a major C-terminal substrate and – like wild type RizA – contains a threonine at this position in line with the similar high affinity of the wild type enzyme for serine (Arai et al., 2013).

Similar to position 81, the substitution to phenylalanine at position 83 had a larger effect than the other variants K83L/P/R/S/T, where only small effects on product formation with serine, alanine and phenylalanine were detected, while for arginine and aspartic acid it increased by up to 46%. K83F had no effect on the aspartic acid reactions, but increased product formation for serine and alanine by about 20%, by 66% with phenylalanine and finally by 81% with arginine making it the variant with the highest Arg-Arg production alongside S156A. In line

with this, K83F also showed increased Arg-Arg formation as a side product in the reactions with a second amino acid as seen by the lowered specificity ratios (Figure 6-6 to 6-8). A possible explanation for this large effect is that the mutation of lysine to phenylalanine removed a positive charge from the substrate binding pocket, which normally repels the positive charge of the guanidinium moiety of the arginine substrate. However, the other K83 variants also removed this positive charge, so the substitution to phenylalanine must have an additional positive effect on the binding of arginine apart from the charge.

At position 84, substitution to leucine had a detrimental effect on reactions with all amino acids except aspartic acid, where no significant effect was registered. In contrast, S84F dramatically increased Arg-Asp formation by 155% making it the best variant for this dipeptide alongside T81F. Arg-Ser production was also increased by 25% with no significant effect on the other amino acids. Both S84F and S84L showed large increases in the specificity ratios for most reactions (Figure 6-6 to 8). However, S84F mainly increased main product formation and side product formation remained relatively unchanged, while for S84L main product formation decreased, but side product formation decreased even further resulting in an overall increased specificity. This is also reflected in the reactions containing only arginine, where S84F had no detected effect on Arg-Arg formation, but S84L decreased it by 69%.

Substitution of the serine at position 156 to alanine or phenylalanine had similar effects on the substrate specificity, as in both cases product formation with aspartic acid and serine was lowered, and product formation with arginine, alanine and phenylalanine increased, but the variants varied in how severe the decreases/increases were. For example, S156F increased Arg-Phe production by 123%, whereas S156A increased it by 270%. The large increase for phenylalanine correlated with BacD and TabS, which also contain an alanine at the homologous position and accept phenylalanine readily as the C-terminal substrate (Arai et al., 2013; Tabata et al., 2005). However, RsLAL also contains alanine but prefers “non-bulky” C-terminal substrates (Kino et al., 2008a). In general, it is plausible that a smaller, non-polar residue like alanine would be more suitable than serine for a large, non-polar substrate like phenylalanine. The mutation to phenylalanine also reduced the polarity of the substrate binding pocket, but its larger size and thus reduced space in the binding pocket could be an explanation for the smaller increase with the large substrate.

Position A158 was substituted by serine or threonine. Despite the small difference between these two amino acids, they had opposite effects: A158S increased product formation for all

amino acids by 8 to 23% and A158T decreased it by 21 to 58%. It was noted that position 158 cannot be unambiguously assigned to the C-terminal binding pocket and that it seems to be oriented more towards the N-terminal binding pocket in the BacD structure (Figure 6-3a). Due to its position, it might be affecting the overall substrate binding more than the N- and C-terminal substrate specifically.

In the N-terminal binding pocket, the mutations of G289 and I289 all drastically reduced product formation for all examined amino acids. Significant differences between C-terminal amino acids were not observed, as expected from their position in the N-terminal binding pocket. Likely, these mutations inhibited binding of the N-terminal arginine, which is the first step of the catalytic cycle and thus inhibited product formation with all examined amino acids (Shomura et al., 2012). D376E was the only mutation in the N-terminal binding pocket with increases in product formation. While Arg-Ser decreased, Arg-Arg, Arg-Asp and Arg-Ala increased by 36 to 49% and Arg-Phe by 138%, respectively, thus making it the second-best variant for Arg-Phe after S156A. Data of the biocatalytic performance for the two best variants in terms of yield and specificity for each amino acid is summarized in Table 6-1.

**Table 6-1.** Variants with the highest biocatalytic performance for the production of Arg-X dipeptides.

Amino Acid X	Variant	c (Arg-X) (mM)	c(Arg-Arg) (mM)	Arg-X/Arg-Arg	Yield (Arg-X) (%)
Arginine	Wild type	5.6 ± 0.7	-	-	19
	S156F	10.5 ± 0.5	-	-	35
	K83F	10.2 ± 1.1	-	-	34
Aspartic acid	Wild type	2.0 ± 0.2	1.6 ± 0.2	1.3	7
	T81F	5.0 ± 0.5	1.8 ± 0.2	2.8	17
	S84F	5.1 ± 0.6	2.1 ± 0.2	2.4	17
Serine	Wild type	10.0 ± 0.4	1.3 ± 0.1	7.8	33
	T81F	14.1 ± 0.1	1.6 ± 0.0	8.6	47
	S84F	12.5 ± 0.7	1.1 ± 0.1	11.6	42
Alanine	Wild type	3.7 ± 0.1	2.1 ± 0.1	1.8	12
	D376E	5.6 ± 0.3	2.6 ± 0.2	2.1	19
	T81F	5.2 ± 0.6	2.5 ± 0.3	2.1	17
Phenylalanine	Wild type	3.3 ± 0.3	2.4 ± 0.2	1.4	11
	S156A	12.1 ± 0.7	1.2 ± 0.1	9.7	40
	D376E	7.8 ± 0.4	2.0 ± 0.1	3.9	26

T81F was among the best variants for all three examined small amino acids. In the case of the small, polar amino acids aspartic acid and serine, S84F was the second-best variant. Considering the close proximity and orientations of T81 and S84 to each other (Figure 6-3a), it is plausible that the same substitution led to similar effects in T81F and S84F. Overall, decreasing the size of the C-terminal binding pocket with mutations to phenylalanine (T81F, K83F, S84F and S156F) generally increased product formation for small amino acids, although not uniformly. For example, the serine at position 156 possibly had a beneficial effect for the binding of small, polar amino acids, as both substitutions (S156A/F) decreased product formation for serine and aspartic acid. The residue might have a discriminating effect on the polarity of the substrate, as both substitutions instead increased product formation with the non-polar alanine and phenylalanine. Both of these substrates also shared D376E as one of the best variants (Table 6-1). It was the only mutation in the N-terminal binding pocket that had positive effects on product formation. If the hypothesized function of D376 in binding the N-terminal arginine by electrostatic interaction (Kagawa et al., 2015) is correct, then it stands to reason that D376E is also capable of that function, but that it might change the orientation of the substrate as a whole due to the larger size of glutamic compared to aspartic acid. This could explain, why it was the only mutation in the N-terminal binding pocket significantly affecting C-terminal specificity.

For all substrates, variants with significantly improved biocatalytic performance were identified (Table 6-1). Alanine was the substrate with the smallest increases from 12 to 19% yield in D376E and only a modest increase in the specificity ratio Arg-X/Arg-Arg. Aspartic acid was the substrate with the lowest yield, and Arg-X/Arg-Arg ratio in the wild type and both parameters were increased more than two-fold in T81F. Serine was the best among the wild type RizA substrates and was still substantially improved from a yield of 33 to 47% and a small increase in specificity in T81F. In addition, S84F significantly increased the specificity to 11.6. Phenylalanine was the substrate with the second-lowest yield of 11% and specificity of 1.4 after alanine. Conversely, S156A conferred the largest increases for both parameters observed in this work and increased them to 40% and 9.7 resulting in a similar performance than observed with serine.

While the yields for Arg-Ala and Arg-Asp were still relatively low despite the large relative change in yield, T81F and S156A represent suitable candidates for the production of the salt-taste enhancer Arg-Ser and the potential antihypertensive Arg-Phe using RizA. In comparison, the previously highest Arg-Ser yield was 41% using higher wild type RizA

concentrations and 50 mM amino acids concentration (Bordewick et al., 2021b). Arg-Phe has been previously produced with TabS with a yield of 62% using 12.5 mM amino acids. S156A represents a single mutation drastically changing the substrate specificity. However, redesign of the substrate specificity of LALs is likely a more complicated matter not to be solved by single mutations.

Apart from completely random directed evolution approaches, protein engineering always benefits from knowledge on the relationship of protein sequence and function in the form of reaction data, structures and mutagenesis studies (Bilal & Iqbal, 2019; Bornscheuer et al., 2012). In the present work, a total of eight positions were examined and targeted for their role in substrate specificity. It represents the first mutagenesis study of RizA and confirmed the importance of positions 81 and 83 for substrate specificity that were already explored in other LALs. Furthermore, the positions S84, S156 and A158 have never been examined in any LAL regarding their potential for changing the substrate specificity. RizA is both an excellent study object of LAL substrate specificity and the production of arginyl dipeptides due to its high N-terminal specificity and relaxed C-terminal specificity. With the gained knowledge, RizA can be further engineered by combining mutations or performing saturation mutagenesis at the identified positions, as has been previously done for the production of Pro-Gly with TabS (Kino et al., 2016). While the specificity of Arg-X versus Arg-Arg formation has been substantially improved in the created variants (Table 6-1), a further reduction of this side product would be a suitable engineering target. Finally, since proline is the only amino acid not accepted by RizA, and Arg-Pro is the strongest salt-taste enhancer among the arginyl dipeptides (Schindler et al., 2011), adapting RizA for the production of this dipeptide is another worthwhile challenge. A promising approach is the use of protein modelling to guide the selection of mutations, which has been successfully performed recently for the engineering of BaLAL (Liu et al., 2021). New tools like the AI-based AlphaFold software (Jumper et al., 2021) allow for the prediction of the 3D-structure of a protein from its primary sequence. However, enzymes undergo conformational changes while binding the substrate, a process based on a mutual stereochemical fit and a variety of molecular interactions. Until all of these conformational states and interactions can be precisely modeled, experiments as described above will be indispensable for understanding the relationship of protein structure and function.



## 6.4 Materials & Methods

### 6.4.1 Chemicals, Reagents and Strains

All chemicals were purchased from Carl Roth (Karlsruhe, Germany) or Sigma Aldrich (Taufkirchen, Germany) if not otherwise indicated. Enzymes for molecular biology were purchased from Thermo Fisher Scientific (St. Leon-Roth, Germany). The pET28a vector was purchased from Merck KGaA (Darmstadt, Germany). The *E. coli* strains BL21 (DE3) and TOP10 were maintained in our laboratory. Oligonucleotides were synthesized by Microsynth Seqlab GmbH (Goettingen, Germany).

### 6.4.2 Mutagenesis of RizA

Structural alignment and images of protein structures were created with PyMOL version 2.3.1 (2020) by Schrödinger, LLC (New York, NY, USA) (Schrödinger, 2020). Sequence alignments were created with SnapGene version 5.1.7 (2020) from GSL Biotech LLC (Chicago, IL, USA). Mutagenesis of the pET28\_his6-rizA construct (Bordewick et al., 2021b) was performed by whole-plasmid PCR using overlapping, mutagenic primers and was adapted from Liu and Naismith (2008). PCR were performed in a Biometra thermal cycler from Analytik Jena (Jena, Germany) using Phusion DNA polymerase from Thermo Fisher Scientific (St. Leon-Roth, Germany) and the pET28a\_his6-rizA plasmid as template (50 ng). Primers (Supporting Table 6-1) were designed with the software SnapGene version 5.1.7 (2020) from GSL Biotech LLC (Chicago, IL, USA). The three-step protocol started with a denaturing step at 98 °C for 30 s, then 20 cycles of 98 °C for 10s, the annealing temperature (Supporting Table 6-1) for 30 s and 72°C for 130 s. Lastly, final extension was performed at 72 °C for 10 min and PCR products were stored at 8°C. In the two-step protocol (Supporting Table 6-1), the elongation step at the annealing temperature was omitted. PCR products were visualized by agarose gel electrophoresis and digested by addition of 1 µL DpnI to 50 µL PCR and incubation at 37 °C for 2 h followed by inactivation at 80 °C for 5 min. The digested reactions were transformed into chemocompetent *E. coli* TOP10. After confirming the correct mutation through sequencing by Microsynth Seqlab GmbH (Goettingen, Germany), the variant plasmids were transformed into *E. coli* BL21 (DE3) for expression and glycerol stocks were stored at -80 °C.

### 6.4.3 Cultivation and Purification

Cultivation and purification were performed as previously described for wild type RizA (Bordewick et al., 2021b). In short, for each variant 100 mL TB medium were inoculated and incubated at 37°C/160 rpm until induction and harvested after 20 h expression at 20

°C/160 rpm. After cell disruption by sonication, the RizA variants were purified by affinity chromatography and desalted by gel filtration.

#### 6.4.4 Biocatalysis

Biocatalytic reactions were performed according to the previously described conditions (Bordewick et al., 2021b). The reactions were performed in 0.2 mL PCR tubes with 50  $\mu$ L reaction volume and contained 30 mM arginine and the second amino acid, 30 mM AcP, 0.5 mM ATP, 7.5 mM MgSO<sub>4</sub>, 0.2 mg/mL RizA, 0.1 mg/mL AckA and 25 mM tricine buffer pH 8.5. Reactions and substrate controls containing no RizA were set up in triplicates and incubated at 25 °C in a Biometra thermal cycler from Analytik Jena (Jena, Germany). After 20 h, the reactions were inactivated at 70 °C for five min and stored at -20 °C until analysis.

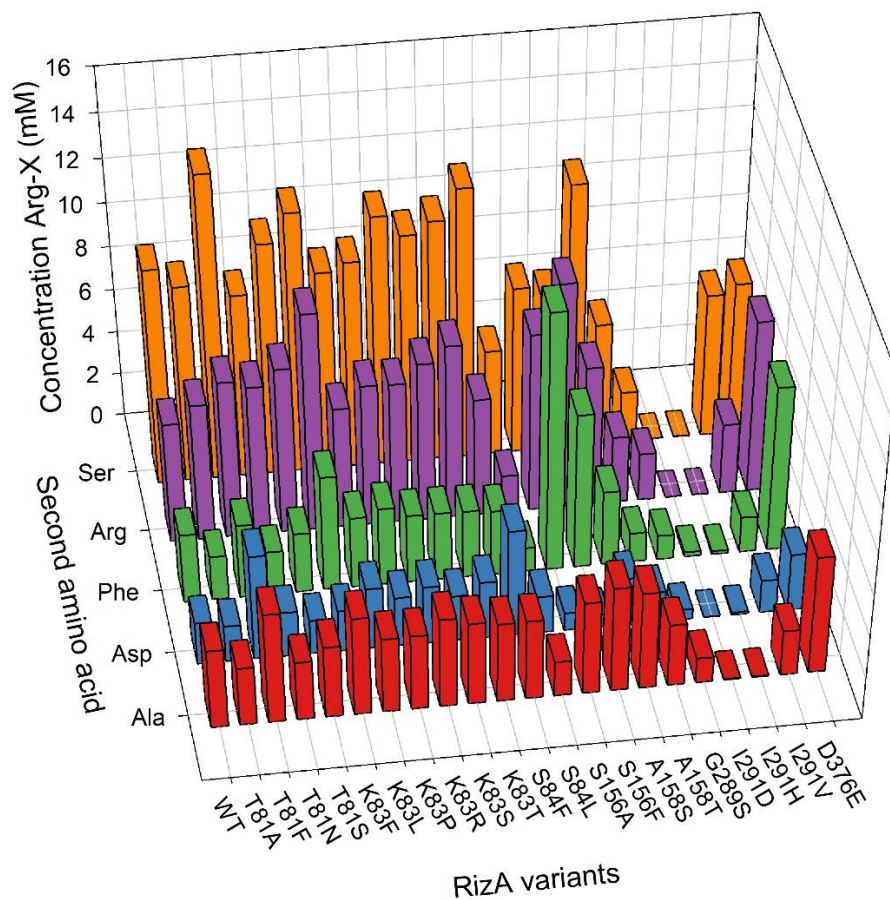
#### 6.4.5 Analysis

The amino groups of dipeptides were derivatized with *o*-phthalaldehyde and analyzed by RP-HPLC with fluorescence detection with the same analytical setup described by Rottmann et al. (2021). Similar to the previous study on RizA (Bordewick et al., 2021b), the gradient consisting of eluent A (0.1 M sodium acetate buffer pH 6.5) and eluent B (Methanol HPLC grade) was modified for the measurement of dipeptides. Two different gradient programs were used: For the measurement of Arg-Asp, Arg-Ser and Arg-Ala alongside Arg-Arg (gradient 1), the gradient was as follows: 0 min: 70% A, 5 min: 70% A, 10 min: 60% A, 15 min: 0% A, 20 min: 0% A, 25 min: 70% A, 30 min: 70% A. For the measurement of Arg-Phe alongside Arg-Arg (gradient 2), the gradient was: 0 min: 60% A, 5 min: 60% A, 10 min: 50% A, 15 min: 0% A, 20 min: 0% A, 25 min: 60% A, 30 min: 60% A. Exemplary chromatograms for each gradient program are shown in Supporting Figure 6-3 and Supporting Figure 6-4. Beta-alanine was added as an internal standard for the derivatization. External calibration was performed with analytical standards of the dipeptides Arg-Arg, Arg-Asp, Arg-Ser, Arg-Ala and Arg-Phe, which were purchased from Bachem (Bubendorf BL, Switzerland). All standard solutions were set up in triplicate. Data was visualized with SigmaPlot 14.5 (2020) from Systat Software GmbH (Erkrath, Germany).

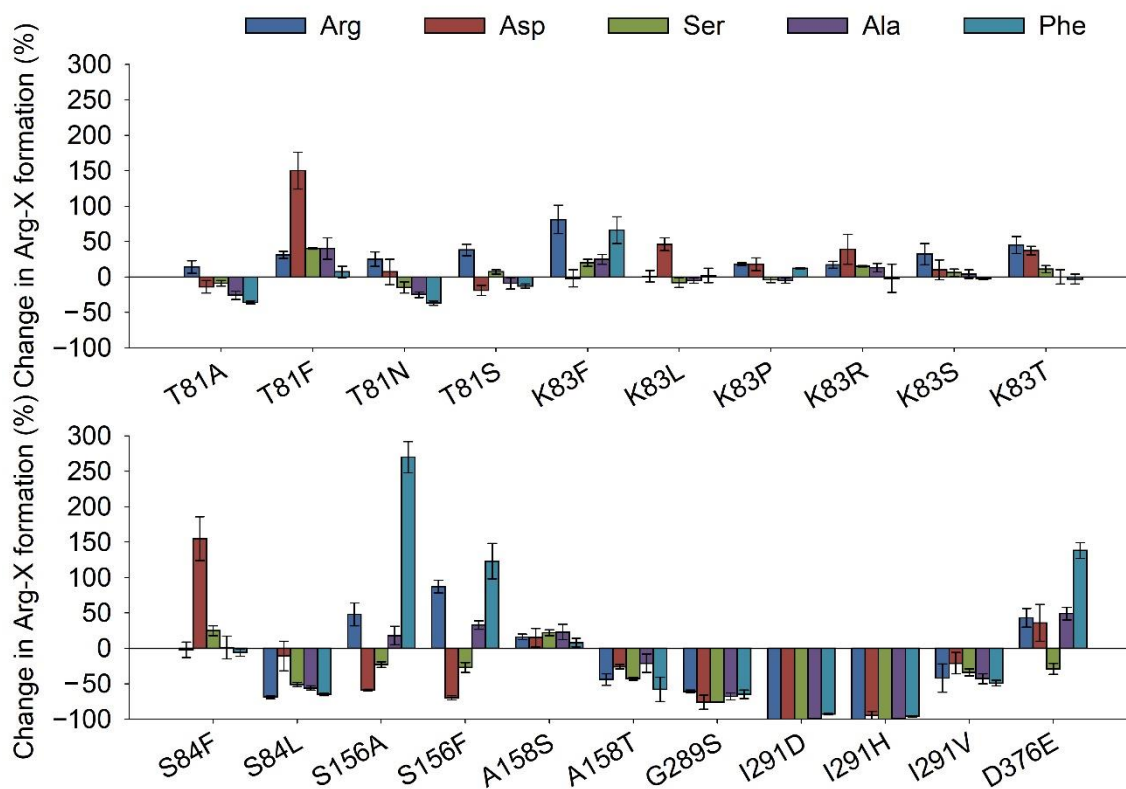
#### 6.5 Conclusions

Mutagenesis of RizA improved the yield and substrate specificity for the production of bioactive dipeptides. The gained data both confirmed the roles of several residues already implicated in substrate specificity and identified new ones that can be used in future protein engineering studies.

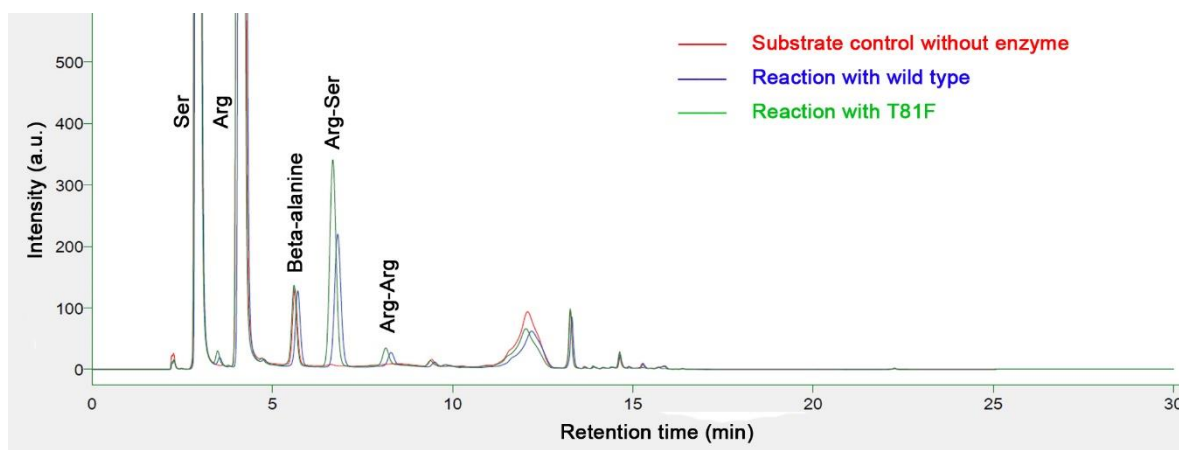
6.6 Supplementary Materials



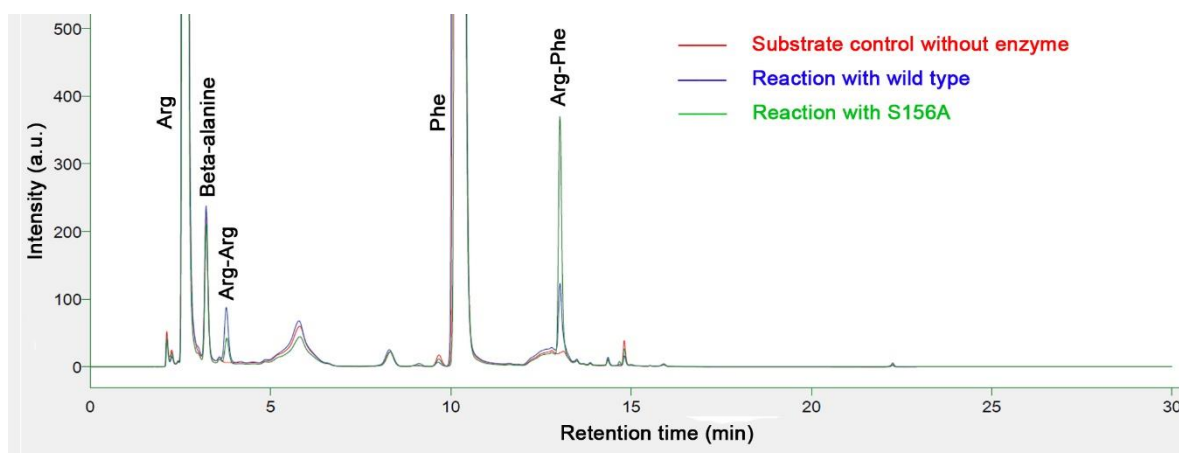
Supporting Figure 6-1. 3D bar chart of dipeptide formation. Created with data from Figure 6-5 to Figure 6-9.



**Supporting Figure 6-2.** Change in product formation of RizA. Reactions were set up in triplicate and data is presented as mean  $\pm$  standard deviation.



**Supporting Figure 6-3.** Exemplary chromatogram with gradient program 1 for measurement of Arg-Ser. For each reaction, only one of the triplicates is shown. The amino acids could not be quantitated due to the significantly higher intensity of their derivates overloading the fluorescence detector. Substrate controls without enzyme were used to account for signals resulting from impurities.



**Supporting Figure 6-4.** Exemplary chromatogram with gradient program 2 for measurement of Arg-Phe. For each reaction, only one of the triplicates is shown. The amino acids could not be quantitated due to the significantly higher intensity of their derivatives overloading the fluorescence detector. Substrate controls without enzyme were used to account for signals resulting from impurities.

**Supporting Table 6-1.** Primer pairs for mutagenesis. The given annealing temperatures are for the three-step protocol, in the two-step protocol annealing and elongation were both performed at 72 °C (see Materials & Methods).

Name	Sequence (5'->3')	Annealing temperature (°C)
T81F_fw	TTAGCACCTTTGAAAAAAGCATTCTGACC	66
T81F_rv	TTTTTCAAAGGTGCTAACAATATGATCAAACG	66
T81S_fw	AGCACCAGCGAAAAAAGCATTCTGACCG	69
T81S_rv	TTTTTCGCTGGTGCTAACAATATGATCAAACG	69
K83F_fw	ACCGAATTTAGCATTCTGACCGGTGGTTTTTC	67
K83F_rv	AATGCTAAATTCGGTGGTGCTAACAATATG	67
K83R_fw	ACCGAACGTAGCATTCTGACCGGTG	68
K83R_rv	AATGCTACGTTTCGGTGGTGCTAAC	68
S156A_fw	TTAGGTGCGGGTGCCTGAATACCTTTATTATC	Two-step protocol
S156A_rv	TGCACCCGCACCTAATGCCGGTTTAAC	Two-step protocol
S156F_fw	TTAGGTTTTGGTGCCTGAATACCTTTATTATC	67
S156F_rv	TGCACCAAACCTAATGCCGGTTTAACAATAATC	67
A158S_fw	AGCGTTTCTCTGAATACCTTTATTATCCATAGC	69
A158S_rv	ATTCAGAGAACCGCTACCTAATGCCGGTTTAAC	69
G289S_fw	TATTGGTGGTAGCGGCATTAGCCGTATG	Two-step protocol
G289S_rv	AATGCCGCTACCACCAATACGCATTG	Two-step protocol
I291V_fw	GGTGGCGTGAGCCGTATGATTGAGAAAAAATTC	Two-step protocol

---

I291V_rv	AATCATACGGCTCACGCCACCACCACCAATAC	Two-step protocol
D376E_fw	TCATTTGAACTGGCACGTCTGTATTTTTG	67
D376E_rv	TGCCAGTTCAAATGAGCTGCTCTGTTTTTC	67
T81A_fw	AGCACCGCGGAAAAAAGCATTCTGAC	Two-step protocol
T81A_rv	TTTTTCCGCGGTGCTAACAATATGATCAAACG	Two-step protocol
T81N_fw	AGCACCAACGAAAAAAGCATTCTGACCG	Two-step protocol
T81N_rv	TTTTTCGTTGGTGCTAACAATATGATCAAACGGAC	Two-step protocol
T81R_fw	AGCACCCGCGGAAAAAAGCATTCTGAC	Two-step protocol
T81R_rv	TTTTTCGCGGGTGCTAACAATATGATCAAACG	Two-step protocol
K83S_fw	ACCGAAAGCAGCATTCTGACCGGTG	Two-step protocol
K83S_rv	AATGCTGCTTTCGGTGGTGCTAACAATATG	Two-step protocol
K83T_fw	ACCGAAACCAGCATTCTGACCGGTG	Two-step protocol
K83T_rv	AATGCTGGTTCGGTGGTGCTAACAATATG	Two-step protocol
K83L_fw	ACCGAACTGAGCATTCTGACCGGTG	Two-step protocol
K83L_rv	AATGCTCAGTTCGGTGGTGCTAACAATATG	Two-step protocol
K83P_fw	ACCGAACCGAGCATTCTGACCGGTG	Two-step protocol
K83P_rv	AATGCTCGGTTCGGTGGTGCTAACAATATG	Two-step protocol
S84F_fw	GAAAAATTTATTCTGACCGGTGGTTTTCTGCG	68
S84F_rv	CAGAATAAATTTTTCGGTGGTGCTAACAATATGATC	68
S84L_fw	GAAAACTGATTCTGACCGGTGGTTTTTC	68
S84L_rv	CAGAATCAGTTTTTCGGTGGTGCTAACAATATG	68
A158T_fw	AGCGGTACCCTGAATACCTTTATTATCCATAG	68
A158T_rv	ATTCAGGGTACCGCTACCTAATGCCG	68
I291H_fw	GGTGGCCATAGCCGTATGATTGAGAAAAAATTC	Two-step protocol
I291H_rv	ACGGCTATGGCCACCACCACCAATACG	Two-step protocol
I291D_fw	GGTGGCGATAGCCGTATGATTGAGAAAAAATTC	Two-step protocol
I291D_rv	ACGGCTATCGCCACCACCACCAATACG	Two-step protocol

---

## 6.7 Disclosures

**Author Contributions:** Conceptualization, S.B. and R.G.B.; methodology, S.B.; validation, S.B.; formal analysis, S.B.; investigation, S.B. and F.E.; writing—original draft preparation, S.B.; writing—review and editing, R.G.B. and F.E.; visualization, S.B.; supervision, R.G.B. and F.E.; project administration, R.G.B. and F.E.; funding acquisition, R.G.B. All authors have read and agreed to the published version of the manuscript.

**Funding:** The project was supported by funds of the Federal Ministry of Food and Agriculture (BMEL) based on a decision of the Parliament of the Federal Republic of Germany via the Federal Office for Agriculture and Food (BLE) under the innovation support programme. The publication of this article was funded by the Open Access Fund of Leibniz Universität Hannover.

**Data Availability Statement:** Data is contained within the article and the Supplementary Materials.

**Acknowledgements:** The authors would like to gratefully acknowledge the assistance of Selina Quehl, Lara Mahnke and Tim A. Mast during mutagenesis and purification of the variants.

**Conflicts of Interest:** The authors declare no conflicts of interest.

## **7 Preamble to the publication “Co-Immobilization of RizA Variants with Acetate Kinase for the Production of Bioactive Arginyl Dipeptides”**

After establishing ATP regeneration (Chapter 4) and producing improved RizA variants (Chapter 6), co-immobilization was the next step towards a possible industrial application of this system. As mentioned before, immobilization of LALs had not been investigated in the scientific literature yet (Chapter 2).

In preparation for immobilization, new variants of RizA were created by combining mutations from the previous study (Chapter 6). While most combinations had no additive or synergistic effects, some combinations of two mutations improved product formation and especially specificity in comparison to the single mutation variants. Regarding the immobilization conditions, experiments showed that co-immobilization of both enzymes conferred no disadvantages in comparison to immobilizing only AckA and only small amounts of AckA were necessary. After investigation of the effect of pH and temperature on the reactions with the immobilisates, a selection of variants was immobilized. Finally, the best variants for Arg-Ser (T81F\_A158S) and Arg-Phe (K83F\_S156A) were characterized in terms of their reusability.

I conceptualized the study and all published data was generated and interpreted by me. Prof. Berger was involved in conceptualization, supervision and administration of the project and funding acquisition. Dr. Ersoy was also involved in supervision and administration of the project. Hermine Coenders worked during her bachelor thesis on the co-immobilization of RizA and AckA (Coenders, 2022) under my supervision. Tim A. Mast was involved in the creation of the variants and enzyme purifications as a student assistant. The work was published in the peer-reviewed journal *Molecules* on 7<sup>th</sup> of July 2022 as part of the Special issue “The Latest Trends in Catalyst Immobilization”.

DOI: 10.3390/molecules27144352



## 8 Co-Immobilization of RizA Variants with Acetate Kinase for the Production of Bioactive Arginyl Dipeptides

### 8.1 Abstract

The biocatalytic system comprised of RizA and acetate kinase (AckA) combines the specific synthesis of bioactive arginyl dipeptides with efficient ATP regeneration. Immobilization of this coupled enzyme system was performed and characterized in terms of activity, specificity and reusability of the immobilisates. Co-immobilization of RizA and AckA into a single immobilisate conferred no disadvantage in comparison to immobilization of only RizA, and a small addition of AckA (20:1) was sufficient for ATP regeneration. New variants of RizA were constructed by combining mutations to yield variants with increased biocatalytic activity and specificity. A selection of RizA variants were co-immobilized with AckA and used for the production of the salt-taste enhancers Arg-Ser and Arg-Ala, and the antihypertensive Arg-Phe. The best variants yielded final dipeptide concentrations of 11.3 mM Arg-Ser (T81F\_A158S) and 11.8 mM Arg-Phe (K83F\_S156A), the latter of which represents a five-fold increase in comparison to the wild type enzyme. T81F\_A158S retained more than 50 % activity for over 96 h and K83F\_S156A for over 72 h. This study provides the first example of the successful co-immobilization of an L-amino acid ligase with an ATP-regenerating enzyme and paves the way towards a bioprocess for the production of bioactive dipeptides.

**Keywords:** covalent immobilization; co-immobilization; biocatalysis; L-amino acid ligase; acetate kinase; ATP regeneration; arginyl dipeptides; salt-taste enhancer; protein engineering; antihypertensive dipeptide

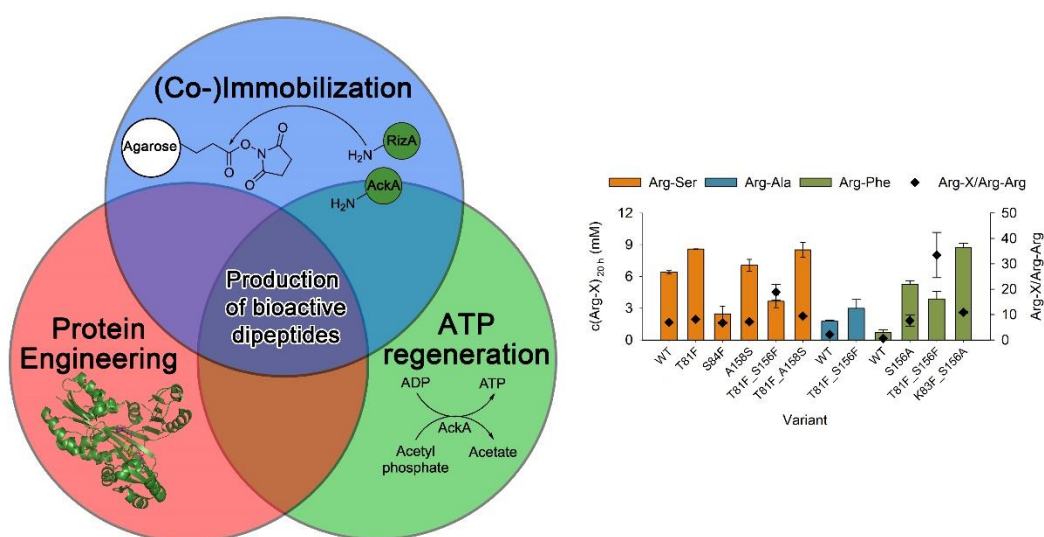


**Figure 8-1.** Graphical abstract of the publication (Bordewick et al., 2022).

## 8.2 Introduction

L-amino acid ligases (LALs; EC 6.3.2.28) are a relatively novel enzyme class that synthesizes dipeptides from their respective amino acids. They belong to the ATP-grasp superfamily and hydrolyze ATP to ADP and P<sub>i</sub> to catalyze the amide bond formation through an acyl phosphate intermediate (Wang et al., 2020). The first LAL ywfE (also called BacD) was discovered in *B. subtilis* in 2005 (Tabata et al., 2005). Since then, LALs with different specificities have been identified (Arai et al., 2013; Kino et al., 2008a; Kino et al., 2008b). The LAL RizA from *B. subtilis* NBRC3134 has a very high specificity for the synthesis of dipeptides containing an N-terminal arginine (Arg-X), many of which (e.g., Arg-Ser, Arg-Ala, Arg-Gly) have been found to have salt-taste enhancing effects (Harth et al., 2018; Kino et al., 2009; Schindler et al., 2011; Xu et al., 2017). Additionally, Arg-Phe is a potential antihypertensive (Arai et al., 2013; Kagebayashi et al., 2012). Due to the very high cost of the cofactor ATP, we previously worked on employing acetate kinase (AckA) from *E. coli* to regenerate ATP from acetyl phosphate (AcP), which is cheaply accessible through acetylation of phosphoric acid by acetic anhydride (Alissandratos et al., 2016; Crans & Whitesides, 1983). The optimized enzyme system produced up to 23 mM Arg-Ser (46 % yield) while only necessitating 0.5 mM ATP (Bordewick et al., 2021b).

Immobilization can significantly improve the economic viability of a bioprocess by increasing stability, enabling reusability and thus decreasing production costs (Sheldon, 2007). Additionally, it can also improve downstream processing through easier enzyme removal and improve enzyme properties like activity or specificity. Immobilization techniques are usually classified by the method through which a carrier is bound (Datta et al., 2013; Garcia-Galan et al., 2011; Mohamad et al., 2015; Sheldon, 2007; Yushkova et al., 2019). The strongest interaction is achieved through covalent immobilization. The induced rigidity can lead to high increases in stability (Bilal et al., 2019; Rodrigues et al., 2008), but also decreases in activity, as enzymatic mobility might be restricted or residues of the active site blocked (Garcia-Galan et al., 2011). Additionally, covalent methods often employ harsh reagents or reaction conditions that can potentially denature the protein (Ruzicka et al., 2006). One particularly mild covalent coupling method is the usage of carriers activated with esters of *N*-hydroxysuccinimide (NHS-esters). Both N-terminal amino groups and lysine residues form strong amide bonds after immobilization for one hour at near physiological pH (Kalkhof & Sinz, 2008; ThermoScientific, 2022). Recently, NHS-activated agarose was used for food-grade immobilization of asparaginase for the removal of acrylamide (Li et al., 2020a).

Agarose beads have remarkable mechanical, chemical and biological stability, which can be further improved by crosslinking (Bié et al., 2022; Zucca et al., 2016).

The co-immobilization of multiple enzymes is reminiscent of the organization of enzymes into enzyme complexes in living cells with short diffusion distances between enzymes in a reaction sequence (Bié et al., 2022; Kazenwadel et al., 2015). It is also helpful if intermediate products are unstable or inhibitory and accumulation is not wanted (Bié et al., 2022). Apart from enzyme cascades, cofactor regeneration is one of the most prominent applications. Regeneration of the electron donor NAD(P)H is a challenge for the application of many oxidoreductases. Examples include ketoreductases or xylose dehydrogenase, which were co-immobilized with glucose or alcohol dehydrogenase, respectively (Bachosz et al., 2022; Basso et al., 2022; Petrovičová et al., 2018; Plž et al., 2020). Regeneration of ATP has been described in the co-immobilization of glutathione synthetase with a polyphosphate kinase (Cui et al., 2020). Perhaps the most impressive example is the co-immobilization of a thermostable acetate kinase with a pantothenate kinase in the multi-enzymatic cascade for the production of the potential antiviral islatravir (Huffman et al., 2019). This work also sets a good example of the possibilities of integrating immobilization and protein engineering: five of the nine enzymes were engineered, and three were (co-)immobilized. Protein engineering can act as the means to prepare an enzyme for successful immobilization (*e.g.*, by improving its stability or introducing sites for immobilization like affinity tags) (Basso et al., 2022; Bernal et al., 2018).

In a previous study, variants of RizA with improved activity and specificity for the production of several dipeptides were created (Bordewick et al., 2021a). After improving the applicability of RizA for a future industrial process both by establishing ATP regeneration (Bordewick et al., 2021b) and protein engineering, co-immobilization was the next step towards this goal. Covalent immobilization using NHS-agarose was performed on both, the unmodified enzymes and a selection of RizA variants generated through a combination of mutations from the previous study to examine how these mutations would affect immobilization. Lastly, the best variants for the production of the salt-taste enhancer Arg-Ser and the antihypertensive Arg-Phe were recycled for multiple reaction cycles to investigate the reusability of the immobilisates.

### 8.3 Results and Discussion

#### 8.3.1 (Co-)Immobilization Conditions

To examine whether co-immobilizing both RizA and AckA into a single immobilisate was viable, immobilizations were set up with different amounts of RizA ranging from 0.2 to 0.8 mg and 20 mg NHS-agarose. AckA was added in a mass ratio of 5:1 (RizA:AckA). For comparison, immobilisates containing only RizA were produced analogously. Protein concentrations before and after immobilization were measured and the difference was used to calculate the coupling efficiency and determine the apparent amount of RizA immobilized on the agarose support (Figure 8-2a).

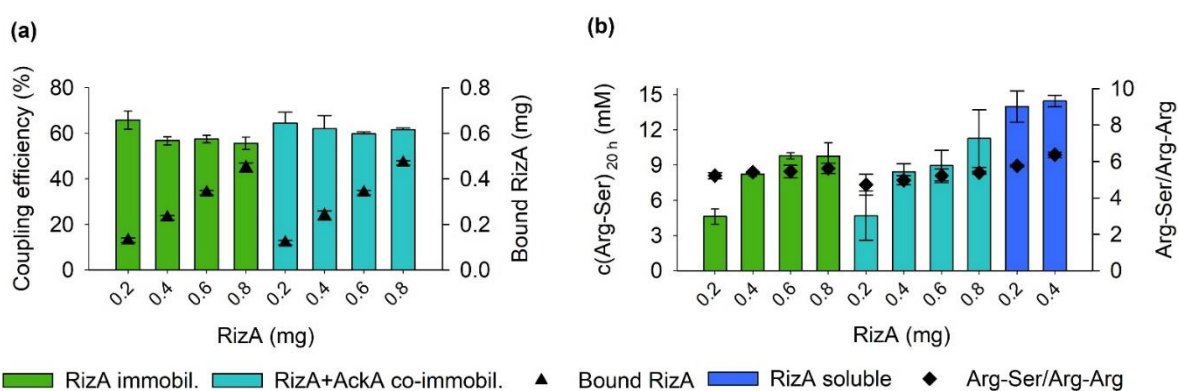


**Figure 8-2.** Immobilization of RizA in comparison to co-immobilization of RizA and AckA. (a) Coupling efficiencies and calculated amount of RizA bound to the agarose support (b) Product and side product formation in 500 µL reaction volume with 30 mM Arg and Ser after 20 h at 25 °C. Reactions were performed in duplicates with error bars representing the upper and lower value.

Coupling efficiencies were similar regardless of the applied amount of protein and ranged from 56 to 66 %. Thus, the amount of RizA bound to the support increased approximately linearly with the applied amount. Overall, the coupling efficiencies were lower than anticipated as the manufacturer states that they are “typically greater than 80 %, regardless of the ligand’s molecular weight or pI” (ThermoScientific, 2022). However, the isoelectric point (pI) of RizA was calculated to be 5.9, and acidic pIs up to 5.9 were previously identified to inhibit coupling to agarose supports using NHS-esters (Frost et al., 1981). Another possibility is that tricine, a secondary amine, in the purification/coupling buffer competed with the enzymes for coupling to the support, although both the lower basicity and steric hindrance of the amino nitrogen in tricine should generally limit this potential competition (Cline & Hanna, 1987). Lastly, there is competition between the desired aminolysis of the NHS-ester by the protein amino groups and hydrolysis by water, which can also reduce the coupling efficiency (Lim et al., 2014).

The immobilisates were used in a batch setup in reaction tubes for the biocatalytic production of Arg-Ser. The reactions with only immobilized RizA contained 0.05 mg soluble AckA. Control reactions with 0.2 and 0.4 mg soluble RizA and 0.05 mg AckA were included. After 20 h, concentrations of the product Arg-Ser and side product Arg-Arg were determined by RP-HPLC (Figure 8-2b). While the reactions with the lowest amount of RizA led to a decreased product concentration, all other immobilisates produced similar product concentrations of around 9 mM Arg-Ser. The reaction with 0.8 mg co-immobilized RizA produced 11 mM, but with a larger error bar. No substantial differences were found between immobilization of only RizA and the co-immobilization of both RizA and AckA. In comparison with the reactions with soluble RizA, the immobilisates showed a significantly lower activity since 0.2 mg (co-)immobilized RizA produced approximately 5 mM and 0.2 mg soluble RizA 14 mM Arg-Ser. Due to the incomplete coupling, part of the lower activity can be attributed to the lower actual amount of enzyme present in the reactions. However, higher enzyme amounts during the immobilization did not increase the product concentration. Decreases in activity are a known drawback of covalent immobilization techniques (Datta et al., 2013; Sheldon, 2007). Apart from denaturing during the immobilization procedure, the rigid covalent attachment can distort the enzyme structure or bind it in such an orientation that the transfer of substrates and products to and from the enzyme is limited (Garcia-Galan et al., 2011). Side product formation was similar in all reactions with specificity ratios (Arg-Ser/Arg-Arg) of approximately 6.

Next, the ratio between both enzymes was optimized. Former experiments with free RizA and AckA showed that supplying AckA in a ratio of 4 to 1 was sufficient to supply ATP for the reaction (Bordewick et al., 2021b). To examine this factor for the co-immobilized enzyme system, reactions were set up with a constant amount of 0.4 mg RizA and different mass ratios of AckA ranging from 1:1 to 20:1 (RizA:AckA). During the first two hours, samples were taken each half-hour to determine the initial activities (Figure 8-3a). The final product concentrations were measured after 20 h (Figure 8-3b).

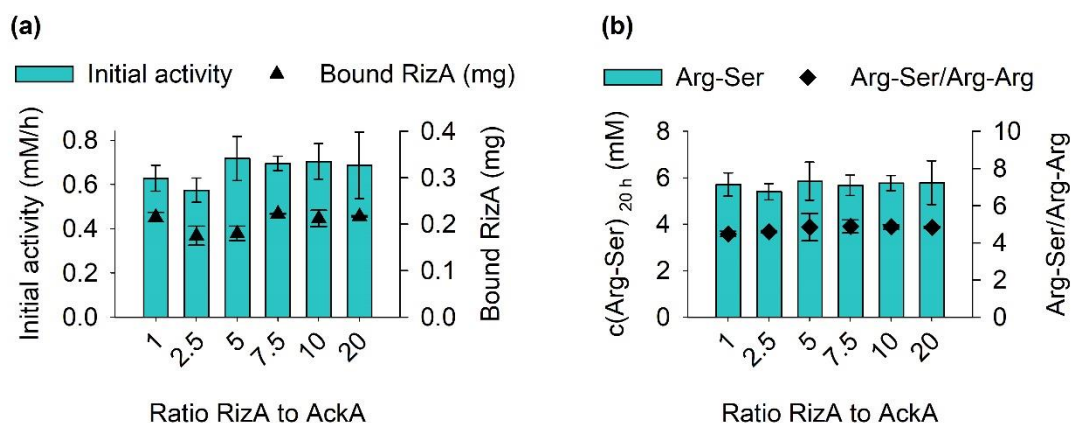


**Figure 8-3.** Effect of different ratios of RizA and AckA during co-immobilization. 0.4 mg of RizA were used, as well as a corresponding amount of AckA. Reaction conditions were identical to Figure 8-2. **(a)** Initial activities were determined in the first two hours of reaction time with linear regression. All  $R^2$  were above 0.96. **(b)** Final product and side product concentrations were determined after 20 h. Reactions were performed in duplicates with error bars representing the upper and lower value.

The two highest additions of AckA decreased the initial activities of the immobilisates slightly, possibly indicating a negative effect of the bound AckA on RizA. Overall, no large differences in product or side product formation were determined, and even the smallest addition of AckA was sufficient to drive ATP regeneration at a low ATP concentration of 0.5 mM. For all following experiments, AckA was added in a ratio of 1 to 10. While the lowest addition of 1 to 20 would be the most efficient, a higher addition was chosen to not risk limiting the cofactor supply, since the demand for ATP regeneration is dependent on the reaction conditions.

### 8.3.2 Co-Immobilization of RizA Variants

#### 8.3.2.1 Combination of Mutations to Yield Improved Variants

In a previous study, a total of 21 variants of RizA were created and characterized (Bordewick et al., 2021a). Arg-Ser formation was increased up to 41 % in T81F, while K83F/R, S84F and A158S also substantially increased it. Arg-Ala formation was increased by T81F, K83F and A158S, and also by S156A/F and D376E. The largest increase was found for S156A, which increased Arg-Phe formation by 270 % in comparison to the wild type. Additionally, Arg-Phe formation was also increased by S156F and D376E.

Here, these 8 best mutations from the previous study were combined to generate 14 new variants. For Arg-Ser, most combinations had no beneficial effect and showed lower product concentrations than the wild type (Figure 8-4a). Only T81F\_K83R and T81F\_A158S yielded higher Arg-Ser concentrations, with the last showing the highest with 12 mM. Variants also

increased specificity up to a ratio of 13 for T81F\_K83F. The highest specificity (15) was detected for T81F\_S156F, but with a slightly reduced product formation.

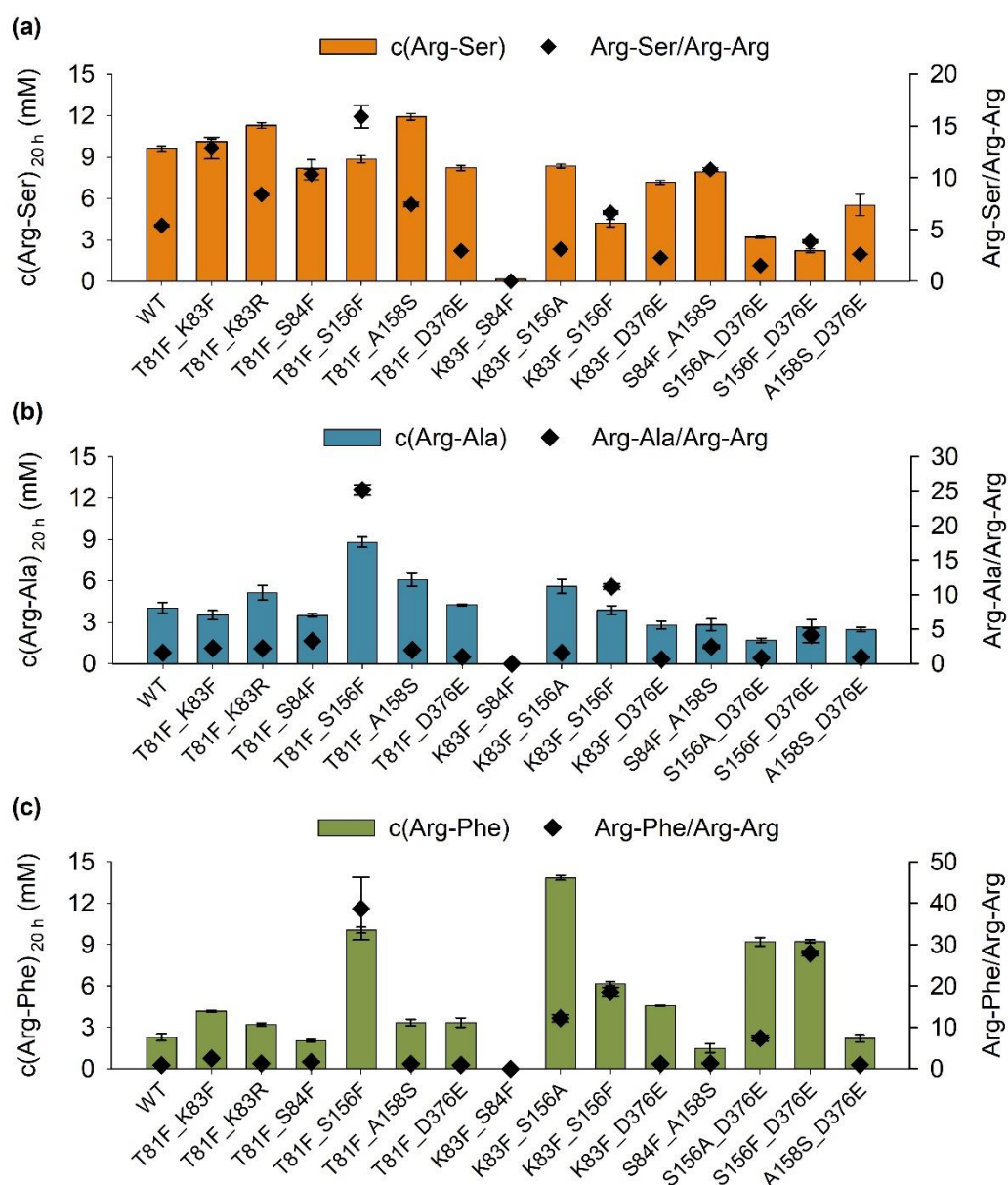


**Figure 8-4.** Production of Arg-X dipeptides by soluble variants containing two mutations. Reactions were set up in triplicates and contained 30 mM each Arg and (a) Ser, (b) Ala or (c) Phe. A total of 0.2 mg/mL RizA variant and 0.1 mg/mL AckA were used.

For Arg-Ala, T81F\_S156F also displayed the highest specificity ratio, in this case 25, along with the highest product formation of 9 mM, which was more than a two-fold increase in comparison to the wild type enzyme (Figure 8-4b). T81F\_K83R, T81F\_A158S and K83F\_S156A also increased product formation, but to a lesser degree. Combinations with D376E showed no increase in comparison to the wild type. Similar to the other two products, T81F\_S156F, led to a large increase in specificity to 39 for the production of Arg-Phe, while



also significantly increasing product formation to 10 mM (Figure 8-4c). Only K83F\_S156A generated more product (14 mM). K83F\_S156F, S156A\_D376E and S156F\_D376E also increased product formation and specificity.

Overall, most combinations of mutations had no additive effect, which is a known phenomenon and challenge in protein engineering (Reetz, 2013a). The two significant exceptions were T81F\_S156F, which increased the Arg-Ala concentration to 8.8 mM (best single variant D376E: 5.6 mM) and K83F\_S156A, which increased Arg-Phe concentration to 13.8 mM (best single variant S156A: 12.1 mM). While T81F\_A158S did not increase Arg-Ser formation over T81F, it raised the specificity ratio to 12 in comparison to 9. With the exception of D376E, all of the examined mutations were located in the binding pocket for the C-terminal substrate (Bordewick et al., 2021a). Interestingly, in most cases where combinations of mutations had a beneficial effect, the two residues were located on different loops (*e.g.*, T81F and A158S). Since increasing the number of mutations can destabilize an enzyme (Behrens et al., 2011), not accumulating too many changes in one part of the protein is likely a sound strategy. In contrast, mutation of both neighboring residues K83 and S84 to the large phenylalanine was the only example where activity was completely destroyed. While the combination of mutations did not lead to considerable increases in activity in most cases, it produced multiple variants with the highest specificities to date. While the highest specificity for a single variant was 12 (S84F for Arg-Ser), T81F\_S156F displayed specificities of up to 39 for Arg-Phe production. It was the variant with the lowest side product formation and showed the highest specificity ratios for Arg-Ser and Arg-Ala production as well.

### 8.3.2.2 Immobilization of RizA Variants

A selection of nine RizA variants from both this and the previous study were chosen based on activities and specificities. They were co-immobilized analogously to the wild type enzyme with AckA and characterized. Most variants were immobilized with a similar efficiency to the wild type, corresponding to 0.27 to 0.33 mg RizA bound to the support from an application of 0.4 mg (Figure 8-5a). S84F could only be immobilized to a reduced degree (0.22 mg). Both the initial activities (Figure 8-5a) and the final product concentrations after 20 h (Figure 8-5b) were determined.

For Arg-Ser, both T81F and T81F\_A158S showed the highest final product concentration, but T81F\_A158S had a higher initial activity and the highest specificity ratio of 9 compared to 8 for T81F and 7 for the wild type. S84F and T81F\_S156F showed the lowest Arg-Ser



formation. S84F was the variant with the second-highest product formation of Arg-Ser (Bordewick et al., 2021a), but lost the majority of its activity due to immobilization. The unusually low binding to the support also contributed to the decrease in activity. For Arg-Ala, T81F\_S156F had a similar increase in activity compared to the immobilized wild type and reached a slightly improved final product concentration of 3 mM, although with very high specificity as no Arg-Arg could be detected. Of the three dipeptides, the variants generated the strongest improvements for the production of Arg-Phe. In comparison to the wild type, the product concentration of 9 mM generated by K83F\_S156A represents a nine-fold increase with a substantial increase in specificity from 1 to 11. The highest overall specificity of 33 was also generated for Arg-Phe by T81F\_S156F and went along with an increased product concentration of 4 mM.

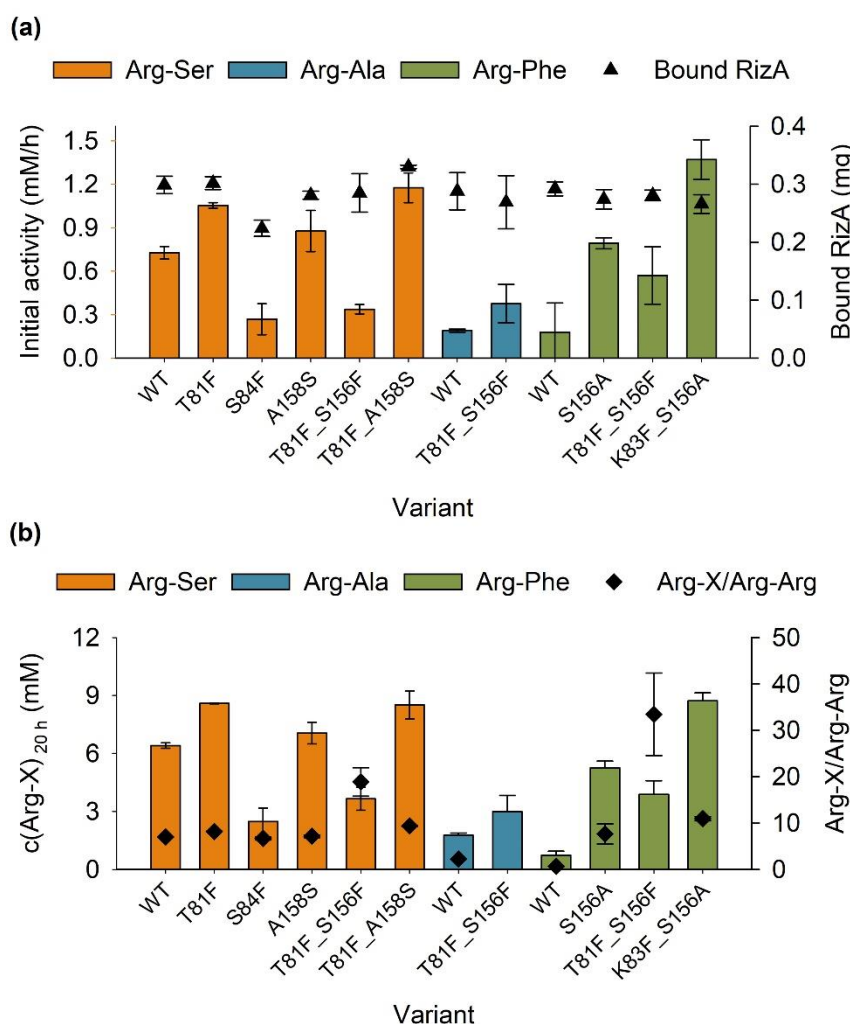


**Figure 8-5.** Co-immobilization of RizA variants. A total of 0.4 mg of RizA variant and 0.04 mg AckA were used. Reaction conditions were identical to Figure 8-2. **(a)** Initial activities were determined in the first two hours of reaction time with linear regression. All  $R^2$  were above 0.95. **(b)** Final product and side product concentrations were determined after 20 h. Reactions were performed in duplicates with error bars representing the upper and lower value.

### 8.3.3 Characterization of the Immobilisates

In a first step, reactions were performed with wild type immobilisate at different reaction temperatures and pH and characterized in terms of initial (Figure 8-6a) and final Arg-Ser product concentration (Figure 8-6b). All reaction conditions led to similar initial Arg-Ser concentrations between 1.5 and 2.3 mM after 2 h, with the reaction at 30 °C and pH 8.5 producing the highest concentration. However, after 20 h, all reactions at 25 and 30 °C yielded similar product concentrations between 6 and 7 mM, while reactions at 35 °C only contained approximately 4 mM. This was in line with the results for free RizA and AckA where 25 and 30 °C produced similar results, and 37 °C led to significantly lower product concentrations. Since 37 °C has been determined as the temperature optimum of free RizA (Kino et al., 2009), this disparity was likely related to the cofactor regeneration. Since the initial product formation at 35 °C was similar, the limitation manifested at longer reaction times. AckA was determined to be stable up to 40 °C (Nakajima et al., 1978). Hydrolysis of both ATP and AcP is known to accelerate at higher temperatures (Leibrock et al., 1995). While approximately 20 % of the latter is hydrolyzed after 5 h at 20 °C, it is hydrolyzed completely in 3 to 5 h at 60 °C (Whicher et al., 2018).

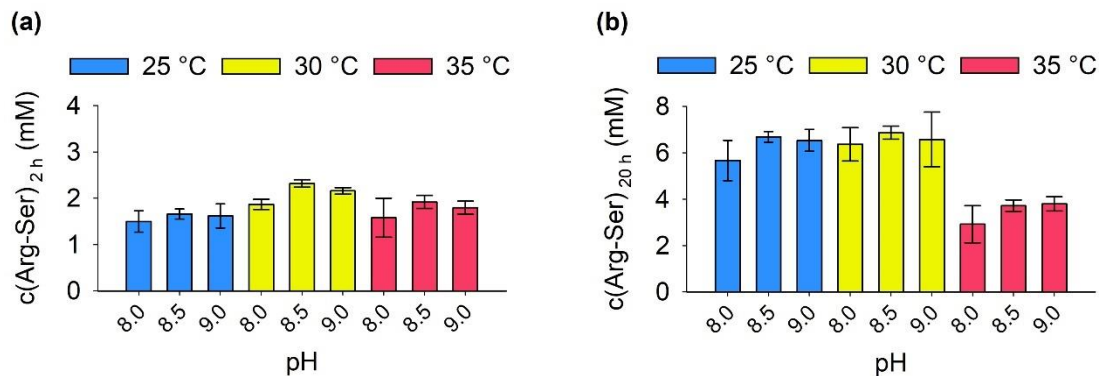


**Figure 8-6.** Effect of reaction temperature and pH. A total of 0.4 mg of RizA and 0.04 mg AckA were used for immobilization. 50 mM each Arg and Ser were used. Product concentrations were measured (a) after 2 and (b) after 20 h reaction time.

For the free enzymes, increasing the amino acid concentrations substantially improved product formation (Bordewick et al., 2021b). Here, the increase in substrate concentration to 50 mM while maintaining the applied amount of RizA at 0.4 mg did not increase product formation in the 25 °C and pH 8.5 reaction compared to the previous reactions at 30 mM under comparable reaction conditions (Figure 8-3b). In an attempt to increase the product concentration, the applied amount of RizA was increased to 0.8 mg for all following experiments.

The best variants for Arg-Ser (T81F\_A158S) and Arg-Phe production (K83F\_S156A) were selected for further characterization of the activity and reusability. Since 25 and 30 °C at pH 8.5 led to the highest product concentrations with the wild type enzyme (Figure 8-6b), both were tested. Time courses for product formation were determined (Figure 8-7a) and the reusability of the immobilisates was examined by recycling them after 24 h reaction time over a total of seven cycles (Figure 8-7b).

With the increase in both substrate concentration and enzyme amount, product concentrations of up to 11.2 mM Arg-Ser were reached by T81F\_A158S at 25 °C, while the wild type enzyme produced 10.3 mM under the same conditions (Figure 8-7a, left panel). Similar to the previous results (Figure 8-5a), T81F\_A158S displayed a substantially higher initial activity producing 6.5 mM Arg-Ser during the first four hours, while the wild type only reached 3.9 mM. After that, the differences decreased, and similar product concentrations were reached after 24 h. At 30 °C, final product concentrations after 24 h were lower with the wild type producing 7.1 mM and T81F\_A158S producing 7.7 mM Arg-Ser. At this temperature, no differences were visible in the time course of the product formation (Figure 8-7a, right panel). As expected from the previous experiments (Figure 8-5b), K83F\_S156A generated a significantly higher Arg-Phe concentration of 11.8 mM compared to the wild type with 2.3 mM. Similar to the Arg-Ser reaction, product concentrations were decreased at 30 °C.

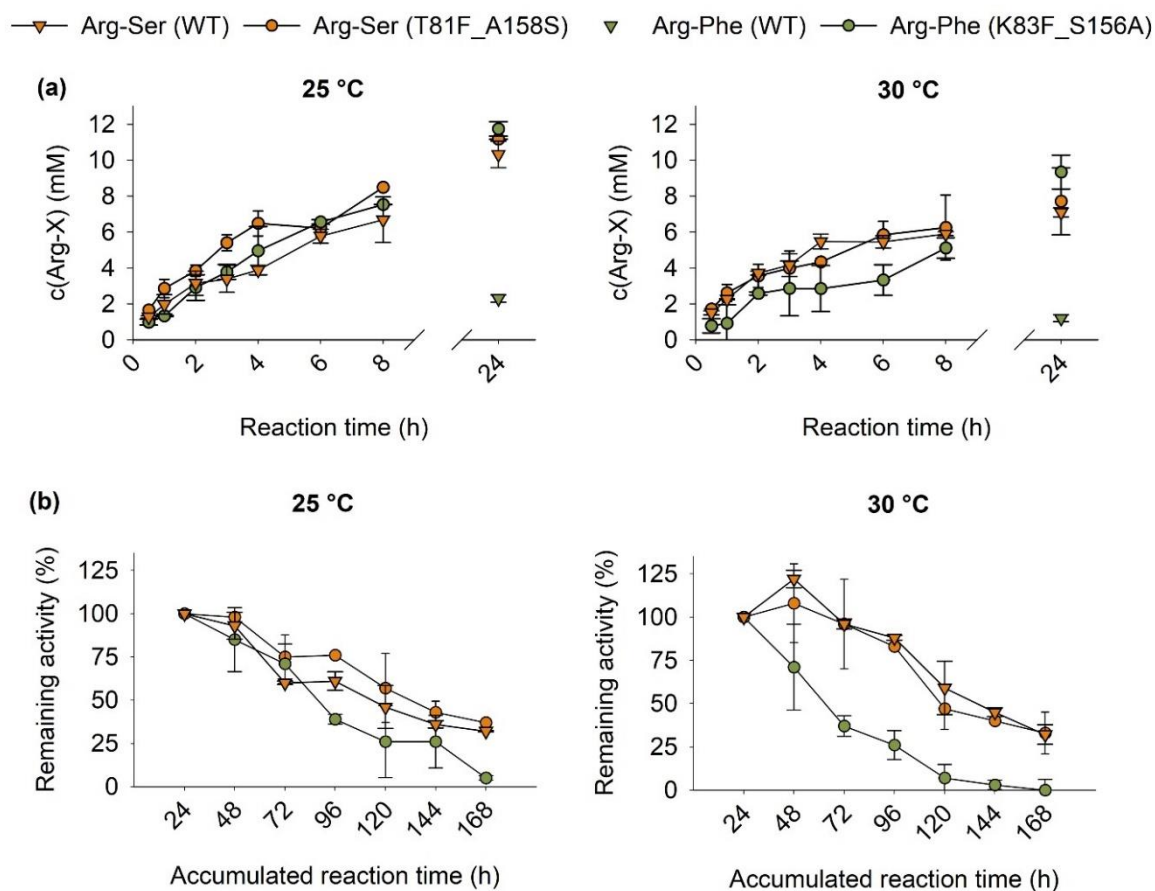


**Figure 8-7.** Effect of reaction temperature on (a) the time course of dipeptide formation and (b) reusability of the immobilisates of RizA wild type and variants. The remaining activity was calculated as the product concentration reached after an additional cycle of 24 h in comparison to that after the first cycle. A total of 0.8 mg RizA and 0.08 mg AckA were used for immobilization. 50 mM Arg and Ser were used. No time course and remaining activity could be determined for the WT producing Arg-Phe due to the low product concentrations.

Both immobilisates for Arg-Ser production retained more than 50 % activity at both temperatures for at least 96 h of accumulated reaction time, corresponding to four reaction cycles. At 25 °C, T81F\_A158S displayed a slightly higher retention of 76 % activity at 96 h compared to the 61 % of the wild type. While overall product concentrations were lower at 30 °C, both immobilisates retained a higher percentage of their activity at this temperature, with 88 % and 83 % for wild type and variant remaining after 96 h, respectively. In contrast, K83F\_S156A displayed a very sharp decline in activity at 30 °C, with only 26 % remaining after 96 h. At 25 °C, it showed a similar decrease to the Arg-Ser reactions during the first 72 h, but then sharply dropped to 39 % at 96 h. At the end of the seven cycles, all Arg-Ser immobilisates had similar remaining activities ranging from 32 to 37 %, while K83F\_S156A displayed no significant remaining activity. Apart from enzyme inactivation, there was a noticeable loss of immobilisate from cycle to cycle during washing, as evidenced by immobilisate sedimenting in the used wash buffer. The discarded immobilisate was collected,

and at the end of the seven cycles, approximately half of the immobilisate was lost from the reactions as judged by comparison of the discarded with the remaining immobilisate. For future applications, a different separation technique such as the use of small chromatography columns is thus advised. The choice of the washing buffer also had a large effect on the remaining activity as washing the immobilisates with the phosphate coupling buffer reduced activities to less than 30 % in the third cycle regardless of pH or temperature (Supporting Figure 8-1). All major results were summarized in Table 8-1.

**Table 8-1.** Comparison of the biocatalytic performances of the RizA immobilisates.

Dipeptide	Variant	Temperature (°C)	c(Arg-X) <sub>24h</sub> (mM)	c(Arg-Arg) <sub>24h</sub> (mM)	Arg-X/Arg-Arg	Yield (Arg-X) <sub>24h</sub> (%)	> 50 %activity*
Arg-Ser	Wild type	25	10.3 ± 0.8	1.9 ± 0.3	5.4 ± 1.1	21	> 96 h
		30	7.1 ± 0.2	1.1 ± 0.0	6.7 ± 0.3	14	> 120 h
	T81F_A158S	25	11.2 ± 0.0	1.6 ± 0.1	7.2 ± 0.6	22	> 120 h
		30	7.7 ± 1.9	1.0 ± 0.0	8.1 ± 0.4	15	> 96 h
Arg-Phe	Wild type	25	2.3 ± 0.2	1.5 ± 0.3	1.5 ± 0.2	5	n. d.†
		30	1.2 ± 0.3	1.1 ± 0.0	1.1 ± 0.3	2	n. d.†
	K83F_S156A	25	11.8 ± 0.4	0.7 ± 0.0	16 ± 0.2	24	> 72 h
		30	9.3 ± 0.9	0.4 ± 0.2	24 ± 15	19	> 48 h

\* Time that the immobilisates displayed more than 50 % remaining activity, † Could not be accurately determined due to overall low activity

Reactions at 25 °C led to higher final product concentrations, while 30 °C generally led to higher specificities. Both immobilisates of RizA variants showed improved performances in comparison to the wild type. In the case of Arg-Ser, this mainly constituted an increase in the initial activity (Figure 8-5a and Figure 8-7a), higher specificity and a slightly increased reusability and final product concentration at 25 °C (Table 8-1). For Arg-Phe, K83F\_S156A dramatically increased the product concentration five-fold and specificity almost ten-fold (Table 8-1). No time course was determined for Arg-Phe production of the wild type due to very low concentrations during the early reaction time. The calculation of the remaining activity also fluctuated highly and could not be interpreted. In comparison to K83F\_S156A with the Arg-Ser reactions, the reusability was significantly lower. This could be due to phenylalanine as a substrate or a decreased stability of the variant.

In comparison to the free enzymes, activities and yields of the immobilisates were reduced. For Arg-Ser, yields of up to 33 % were achieved with the wild type enzyme and up to 47 % with T81F with 30 mM substrate (Bordewick et al., 2021a). With 50 mM substrate, up to 23 mM Arg-Ser, corresponding to a yield of 46 %, were produced (Bordewick et al., 2021b). The disadvantage of lower activities was partially offset by the ability to easily separate the immobilized enzymes from the reaction and to reuse them. Thus, the cumulative product formation of the reusable immobilisates was already higher than for the free enzymes, which can only be used once. In order to improve this further, the apparent loss of activity could be addressed by exploring other immobilization supports or coupling techniques. Since both RizA and AckA were produced with a his-tag for affinity purification, the analogous affinity immobilization would be a plausible next step (Bié et al., 2022).

Apart from the reduced activity, a decline in product formation after the first eight hours of reaction time limited the yield and was a phenomenon witnessed both for the free and immobilized RizA and AckA system (Bordewick et al., 2021b). While a decrease in enzyme activity by enzyme denaturing was plausible for the free enzymes, the reusability of the immobilisates showed that this could not be the sole factor. The possible degradation of the cofactors has already been discussed above in this section. Another likely factor is accumulation and inhibition by side products of the reaction, most notably phosphate. Phosphate is produced during the reaction both through the desired hydrolysis of ATP to ADP catalyzed by the L-amino acid ligase (Kino et al., 2009), but also over time by the inevitable hydrolysis of ATP and AcP by water (Leibroek et al., 1995; Whicher et al., 2018), thus leading to the accumulation of inorganic phosphate. Apart from direct product inhibition by phosphate (Dean, 2002; Tasnádi et al., 2018), its accumulation can lead to the precipitation of magnesium phosphate (Wang & Zhang, 2009). Since both RizA and AckA require  $Mg^{2+}$  as a cofactor, this could be an additional factor limiting the yield. In the sophisticated design of the biocatalytic cascade for the synthesis of islatravir, the addition of sucrose and a sucrose phosphorylase provided the depletion of phosphate (Chen & Zhang, 2021; Huffman et al., 2019).

Since regeneration of the expensive ATP is an absolute necessity for industrial application of the whole class of L-amino acid ligases, establishing an efficient ATP regeneration was an important step (Bordewick et al., 2021b). In order to further limit the cost of enzymes and improve downstream processing, immobilization of RizA was the next step. The presented work is, to our knowledge, the first published example of an L-amino acid ligase

co-immobilized with an ATP-regenerating enzyme. While the developed immobilisates are not yet fit for practical applications due to their insufficient activities and yields, the results showed that both RizA and AckA can successfully be covalently immobilized and reused for several cycles. It is likely that both activity and stability can be improved upon in future work with different immobilization techniques. Another promising option would be to adapt the created immobilisates to a continuous flow setup, in which the reagents flow through the immobilisate producing a steady flow of products (Naramittanakul et al., 2021). While flow chemistry is an established field (Porta et al., 2016), flow biocatalysis has only begun to expand significantly in recent years (Britton et al., 2018). Advantages include less downtime of the reactor for cleaning/refilling between batches, improved mass transfer of substrates towards the immobilisate, simplified downstream processing and reduced product inhibition through continuous removal of products (Naramittanakul et al., 2021; Thompson et al., 2019). Apart from preventing the accumulation of phosphate, a continuous setup could also provide a steady stream of cofactors circumventing their discussed stability issues. Continuous systems present a challenge for cofactor regeneration as they are mono-directional and diffusion of the cofactor to and from the regenerating enzyme is severely limited (Britton et al., 2018). Co-immobilization of the regenerating enzyme addresses this issue and is likely a necessity for employing L-amino acid ligases in such a system. The employed agarose support is also well suited for flow applications (ThermoScientific, 2022; Zucca et al., 2016). We hope that this study lays the foundation for further work in this direction and the application of both this interesting enzyme class and its equally interesting products.

## 8.4 Materials & Methods

### 8.4.1 Chemicals, Reagents and Strains

Chemicals were purchased from Carl Roth (Karlsruhe, Germany) or Sigma Aldrich (Taufkirchen, Germany) if not otherwise indicated. Enzymes for molecular biology were purchased from Thermo Fisher Scientific (St. Leon-Roth, Germany). The pET28a vector was purchased from Merck KGaA (Darmstadt, Germany). The *E. coli* strains BL21 (DE3) and TOP10 were maintained in our laboratory. Oligonucleotides were synthesized by Microsynth Seqlab GmbH (Goettingen, Germany).

### 8.4.2 Mutagenesis

Mutagenesis was performed as previously described (Bordewick et al., 2021a). In short, site-specific mutations were inserted by whole-plasmid PCR with two overlapping mutagenic

primers on a construct already containing the other mutation. In the cases where neighboring codons were mutated, new primers combining both mutations (Supporting Table 8-1) were designed with the software SnapGene version 5.1.7 (2020) from GSL Biotech LLC (Chicago, IL, USA). The three-step protocol started with a denaturing step at 98 °C for 30 s and was then followed by 20 cycles of 98 °C for 10 s, the annealing temperature (Supporting Table 8-1) for 30 s, and 72 °C for 130 s. Lastly, a final extension was performed at 72 °C for 10 min, and PCR products were stored at 8 °C. In the two-step protocol (Supporting Table 8-1), the elongation step at the annealing temperature was omitted.

### 8.4.3 Production of Soluble Enzymes

RizA, its variants and AckA were recombinantly produced in *E. coli* BL21 (DE3) and purified by affinity chromatography followed by desalting through gel filtration as previously described (Bordewick et al., 2021a; Bordewick et al., 2021b).

### 8.4.4 Immobilization

Immobilization was performed using Pierce NHS-Activated Agarose from Thermo Fisher Scientific (St. Leon-Roth, Germany). Here, 20 mg NHS-agarose was used for the experiments in chapter 8.3.1, while 33 mg NHS-agarose was used for all other experiments. The respective amount of enzyme solution in coupling buffer (50 mM phosphate, 150 mM NaCl, pH 7.2) was added to the NHS-agarose in 2 mL reaction tubes and incubated with end-over-end mixing for 1 h at room temperature. Afterwards, the immobilisates were subjected to centrifugation at 1.0× g for 1 min and the supernatant was removed, which was followed by two washing steps (with intermittent centrifugation) with 800 µL desalting buffer (50 mM tricine, 100 mM NaCl, pH 8.0). Subsequently, 800 µL quenching buffer (1 M TRIS-HCl, pH 7.4) was added, followed by end-over-end mixing for 30 min. After centrifugation, the supernatant was removed, and the immobilisates were washed three times (with intermittent centrifugation) with 800 µL desalting buffer. Finally, the immobilisates were stored at 4 °C until usage. Samples of the enzyme solution added to the NHS-agarose and samples of the supernatant after the first incubation were collected to determine the coupling efficiency. Protein concentrations were determined with Bradford solution from Sigma-Aldrich (Taufkirchen, Germany).

### 8.4.5 Biocatalysis

Biocatalytic reactions with the free variants were performed as previously for comparability reasons (Bordewick et al., 2021a). Reactions using immobilisate were performed in a reaction volume of 500 µL with the designated amino acid concentrations, equimolar amounts of



acetyl phosphate, 7.5 mM MgSO<sub>4</sub> and 0.5 mM ATP. In the cases where RizA or AckA were not (co-)immobilized, the designated amounts of soluble enzyme were added. Reactions were performed on a Thermomixer comfort from Eppendorf SE (Hamburg, Germany) and incubated at the designated reaction temperature and 1200 rpm. Samples were taken at the designated times and inactivated for 5 min at 70 °C in a Biometra thermal cycler from Analytik Jena (Jena, Germany) and stored at -20 °C until analysis. The immobilisates were recycled by removing the old reaction solution after centrifugation followed by two washing steps with 800 µL desalting buffer. After removing the last washing solution, the immobilisate was used again.

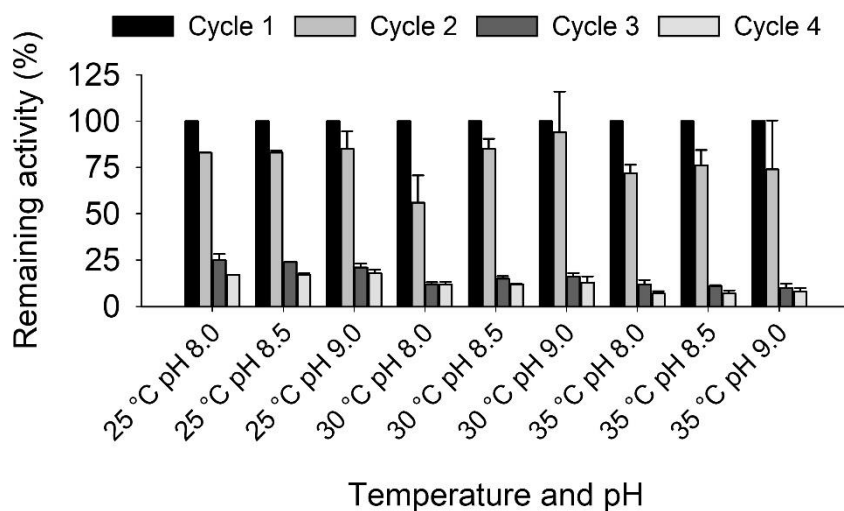
#### 8.4.6 Analysis

Product and side product analysis was performed as previously described by RP-HPLC with pre-column derivatization using *o*-phthalaldehyde and fluorescence detection of the dipeptide derivatives (Bordewick et al., 2021a; Bordewick et al., 2021b; Rottmann et al., 2021). Data were visualized with SigmaPlot 14.5 (2020) from Systat Software GmbH (Erkrath, Germany).

#### 8.5 Conclusions

New variants of RizA were created through the combination of the best single mutations from a former study to improve the enzyme's activity and specificity. Both the RizA wild type enzyme and a selection of seven variants were successfully co-immobilized with AckA for ATP regeneration. Immobilisates of the two variants with the highest activities for the production of Arg-Ser (T81F\_A158S) and Arg-Phe (K83F\_S156A) retained more than 50 % activity for at least 96 and 72 h, respectively. The variant for Arg-Phe also significantly increased product concentration and specificity by factors of 5 and nearly 10, respectively, in comparison to the wild type enzyme.

## 8.6 Supplementary Materials



**Supporting Figure 8-1.** Reusability of the immobilisates when using coupling buffer for washing. The remaining activity was calculated as the product concentration reached after an additional cycle of 24 h in comparison to that after the first cycle. 0.4 mg of RizA and 0.04 mg AckA were used for immobilization. 50 mM of Arg and Ser were used.

**Supporting Table 8-1.** Primer pairs for mutagenesis. The given annealing temperatures are for the three-step protocol, in the two-step protocol annealing and elongation were both performed at 72 °C (see Materials & Methods).

Name	Sequence (5'→3')	Annealing temperature (°C)
T81F_K83F fw	TTTGAATTTAGCATTCTGACCGGTGGTTTTTC	64.4
T81F_K83F rv	AATGCTAAATTCAAAGGTGCTAACAATATG	64.4
T81F_K83R fw	TTTGAACGTAGCATTCTGACCGGTG	64.7
T81F_K83R rv	AATGCTACGTTCAAAGGTGCTAAC	64.7
T81F_S84F fw	GAAAAATTTATTCTGACCGGTGGTTTTCTGCG	65.5
T81F_S84F rv	CAGAATAAATTTTTCAAAGGTGCTAACAATATGATC	65.5
K83F_S84F fw	GAATTTTTTCATTCTGACCGGTGGTTTTCTGCG	Two-step protocol
K83F_S84F rv	CAGAATGAAAAATTCGGTGGTGCTAACAATATGATC	Two-step protocol

## 8.7 Disclosures

**Author Contributions:** Conceptualization, S.B. and R.G.B.; methodology, S.B. and F.E.; validation, S.B.; formal analysis, S.B.; investigation, S.B.; writing—original draft preparation, S.B.; writing—review and editing, R.G.B. and F.E.; visualization, S.B.;

supervision, R.G.B. and F.E.; project administration, R.G.B. and F.E.; funding acquisition, R.G.B. All authors have read and agreed to the published version of the manuscript.

**Funding:** The project was supported by funds from the Federal Ministry of Food and Agriculture (BMEL) based on a decision of the Parliament of the Federal Republic of Germany via the Federal Office for Agriculture and Food (BLE) under the innovation support program. The publication of this article was funded by the Open Access Fund of Leibniz Universität Hannover.

**Data Availability Statement:** Data are contained within the article and the Supplementary Materials.

**Acknowledgments:** The authors would like to gratefully acknowledge the assistance of Hermine Coenders with immobilization and Tim A. Mast with mutagenesis and purification of the variants.

**Conflicts of Interest:** The authors declare no conflicts of interest.

## 9 Conclusion and Outlook

In this thesis, three strategies for the engineering of biocatalytic reactions (Chapter 1.1.2) were applied for the production of bioactive dipeptides: ATP regeneration through coupling with a second enzyme, protein engineering to improve the activity and specificity of the LAL, and finally co-immobilization of the improved variants with the ATP-regenerating enzyme in order to reuse the enzymes.

Without regeneration, ATP concentrations equimolar to the substrate were usually used in literature (see references in Table 1-4). Therefore, only a maximum of approximately 0.5 g Arg-Ser can be produced per gram of ATP assuming total conversion. Due to the incomplete conversion and background hydrolysis of ATP, even less of ATP was effectively used for the formation of the desired product. Another issue that was discovered during the work on hand was a strong inhibition of RizA by ATP that drastically reduces enzyme activity in the presence of ATP concentrations over 5 mM (Chapter 4.3.2 and Supporting Figure 4-1). Using ATP regeneration, a low ATP concentration of 0.5 mM was sufficient for a reaction with 50 mM substrates and a yield of 41 %, corresponding to 23 g Arg-Ser per gram ATP. ATP regeneration by acetate kinase was a highly effective strategy for RizA and further work could explore application of this strategy to other LALs. It would be interesting to examine if ATP regeneration for other LALs is as efficient as for RizA. The fact that a steady-state supply of 0.5 mM ATP or less was sufficient for RizA suggests a high affinity of RizA for the cofactor. Apparent  $K_m$  values for ATP as a measure for substrate affinity have been determined for some LALs and were 0.1 mM for YwfE (Tabata et al., 2005), 0.5 mM for RSp1486a (Kino et al., 2008a) and 2.5 mM TabS (Arai et al., 2013). Due to the possible advantages of regeneration from polyphosphate (Chapter 1.1.3), examining a PPK-based regeneration strategy would also be a worthwhile endeavor.

Protein engineering of RizA was successful in improving yields and specificity for Arg-Ser and Arg-Ala production and dramatically improved these for production of Arg-Phe (Chapters 6 and 8). However, production of the strongest Arg-X salt-taste enhancer Arg-Pro was not possible. The inability of RizA to accept proline was already discussed in its original publication (Kino et al., 2009) and remains an interesting engineering target. In addition to the wild type, none of the 35 variants (both with one and two mutations) from this thesis were able to produce Arg-Pro (data not shown). The likely reason is that proline contains a secondary instead of a primary amino group like all other amino acids. The only published example of an LAL incorporating proline as the C-terminal amino acid was TabS, for which

formation of Pro-Pro and Gly-Pro was detected; however, no concentrations were determined (Kino et al., 2016).

All engineering studies on LALs so far have been restricted to mutating distinct amino acids. Due to the potential of directed evolution and focused directed evolution approaches (Chapter 1.1.2), these constitute unexplored potential for this enzyme class. The main bottleneck for attempting these approaches is the availability of suitable assays. Screening a large library with the HPLC analysis used in this thesis is not feasible due to the relatively long analysis time of 30 min and associated costs for HPLC-grade solvents. Similar methods using derivatization followed by HPLC analysis are the most widely used strategy for the analysis of LAL reactions (see references in Table 1-4). Another is an assay based on the colorimetric detection of phosphate formed due to ATP hydrolysis, for example by using malachite green (Carter & Karl, 1982; Feng et al., 2011). While this assay can be performed in microtiter plates, the indirect nature of the assay cannot screen for the formation of a specific dipeptide. When two amino acids X and Y are given, it cannot differentiate between formation of X-X, Y-Y, X-Y, Y-X or even a simple phosphatase activity without dipeptide formation. In addition to this “total dipeptide” formation, background ATP hydrolysis also results in a signal, therefore an additional blank reaction needs to be included, thus doubling the number of assay reactions.

The assay used for the discovery of RizA provides an interesting strategy for assaying the N-terminal specificity of LALs (Chapter 1.3.2). If only the desired N-terminal amino acid X is present in the reaction, formation and colorimetric detection of the “X hydroxamate” could be used to identify variants for the formation of these “X N-terminal” dipeptides. This approach could be combined with screening by phosphate depletion to yield candidates for the desired dipeptides, which could then be investigated further by methods like HPLC. Creation of “smart” libraries could significantly increase the chance of producing the desired variants, by restricting mutagenesis of a CAST or ISM approach to the N- or C-terminal substrate binding pocket (Chapter 1.1.2).

An interesting area of study could be the usage of non-proteinogenic amino acids. Examples like the production of bacilysin by YwfE or rhizoctin A by RizA show that non-proteinogenic amino acids can be incorporated using LALs, which further expands the potential diversity of dipeptides and their bioactivities (Chapter 1.2.1). Due to the high promiscuity of RizA for its C-terminal substrate, the usage of other C-terminal substrates should be possible. Another possibility would be to examine if substrates similar to arginine

like ornithine, citrulline or homocitrulline were accepted as N-terminal substrates. The variant library created in this thesis could be screened for these purposes.

Finally, the third part of the thesis showed that a biocatalytic system, comprised of AckA for ATP regeneration and variants of RizA improved by protein engineering, was successfully co-immobilized and could be reused. The limitations of this approach, namely enzyme inactivation by the covalent immobilization and likely limitation of the yield by phosphate accumulation were discussed in Chapter 8.3 alongside possible solutions. If an immobilization strategy could be identified that further improved stability and reusability of the immobilisates, without causing such a significant decrease in activity, and the limitation of the yield could be remedied towards (near) complete conversion, this system would provide a very specific and efficient method to produce arginyl dipeptides. Finally, the next steps towards industrial application would be upscaling of the reaction and establishing downstream processing of the reaction mixture to yield the pure dipeptides.

## 10 References

- Albers, S., Wernerman, J., Stehle, P., Vinnars, E., & Fürst, P. (1988). Availability of amino acids supplied intravenously in healthy man as synthetic dipeptides: Kinetic evaluation of L-alanyl-L-glutamine and glycyl-L-tyrosine. *Clin. Sci.*, *75*(5), 463-468.
- Alissandratos, A., Caron, K., Loan, T. D., Hennessy, J. E., & Easton, C. J. (2016). ATP Recycling with Cell Lysate for Enzyme-Catalyzed Chemical Synthesis, Protein Expression and PCR. *ACS Chem. Biol.*, *11*(12), 3289-3293.
- Anderson, C. A. M., Appel, L. J., Okuda, N., Brown, I. J., Chan, Q., Zhao, L., Ueshima, H., Kesteloot, H., Miura, K., Curb, J. D., Yoshita, K., Elliott, P., Yamamoto, M. E., & Stamler, J. (2010). Dietary Sources of Sodium in China, Japan, the United Kingdom, and the United States, Women and Men Aged 40 to 59 Years: The INTERMAP Study. *J. Am. Diet. Assoc.*, *110*(5), 736-745.
- Andexer, J. N., & Richter, M. (2015). Emerging Enzymes for ATP Regeneration in Biocatalytic Processes. *ChemBioChem*, *16*(3), 380-386.
- Ano, Y., Ayabe, T., Ohya, R., Kondo, K., Kitaoka, S., & Furuyashiki, T. (2019a). Tryptophan-Tyrosine Dipeptide, the Core Sequence of  $\beta$ -Lactolin, Improves Memory by Modulating the Dopamine System. *Nutrients*, *11*(2), 348.
- Ano, Y., Kita, M., Kitaoka, S., & Furuyashiki, T. (2019b). Leucine–Histidine Dipeptide Attenuates Microglial Activation and Emotional Disturbances Induced by Brain Inflammation and Repeated Social Defeat Stress. *Nutrients*, *11*(9), 2161.
- Ano, Y., Yoshino, Y., Uchida, K., & Nakayama, H. (2019c). Preventive Effects of Tryptophan–Methionine Dipeptide on Neural Inflammation and Alzheimer’s Pathology. *Int. J. Mol. Sci.*, *20*(13), 3206.
- Apostolopoulos, V., Bojarska, J., Chai, T.-T., Elnagdy, S., Kaczmarek, K., Matsoukas, J., New, R., Parang, K., Lopez, O. P., Parhiz, H., Perera, C. O., Pickholz, M., Remko, M., Saviano, M., Skwarczynski, M., Tang, Y., Wolf, W. M., Yoshiya, T., Zabrocki, J., Zielenkiewicz, P., AlKhazindar, M., Barriga, V., Kelaidonis, K., Sarasia, E. M., & Toth, I. (2021). A Global Review on Short Peptides: Frontiers and Perspectives. *Molecules*, *26*(2), 430.
- Arai, T., & Kino, K. (2008). A Novel L-Amino Acid Ligase Is Encoded by a Gene in the Phaseolotoxin Biosynthetic Gene Cluster from *Pseudomonas syringae* pv. *phaseolicola* 1448A. *Biosci. Biotechnol. Biochem.*, *72*(11), 3048-3050.
- Arai, T., Arimura, Y., Ishikura, S., & Kino, K. (2013). L-Amino Acid Ligase from *Pseudomonas syringae* Producing Tabtoxin Can Be Used for Enzymatic Synthesis of Various Functional Peptides. *Appl. Environ. Microbiol.*, *79*(16), 5023-5029.
- Arnold, F. H. (2018). Directed Evolution: Bringing New Chemistry to Life. *Angew. Chem. Int. Ed.*, *57*(16), 4143-4148.
- Aso, K., Kodaka, H., Fukushi, H., & Lee, H.-H. (1992). Trypsin-catalyzed synthesis of the arginyl-arginine dipeptide from L-arginine ethyl ester. *Biotechnol. Lett.*, *14*(6), 451-454.
- Bachosz, K., Piasecki, A., Zdarta, A., Kaczorek, E., Pinelo, M., Zdarta, J., & Jesionowski, T. (2022). Enzymatic membrane reactor in xylose bioconversion with simultaneous cofactor regeneration. *Bioorg. Chem.*, *123*, 105781.
- Basso, A., Brown, M. S., Cruz-Izquierdo, A., Martinez, C. A., & Serban, S. (2022). Optimization of Metal Affinity Ketoreductase Immobilization for Application in Batch and Flow Processes. *Org. Process Res. Dev.*
- Behrens, G. A., Hummel, A., Padhi, S. K., Schätzle, S., & Bornscheuer, U. T. (2011). Discovery and Protein Engineering of Biocatalysts for Organic Synthesis. *Adv. Synth. Catal.*, *353*(13), 2191-2215.

- Beier, A., Bordewick, S., Genz, M., Schmidt, S., van den Bergh, T., Peters, C., Joosten, H.-J., & Bornscheuer, U. T. (2016). Switch in Cofactor Specificity of a Baeyer–Villiger Monooxygenase. *ChemBioChem*, *17*(24), 2312-2315.
- Bell, E. L., Finnigan, W., France, S. P., Green, A. P., Hayes, M. A., Hepworth, L. J., Lovelock, S. L., Niikura, H., Osuna, S., Romero, E., Ryan, K. S., Turner, N. J., & Flitsch, S. L. (2021). Biocatalysis. *Nat. Rev. Methods Primers*, *1*(1), 46.
- Bernal, C., Rodríguez, K., & Martínez, R. (2018). Integrating enzyme immobilization and protein engineering: An alternative path for the development of novel and improved industrial biocatalysts. *Biotechnol. Adv.*, *36*(5), 1470-1480.
- Bhat, S., Marklund, M., Henry, M. E., Appel, L. J., Croft, K. D., Neal, B., & Wu, J. H. Y. (2020). A Systematic Review of the Sources of Dietary Salt Around the World. *Adv. Nutr.*, *11*(3), 677-686.
- Bié, J., Sepodes, B., Fernandes, P. C. B., & Ribeiro, M. H. L. (2022). Enzyme Immobilization and Co-Immobilization: Main Framework, Advances and Some Applications. *Processes*, *10*(3), 494.
- Bilal, M., Asgher, M., Cheng, H., Yan, Y., & Iqbal, H. M. N. (2019). Multi-point enzyme immobilization, surface chemistry, and novel platforms: a paradigm shift in biocatalyst design. *Crit. Rev. Biotechnol.*, *39*(2), 202-219.
- Bilal, M., & Iqbal, H. M. N. (2019). Tailoring Multipurpose Biocatalysts via Protein Engineering Approaches: A Review. *Catal. Lett.*, *149*(8), 2204-2217.
- Bordewick, S., Berger, R. G., & Ersoy, F. (2021a). Mutagenesis of the L-Amino Acid Ligase RizA Increased the Production of Bioactive Dipeptides. *Catalysts*, *11*(11), 1385.
- Bordewick, S., Mast, T. A., Berger, R. G., & Ersoy, F. (2021b). Recombinant Production of Arginyl Dipeptides by L-Amino Acid Ligase RizA Coupled with ATP Regeneration. *Catalysts*, *11*(11), 1290.
- Bordewick, S., Berger, R. G., & Ersoy, F. (2022). Co-Immobilization of RizA Variants with Acetate Kinase for the Production of Bioactive Arginyl Dipeptides. *Molecules*, *27*(14), 4352.
- Bornscheuer, U. T., & Buchholz, K. (2005). Highlights in Biocatalysis – Historical Landmarks and Current Trends. *Eng. Life Sci.*, *5*(4), 309-323.
- Bornscheuer, U. T., Huisman, G. W., Kazlauskas, R. J., Lutz, S., Moore, J. C., & Robins, K. (2012). Engineering the third wave of biocatalysis. *Nature*, *485*(7397), 185-194.
- Bornscheuer, U. T., Hauer, B., Jaeger, K. E., & Schwaneberg, U. (2019). Directed Evolution Empowered Redesign of Natural Proteins for the Sustainable Production of Chemicals and Pharmaceuticals. *Angew. Chem. Int. Ed.*, *58*(1), 36-40.
- Breslin, P. A. S., & Beauchamp, G. K. (1997). Salt enhances flavour by suppressing bitterness. *Nature*, *387*(6633), 563-563.
- Britton, J., Majumdar, S., & Weiss, G. A. (2018). Continuous flow biocatalysis. *Chem. Soc. Rev.*, *47*(15), 5891-5918.
- Buchholz, K., & Collins, J. (2013). The roots—a short history of industrial microbiology and biotechnology. *Appl. Microbiol. Biotechnol.*, *97*(9), 3747-3762.
- Buchner, E. (1897). Alkoholische Gärung ohne Hefezellen. *Ber. Dtsch. Chem. Ges.*, *30*(1), 117-124.
- Burgener, S., Luo, S., McLean, R., Miller, T. E., & Erb, T. J. (2020). A roadmap towards integrated catalytic systems of the future. *Nat. Catal.*, *3*(3), 186-192.
- Carter, S. G., & Karl, D. W. (1982). Inorganic phosphate assay with malachite green: An improvement and evaluation. *J. Biochem. Biophys. Methods*, *7*(1), 7-13.
- Chen, H., & Zhang, Y.-H. P. J. (2021). Enzymatic regeneration and conservation of ATP: challenges and opportunities. *Crit. Rev. Biotechnol.*, *41*(1), 16-33.



- Choi, J.-M., Han, S.-S., & Kim, H.-S. (2015). Industrial applications of enzyme biocatalysis: Current status and future aspects. *Biotechnol. Adv.*, *33*(7), 1443-1454.
- Cline, G. W., & Hanna, S. B. (1987). The aminolysis of N-hydroxysuccinimide esters. A structure-reactivity study. *J. Am. Chem. Soc.*, *109*(10), 3087-3091.
- Coenders, H. (2022). *Immobilisierung der L-Aminosäureligase RizA* [Bachelor thesis, Leibniz Universität Hannover].
- Crans, D. C., & Whitesides, G. M. (1983). A convenient synthesis of disodium acetyl phosphate for use in *in situ* ATP cofactor regeneration. *J. Org. Chem.*, *48*(18), 3130-3132.
- Cui, C., Ming, H., Li, L., Li, M., Gao, J., Han, T., & Wang, Y. (2020). Fabrication of an *in-situ* co-immobilized enzyme in mesoporous silica for synthesizing GSH with ATP regeneration. *Mol. Catal.*, *486*, 110870.
- Datta, S., Christena, L. R., & Rajaram, Y. R. S. (2013). Enzyme immobilization: an overview on techniques and support materials. *3 Biotech*, *3*(1), 1-9.
- Dean, R. L. (2002). Kinetic studies with alkaline phosphatase in the presence and absence of inhibitors and divalent cations. *Biochem. Mol. Biol. Educ.*, *30*(6), 401-407.
- Demirjian, D. C., Moris-Varas, F., & Cassidy, C. S. (2001). Enzymes from extremophiles. *Curr. Opin. Chem. Biol.*, *5*(2), 144-151.
- Desai, A. A. (2011). Sitagliptin Manufacture: A Compelling Tale of Green Chemistry, Process Intensification, and Industrial Asymmetric Catalysis. *Angew. Chem. Int. Ed.*, *50*(9), 1974-1976.
- Desmond, E. (2006). Reducing salt: A challenge for the meat industry. *Meat Sci.*, *74*(1), 188-196.
- Doel, M. T., Eaton, M., Cook, E. A., Lewis, H., Patel, T., & Carey, N. H. (1980). The expression in *E. coli* of synthetic repeating polymeric genes coding for poly(L-aspartyl-L-phenylalanine). *Nucleic Acids Res.*, *8*(20), 4575-4592.
- El-Ashram, S., Al Nasr, I., & Suo, X. (2016). Nucleic acid protocols: Extraction and optimization. *Biotechnol. Rep.*, *12*, 33-39.
- Elleuche, S., Schröder, C., Sahm, K., & Antranikian, G. (2014). Extremozymes—biocatalysts with unique properties from extremophilic microorganisms. *Curr. Opin. Biotechnol.*, *29*, 116-123.
- Feng, J., Chen, Y., Pu, J., Yang, X., Zhang, C., Zhu, S., Zhao, Y., Yuan, Y., Yuan, H., & Liao, F. (2011). An improved malachite green assay of phosphate: Mechanism and application. *Anal. Biochem.*, *409*(1), 144-149.
- Finnigan, W., Hepworth, L. J., Flitsch, S. L., & Turner, N. J. (2021). RetroBioCat as a computer-aided synthesis planning tool for biocatalytic reactions and cascades. *Nat. Catal.*, *4*(2), 98-104.
- Fiske, C. H., & Subbarow, Y. (1929). Phosphorus Compounds of Muscle and Liver. *Science*, *70*(1816), 381-382.
- Frost, R. G., Monthony, J. F., Engelhorn, S. C., & Siebert, C. J. (1981). Covalent immobilization of proteins to N-hydroxysuccinimide ester derivatives of agarose: Effect of protein charge on immobilization. *Biochim. Biophys. Acta Proteins Proteom*, *670*(2), 163-169.
- Fürst, P., Pogan, K., & Stehle, P. (1997). Glutamine dipeptides in clinical nutrition. *Nutrition*, *13*(7), 731-737.
- Fürst, P. (2001). New Developments in Glutamine Delivery. *J. Nutr.*, *131*(9), 2562S-2568S.
- Galperin, M. Y., & Koonin, E. V. (1997). A diverse superfamily of enzymes with ATP-dependent carboxylate-amine/thiol ligase activity. *Protein Sci.*, *6*(12), 2639-2643.

- Gao, D., Song, W., Wu, J., Guo, L., Gao, C., Liu, J., Chen, X., & Liu, L. (2022). Efficient Production of L-homophenylalanine by Enzymatic–Chemical Cascade Catalysis. *Angew. Chem. Int. Ed.*
- Garcia-Galan, C., Berenguer-Murcia, Á., Fernandez-Lafuente, R., & Rodrigues, R. C. (2011). Potential of Different Enzyme Immobilization Strategies to Improve Enzyme Performance. *Adv. Synth. Catal.*, 353(16), 2885-2904.
- Garofalo, C., Borrelli, S., Provenzano, M., De Stefano, T., Vita, C., Chiodini, P., Minutolo, R., Nicola, L. D., & Conte, G. (2018). Dietary Salt Restriction in Chronic Kidney Disease: A Meta-Analysis of Randomized Clinical Trials. *Nutrients*, 10(6), 732.
- Gavrilescu, M., & Chisti, Y. (2005). Biotechnology—a sustainable alternative for chemical industry. *Biotechnol. Adv.*, 23(7), 471-499.
- Gill, I., López-Fandiño, R., Jorba, X., & Vulfson, E. N. (1996). Biologically active peptides and enzymatic approaches to their production. *Enzyme Microb. Technol.*, 18(3), 162-183.
- Graudal, N. A., Hubeck-Graudal, T., & Jurgens, G. (2020). Effects of low sodium diet versus high sodium diet on blood pressure, renin, aldosterone, catecholamines, cholesterol, and triglyceride. *Cochrane Database Syst. Rev.*(12).
- Guzmán, F., Barberis, S., & Illanes, A. (2007). Peptide synthesis: chemical or enzymatic. *Electron. J. Biotechnol.*, 10, 279-314.
- Harth, L., Krah, U., Linke, D., Dunkel, A., Hofmann, T., & Berger, R. G. (2018). Salt Taste Enhancing L-Arginyl Dipeptides from Casein and Lysozyme Released by Peptidases of Basidiomycota. *J. Agric. Food Chem.*, 66(10), 2344-2353.
- Hashimoto, S.-i., Ikeda, H., & Yagasaki, M. (2006). *Process for producing dipeptides or dipeptide derivatives* (United States Patent No. US8257943B2).
- He, F. J., & MacGregor, G. A. (2002). Effect of modest salt reduction on blood pressure: a meta-analysis of randomized trials. Implications for public health. *J. Hum. Hypertens.*, 16(11), 761-770.
- He, F. J., & MacGregor, G. A. (2009). A comprehensive review on salt and health and current experience of worldwide salt reduction programmes. *J. Hum. Hypertens.*, 23(6), 363-384.
- He, F. J., Li, J., & MacGregor, G. A. (2013). Effect of longer term modest salt reduction on blood pressure: Cochrane systematic review and meta-analysis of randomised trials. *BMJ*, 346, f1325.
- Heres, A., Yokoyama, I., Gallego, M., Toldrá, F., Arihara, K., & Mora, L. (2021). Antihypertensive potential of sweet Ala-Ala dipeptide and its quantitation in dry-cured ham at different processing conditions. *J. Funct. Foods*, 87, 104818.
- Hirao, Y., Mihara, Y., Kira, I., Abe, I., & Yokozeki, K. (2013). Enzymatic Production of L-Alanyl-L-glutamine by Recombinant *E. coli* Expressing  $\alpha$ -Amino Acid Ester Acyltransferase from *Sphingobacterium siyangensis*. *Biosci. Biotechnol. Biochem.*, 77(3), 618-623.
- Huang, C., & Yin, Z. (2020). Highly Efficient Synthesis of Glutathione via a Genetic Engineering Enzymatic Method Coupled with Yeast ATP Generation. *Catalysts*, 10(1), 33.
- Huffman, M. A., Fryszkowska, A., Alvizo, O., Borra-Garske, M., Campos, K. R., Canada, K. A., Devine, P. N., Duan, D., Forstater, J. H., Grosser, S. T., Halsey, H. M., Hughes, G. J., Jo, J., Joyce, L. A., Kolev, J. N., Liang, J., Maloney, K. M., Mann, B. F., Marshall, N. M., McLaughlin, M., Moore, J. C., Murphy, G. S., Nawrat, C. C., Nazor, J., Novick, S., Patel, N. R., Rodriguez-Granillo, A., Robaire, S. A., Sherer, E. C., Truppo, M. D., Whittaker, A. M., Verma, D., Xiao, L., Xu, Y., & Yang, H. (2019).

- Design of an in vitro biocatalytic cascade for the manufacture of islatravir. *Science*, 366(6470), 1255-1259.
- Huisman, G. W., & Collier, S. J. (2013). On the development of new biocatalytic processes for practical pharmaceutical synthesis. *Curr. Opin. Chem. Biol.*, 17(2), 284-292.
- Isowa, Y., Ohmori, M., Ichikawa, T., Mori, K., Nonaka, Y., Kihara, K.-i., Oyama, K., Satoh, H., & Nishimura, S. (1979). The thermolysin-catalyzed condensation reactions of n-substituted aspartic and glutamic acids with phenylalanine alkyl esters. *Tetrahedron Lett.*, 20(28), 2611-2612.
- Iwatani, S., & Yamamoto, N. (2019). Functional food products in Japan: A review. *Food Sci. Hum. Wellness*, 8(2), 96-101.
- Jaenicke, L. (2007). Centenary of the Award of a Nobel Prize to Eduard Buchner, the Father of Biochemistry in a Test Tube and Thus of Experimental Molecular Bioscience. *Angew. Chem. Int. Ed.*, 46(36), 6776-6782.
- Jia, Y., & Li, J. (2019). Reconstitution of FoF1-ATPase-based biomimetic systems. *Nat. Rev. Chem.*, 3(6), 361-374.
- Jiang, X., Chen, W., Liu, X., Wang, Z., Liu, Y., Felder, R. A., Gildea, J. J., Jose, P. A., Qin, C., & Yang, Z. (2016). The Synergistic Roles of Cholecystokinin B and Dopamine D5 Receptors on the Regulation of Renal Sodium Excretion. *PLoS One*, 11(1), e0146641.
- Jiang, X., Liu, Y., Zhang, X.-Y., Liu, X., Liu, X., Wu, X., Jose, P. A., Duan, S., Xu, F.-J., & Yang, Z. (2022). Intestinal Gastrin/CCKBR (Cholecystokinin B Receptor) Ameliorates Salt-Sensitive Hypertension by Inhibiting Intestinal Na<sup>+</sup>/H<sup>+</sup> Exchanger 3 Activity Through a PKC (Protein Kinase C)-Mediated NHERF1 and NHERF2 Pathway. *Hypertension*, 79(8), 1668-1679.
- Jones, C. W. (2018). Another Nobel Prize for Catalysis: Frances Arnold in 2018. *ACS Catal.*, 8(11), 10913-10913.
- Jumper, J., Evans, R., Pritzel, A., Green, T., Figurnov, M., Ronneberger, O., Tunyasuvunakool, K., Bates, R., Žídek, A., Potapenko, A., Bridgland, A., Meyer, C., Kohl, S. A. A., Ballard, A. J., Cowie, A., Romera-Paredes, B., Nikolov, S., Jain, R., Adler, J., Back, T., Petersen, S., Reiman, D., Clancy, E., Zielinski, M., Steinegger, M., Pacholska, M., Berghammer, T., Bodenstein, S., Silver, D., Vinyals, O., Senior, A. W., Kavukcuoglu, K., Kohli, P., & Hassabis, D. (2021). Highly accurate protein structure prediction with AlphaFold. *Nature*, 596(7873), 583-589.
- Junge, W., & Nelson, N. (2015). ATP Synthase. *Annu. Rev. Biochem.*, 84(1), 631-657.
- Kagawa, W., Arai, T., Ishikura, S., Kino, K., & Kurumizaka, H. (2015). Structure of RizA, an L-amino-acid ligase from *Bacillus subtilis*. *Acta Cryst. F.*, 71(9), 1125-1130.
- Kagebayashi, T., Kontani, N., Yamada, Y., Mizushige, T., Arai, T., Kino, K., & Ohinata, K. (2012). Novel CCK-dependent vasorelaxing dipeptide, Arg-Phe, decreases blood pressure and food intake in rodents. *Mol. Nutr. Food Res.*, 56(9), 1456-1463.
- Kalkhof, S., & Sinz, A. (2008). Chances and pitfalls of chemical cross-linking with amine-reactive N-hydroxysuccinimide esters. *Anal. Bioanal. Chem. Res.*, 392(1), 305-312.
- Kaushik, S., Kumar, R., & Kain, P. (2018). Salt an Essential Nutrient: Advances in Understanding Salt Taste Detection Using *Drosophila* as a Model System. *J. Exp. Neurosci.*, 12, 1179069518806894.
- Kazenwadel, F., Franzreb, M., & Rapp, B. E. (2015). Synthetic enzyme supercomplexes: co-immobilization of enzyme cascades. *Anal. Methods*, 7(10), 4030-4037.
- Kazlauskas, R. J., & Bornscheuer, U. T. (2009). Finding better protein engineering strategies. *Nat. Chem. Biol.*, 5(8), 526-529.
- Kearney, P. M., Whelton, M., Reynolds, K., Whelton, P. K., & He, J. (2004). Worldwide prevalence of hypertension: a systematic review. *J. Hypertens.*, 22(1), 11-19.

- Kim, D.-M., & Swartz, J. R. (1999). Prolonging cell-free protein synthesis with a novel ATP regeneration system. *Biotechnol. Bioeng.*, *66*(3), 180-188.
- Kino, H., & Kino, K. (2015). Alteration of the substrate specificity of L-amino acid ligase and selective synthesis of Met-Gly as a salt taste enhancer. *Biosci. Biotechnol. Biochem.*, *79*(11), 1827-1832.
- Kino, H., Nakajima, S., Arai, T., & Kino, K. (2016). Effective production of Pro-Gly by mutagenesis of L-amino acid ligase. *J. Biosci. Bioeng.*, *122*(2), 155-159.
- Kino, K., Nakazawa, Y., & Yagasaki, M. (2008a). Dipeptide synthesis by L-amino acid ligase from *Ralstonia solanacearum*. *Biochem. Biophys. Res. Commun.*, *371*(3), 536-540.
- Kino, K., Noguchi, A., Nakazawa, Y., & Yagasaki, M. (2008b). A novel L-amino acid ligase from *Bacillus Licheniformis*. *J. Biosci. Bioeng.*, *106*(3), 313-315.
- Kino, K., Kotanaka, Y., Arai, T., & Yagasaki, M. (2009). A Novel L-Amino Acid Ligase from *Bacillus subtilis* NBRC3134, a Microorganism Producing Peptide-Antibiotic Rhizocticin. *Biosci. Biotechnol. Biochem.*, *73*(4), 901-907.
- Kino, K., Noguchi, A., Arai, T., & Yagasaki, M. (2010). Identification and characterization of a novel L-amino acid ligase from *Photorhabdus luminescens* subsp. *laumondii* TT01. *J. Biosci. Bioeng.*, *110*(1), 39-41.
- Kirk, O., Borchert, T. V., & Fuglsang, C. C. (2002). Industrial enzyme applications. *Curr. Opin. Biotechnol.*, *13*(4), 345-351.
- Koyama, D., Sasai, M., Matsumura, S., Inoue, K., & Ohinata, K. (2020). A milk-derived pentapeptide reduces blood pressure in advanced hypertension in a CCK system-dependent manner. *Food Func.*, *11*(11), 9489-9494.
- Kugler, M., Loeffler, W., Rapp, C., Kern, A., & Jung, G. (1990). Rhizocticin A, an antifungal phosphono-oligopeptide of *Bacillus subtilis* ATCC 6633: biological properties. *Arch. Microbiol.*, *153*(3), 276-281.
- Langer, R. S., Gardner, C. R., Hamilton, B. K., & Colton, C. K. (1977). Enzymatic regeneration of ATP: II. Equilibrium studies with acetate kinase and adenylate kinase. *AIChE J.*, *23*(1), 1-10.
- Leibrock, E., Bayer, P., & Lüdemann, H. D. (1995). Nonenzymatic hydrolysis of adenosinetriphosphate (ATP) at high temperatures and high pressures. *Biophys. Chem.*, *54*(2), 175-180.
- Li, R., Zhang, Z., Pei, X., & Xia, X. (2020a). Covalent Immobilization of L-Asparaginase and Optimization of Its Enzyme Reactor for Reducing Acrylamide Formation in a Heated Food Model System. *Front Bioeng. Biotechnol.*, *8*, 584758.
- Li, Z., Ning, X., Zhao, Y., Zhang, X., Xiao, C., & Li, Z. (2020b). Efficient One-Pot Synthesis of Cytidine 5'-Monophosphate Using an Extremophilic Enzyme Cascade System. *J. Agric. Food Chem.*, *68*(34), 9188-9194.
- Lim, C. Y., Owens, N. A., Wampler, R. D., Ying, Y., Granger, J. H., Porter, M. D., Takahashi, M., & Shimazu, K. (2014). Succinimidyl Ester Surface Chemistry: Implications of the Competition between Aminolysis and Hydrolysis on Covalent Protein Immobilization. *Langmuir*, *30*(43), 12868-12878.
- Liu, H., & Naismith, J. H. (2008). An efficient one-step site-directed deletion, insertion, single and multiple-site plasmid mutagenesis protocol. *BMC Biotechnol.*, *8*(1), 91.
- Liu, L., Wang, J., Rosenberg, D., Zhao, H., Lengyel, G., & Nadel, D. (2018). Fermented beverage and food storage in 13,000 y-old stone mortars at Raqefet Cave, Israel: Investigating Natufian ritual feasting. *J. Archaeol. Sci. Rep.*, *21*, 783-793.
- Liu, X.-h., Ning, L.-x., Zhang, Y.-f., Wang, Y.-f., Lu, Z.-h., & Wang, T. (2021). Rational engineering of BaLal\_16 from a novel *Bacillus amyloliquefaciens* strain to improve catalytic performance. *Enzyme Microb. Technol.*, *146*, 109781.
- Lohmann, K. (1929). Über die Pyrophosphatfraktion im Muskel. *Sci. Nat.*, *17*(31), 624-625.

- Lutz, S. (2010). Beyond directed evolution—semi-rational protein engineering and design. *Curr. Opin. Biotechnol.*, *21*(6), 734-743.
- Lythgoe, B., & Todd, A. R. (1945). Structure of Adenosine Di- and Tri-Phosphate. *Nature*, *155*(3945), 695-696.
- Ma, S. K., Gruber, J., Davis, C., Newman, L., Gray, D., Wang, A., Grate, J., Huisman, G. W., & Sheldon, R. A. (2010). A green-by-design biocatalytic process for atorvastatin intermediate. *Green Chem.*, *12*(1), 81-86.
- Mahnke, L. (2021). *Charakterisierung der Substratspezifität von Varianten der Aminosäureligase RizA* [Bachelor thesis, Leibniz Universität Hannover].
- Maillet, E. L., Cui, M., Jiang, P., Mezei, M., Hecht, E., Quijada, J., Margolskee, R. F., Osman, R., & Max, M. (2015). Characterization of the Binding Site of Aspartame in the Human Sweet Taste Receptor. *Chem. Sens.*, *40*(8), 577-586.
- Manzanares, P., Gandía, M., Garrigues, S., & Marcos, J. F. (2019). Improving Health-Promoting Effects of Food-Derived Bioactive Peptides through Rational Design and Oral Delivery Strategies. *Nutrients*, *11*(10), 2545.
- Martin, M., Kopaliani, I., Jannasch, A., Mund, C., Todorov, V., Henle, T., & Deussen, A. (2015). Antihypertensive and cardioprotective effects of the dipeptide isoleucine-tryptophan and whey protein hydrolysate. *Acta Physiol.*, *215*(4), 167-176.
- Maruyama, K. (1991). The Discovery of Adenosine Triphosphate and the Establishment of Its Structure. *J. Hist. Biol.*, *24*(1), 145-154.
- Mast, T. A. (2020). *Biokatalytische Produktion von salzgeschmacksverstärkenden Arginyldipeptiden durch die Aminosäureligase RizA unter Regeneration von ATP* [Bachelor thesis, Leibniz Universität Hannover].
- Matsui, T., Tamaya, K., Seki, E., Osajima, K., Matsumoto, K., & Kawasaki, T. (2002). Val-Tyr as a natural antihypertensive dipeptide can be absorbed into the human circulatory blood system. *Clin. Exp. Pharmacol. Physiol.*, *29*(3), 204-208.
- Mattes, R. D., & Donnelly, D. (1991). Relative contributions of dietary sodium sources. *J. Am. Coll. Nutr.*, *10*(4), 383-393.
- Messerli, F. H., Williams, B., & Ritz, E. (2007). Essential hypertension. *Lancet*, *370*(9587), 591-603.
- Michelke, L., Deussen, A., Kettner, K., Dieterich, P., Hagemann, D., Kriegel, T. M., & Martin, M. (2018). Biotechnological production of the angiotensin-converting enzyme inhibitory dipeptide isoleucine-tryptophan. *Eng. Life Sci.*, *18*(4), 218-226.
- Miralles, B., Amigo, L., & Recio, I. (2018). Critical Review and Perspectives on Food-Derived Antihypertensive Peptides. *J. Agric. Food Chem.*, *66*(36), 9384-9390.
- Mizushige, T. (2021). Neuromodulatory peptides: Orally active anxiolytic-like and antidepressant-like peptides derived from dietary plant proteins. *Peptides*, *142*, 170569.
- Mohamad, N. R., Marzuki, N. H. C., Buang, N. A., Huyop, F., & Wahab, R. A. (2015). An overview of technologies for immobilization of enzymes and surface analysis techniques for immobilized enzymes. *Biotechnol. Biotechnol. Equip.*, *29*(2), 205-220.
- Murata, T., Horinouchi, S., & Beppu, T. (1993). Production of poly(L-aspartyl-L-phenylalanine) in *Escherichia coli*. *J. Biotechnol.*, *28*(2), 301-312.
- Nakajima, H., Suzuki, K., & Imahori, K. (1978). Purification and Properties of Acetate Kinase from *Bacillus stearothermophilus*. *J. Biochem.*, *84*(1), 193-203.
- Naramittanakul, A., Buttranon, S., Petchsuk, A., Chaiyen, P., & Weeranoppanant, N. (2021). Development of a continuous-flow system with immobilized biocatalysts towards sustainable bioprocessing. *React. Chem. Eng.*, *6*(10), 1771-1790.
- Nitta, A., Nishioka, H., Fukumitsu, H., Furukawa, Y., Sugiura, H., Shen, L., & Furukawa, S. (2004). Hydrophobic dipeptide Leu-Ile protects against neuronal death by inducing

- brain-derived neurotrophic factor and glial cell line-derived neurotrophic factor synthesis. *J. Neurosci. Res.*, 78(2), 250-258.
- Özcengiz, G., & Öğülür, İ. (2015). Biochemistry, genetics and regulation of bacilysin biosynthesis and its significance more than an antibiotic. *New Biotechnol.*, 32(6), 612-619.
- Petrovičová, T., Markošová, K., Hegyi, Z., Smonou, I., Rosenberg, M., & Rebroš, M. (2018). Co-Immobilization of Ketoreductase and Glucose Dehydrogenase. *Catalysts*, 8(4), 168.
- Pitzer, J., & Steiner, K. (2016). Amides in Nature and Biocatalysis. *J. Biotechnol.*, 235, 32-46.
- Plž, M., Petrovičová, T., & Rebroš, M. (2020). Semi-Continuous Flow Biocatalysis with Affinity Co-Immobilized Ketoreductase and Glucose Dehydrogenase. *Molecules*, 25(18), 4278.
- Porta, R., Benaglia, M., & Puglisi, A. (2016). Flow Chemistry: Recent Developments in the Synthesis of Pharmaceutical Products. *Org. Process Res. Dev.*, 20(1), 2-25.
- Prakash, M. D., Fraser, S., Boer, J. C., Plebanski, M., de Courten, B., & Apostolopoulos, V. (2021). Anti-Cancer Effects of Carnosine—A Dipeptide Molecule. *Molecules*, 26(6), 1644.
- Probst, D., Manica, M., Nana Teukam, Y. G., Castrogiovanni, A., Paratore, F., & Laino, T. (2022). Biocatalysed synthesis planning using data-driven learning. *Nat. Comm.*, 13(1), 964.
- Puri, S., & Lee, Y. (2021). Salt Sensation and Regulation. *Metabolites*, 11(3), 175.
- Quehl, S. (2021). *Mutagenese von RizA zur Beeinflussung der Substratspezifität* [Bachelor thesis, Leibniz Universität Hannover].
- Reetz, M. T. (2013a). The Importance of Additive and Non-Additive Mutational Effects in Protein Engineering. *Angew. Chem. Int. Ed.*, 52(10), 2658-2666.
- Reetz, M. T. (2013b). Biocatalysis in Organic Chemistry and Biotechnology: Past, Present, and Future. *J. Am. Chem. Soc.*, 135(34), 12480-12496.
- Rodrigues, D. S., Mendes, A. A., Adriano, W. S., Gonçalves, L. R. B., & Giordano, R. L. C. (2008). Multipoint covalent immobilization of microbial lipase on chitosan and agarose activated by different methods. *J. Mol. Catal. B Enzym.*, 51(3), 100-109.
- Rosenthaler, L. (1909). Durch Enzyme bewirkte asymmetrische Synthesen. 2. Mitteilung. *Biochem. Z.*, 17, 257.
- Rottmann, E., Hauke, K. F., Krings, U., & Berger, R. G. (2021). Enzymatic acrylamide mitigation in French fries – An industrial-scale case study. *Food Control*, 123, 107739.
- Ruiz-Gayo, M., González, M. C., & Fernández-Alfonso, S. (2006). Vasodilatory effects of cholecystokinin: New role for an old peptide? *Regul. Pept.*, 137(3), 179-184.
- Ruzicka, J., Carroll, A. D., & Lähdesmäki, I. (2006). Immobilization of proteins on agarose beads, monitored in real time by bead injection spectroscopy. *Analyst*, 131(7), 799-808.
- Santos, J. A., Tekle, D., Rosewarne, E., Flexner, N., Cobb, L., Al-Jawaldeh, A., Kim, W. J., Breda, J., Whiting, S., Campbell, N., Neal, B., Webster, J., & Trieu, K. (2021). A Systematic Review of Salt Reduction Initiatives Around the World: A Midterm Evaluation of Progress Towards the 2025 Global Non-Communicable Diseases Salt Reduction Target. *Adv. Nutr.*, 12(5), 1768-1780.
- Santos, S., Torcato, I., & Castanho, M. A. R. B. (2012). Biomedical applications of dipeptides and tripeptides. *Peptide Sci.*, 98(4), 288-293.
- Sato, M., Hosokawa, T., Yamaguchi, T., Nakano, T., Muramoto, K., Kahara, T., Funayama, K., Kobayashi, A., & Nakano, T. (2002). Angiotensin I-Converting Enzyme

- Inhibitory Peptides Derived from Wakame (*Undaria pinnatifida*) and Their Antihypertensive Effect in Spontaneously Hypertensive Rats. *J. Agric. Food Chem.*, 50(21), 6245-6252.
- Savile, C. K., Janey, J. M., Mundorff, E. C., Moore, J. C., Tam, S., Jarvis, W. R., Colbeck, J. C., Krebber, A., Fleitz, F. J., Brands, J., Devine, P. N., Huisman, G. W., & Hughes, G. J. (2010). Biocatalytic Asymmetric Synthesis of Chiral Amines from Ketones Applied to Sitagliptin Manufacture. *Science*, 329(5989), 305-309.
- Schindler, A., Dunkel, A., Stähler, F., Backes, M., Ley, J., Meyerhof, W., & Hofmann, T. (2011). Discovery of Salt Taste Enhancing Arginyl Dipeptides in Protein Digests and Fermented Fish Sauces by Means of a Sensomics Approach. *J. Agric. Food Chem.*, 59(23), 12578-12588.
- Schiraldi, C., & De Rosa, M. (2002). The production of biocatalysts and biomolecules from extremophiles. *Trends Biotechnol.*, 20(12), 515-521.
- Schrödinger, L. (2020). *The PyMOL Molecular Graphics System.*(Version 2.3.1 Version) [Type]. Publisher. URL
- Sheldon, R. A. (2007). Enzyme Immobilization: The Quest for Optimum Performance. *Adv. Synth. Catal.*, 349(8-9), 1289-1307.
- Sheldon, R. A., & van Pelt, S. (2013). Enzyme immobilisation in biocatalysis: why, what and how. *Chem. Soc. Rev.*, 42(15), 6223-6235.
- Sheldon, R. A., & Pereira, P. C. (2017). Biocatalysis engineering: the big picture. *Chem. Soc. Rev.*, 46(10), 2678-2691.
- Sheldon, R. A., & Woodley, J. M. (2018). Role of Biocatalysis in Sustainable Chemistry. *Chem. Rev.*, 118(2), 801-838.
- Shen, D., Song, H., Zou, T., Raza, A., Li, P., Li, K., & Xiong, J. (2022). Reduction of sodium chloride: a review. *J. Sci. Food. Agric.*, 102(10), 3931-3939.
- Shi, H., Su, X., Li, C., Guo, W., & Wang, L. (2022). Effect of a low-salt diet on chronic kidney disease outcomes: a systematic review and meta-analysis. *BMJ Open*, 12(1), e050843.
- Shomura, Y., Hinokuchi, E., Ikeda, H., Senoo, A., Takahashi, Y., Saito, J.-i., Komori, H., Shibata, N., Yonetani, Y., & Higuchi, Y. (2012). Structural and enzymatic characterization of BacD, an L-amino acid dipeptide ligase from *Bacillus subtilis*. *Prot. Sci.*, 21(5), 707-716.
- Stehle, P., Ellger, B., Kojic, D., Feuersenger, A., Schneid, C., Stover, J., Scheiner, D., & Westphal, M. (2017). Glutamine dipeptide-supplemented parenteral nutrition improves the clinical outcomes of critically ill patients: A systematic evaluation of randomised controlled trials. *Clin. Nutr. ESPEN*, 17, 75-85.
- Strazzullo, P., D'Elia, L., Kandala, N.-B., & Cappuccio, F. P. (2009). Salt intake, stroke, and cardiovascular disease: meta-analysis of prospective studies. *BMJ*, 339, b4567.
- Strohm, D., Boeing, H., Leschik-Bonnet, E., Hesecker, H., Arens-Azevêdo, U., Bechthold, A., Knorrpp, L., & Kroke, A. (2016). Salt intake in Germany, health consequences, and resulting recommendations for action. A scientific statement from the German Nutrition Society (DGE). *Ernährungs Umschau*, 63(03), 62-70.
- Suzuki, M., Takahashi, Y., Noguchi, A., Arai, T., Yagasaki, M., Kino, K., & Saito, J.-i. (2012). The structure of L-amino-acid ligase from *Bacillus licheniformis*. *Acta Cryst. D.*, 68(11), 1535-1540.
- Tabata, K., Ikeda, H., & Hashimoto, S.-i. (2005). ywfE in *Bacillus subtilis* Codes for a Novel Enzyme L-Amino Acid Ligase. *J. Bacteriol.*, 187(15), 5195-5202.
- Takagi, H., Shiomi, H., Ueda, H., & Amano, H. (1979). A novel analgesic dipeptide from bovine brain is a possible Met-enkephalin releaser. *Nature*, 282(5737), 410-412.

- Tasnádi, G., Jud, W., Hall, M., Baldenius, K., Ditrich, K., & Faber, K. (2018). Evaluation of Natural and Synthetic Phosphate Donors for the Improved Enzymatic Synthesis of Phosphate Monoesters. *Adv. Synth. Catal.*, *360*(12), 2394-2401.
- Tavanti, M., Hosford, J., Lloyd, R. C., & Brown, M. J. B. (2021). Recent Developments and Challenges for the Industrial Implementation of Polyphosphate Kinases. *ChemCatChem*, *13*(16), 3565-3580.
- ThermoScientific. (2022). *Pierce NHS-Activated Agarose Dry Resin Manual*. Retrieved 24.05.2022 from [https://assets.thermofisher.com/TFS-Assets%2FMSG%2Fmanuals%2FMAN0011707\\_Pierce\\_NHSActiv\\_Agarose\\_Dry\\_Resin\\_UG.pdf](https://assets.thermofisher.com/TFS-Assets%2FMSG%2Fmanuals%2FMAN0011707_Pierce_NHSActiv_Agarose_Dry_Resin_UG.pdf)
- Thompson, M. P., Peñafiel, I., Cosgrove, S. C., & Turner, N. J. (2019). Biocatalysis Using Immobilized Enzymes in Continuous Flow for the Synthesis of Fine Chemicals. *Org. Process Res. Dev.*, *23*(1), 9-18.
- Thum, O. (2004). Enzymatic Production of Care Specialties Based on Fatty Acid Esters. *Tenside Surfactants Deterg.*, *41*(6), 287-290.
- Trieu, K., Neal, B., Hawkes, C., Dunford, E., Campbell, N., Rodriguez-Fernandez, R., Legetic, B., McLaren, L., Barberio, A., & Webster, J. (2015). Salt Reduction Initiatives around the World – A Systematic Review of Progress towards the Global Target. *PLoS One*, *10*(7), e0130247.
- Tsuda, T., Asami, M., Koguchi, Y., & Kojima, S. (2014). Single Mutation Alters the Substrate Specificity of L-Amino Acid Ligase. *Biochemistry*, *53*(16), 2650-2660.
- Uchytíl, T. F., & Durbin, R. D. (1980). Hydrolysis of tabtoxins by plant and bacterial enzymes. *Experientia*, *36*(3), 301-302.
- Vandenbeuch, A., & Kinnamon, S. C. (2020). Is the Amiloride-Sensitive Na<sup>+</sup> Channel in Taste Cells Really ENaC? *Chem. Sens.*, *45*(4), 233-234.
- Velasco-Lozano, S., Benítez-Mateos, A. I., & López-Gallego, F. (2017). Co-immobilized Phosphorylated Cofactors and Enzymes as Self-Sufficient Heterogeneous Biocatalysts for Chemical Processes. *Angew. Chem. Int. Ed.*, *56*(3), 771-775.
- Vercruyse, L., Morel, N., Van Camp, J., Szust, J., & Smagghe, G. (2008). Antihypertensive mechanism of the dipeptide Val-Tyr in rat aorta. *Peptides*, *29*(2), 261-267.
- Vorwerk, K. (2022). *Heterologe Produktion basidiomycetischer Peptidasen zur Reduktion von Speisesalz in Lebensmitteln* [Doctoral thesis, Leibniz Universität Hannover]. Hannover.
- Wang, T., Zhang, Y.-f., Ning, L.-x., Wang, Y.-f., Liu, X.-h., Li, R., & Chen, X.-e. (2020). L-amino acid ligase: A promising alternative for the biosynthesis of L-dipeptides. *Enzyme Microb. Technol.*, *136*, 109537.
- Wang, Y., & Zhang, Y. H. P. (2009). Cell-free protein synthesis energized by slowly-metabolized maltodextrin. *BMC Biotechnol.*, *9*(1), 58.
- Webster, J., Trieu, K., Dunford, E., & Hawkes, C. (2014). Target Salt 2025: A Global Overview of National Programs to Encourage the Food Industry to Reduce Salt in Foods. *Nutrients*, *6*(8), 3274-3287.
- Whicher, A., Camprubi, E., Pinna, S., Herschy, B., & Lane, N. (2018). Acetyl Phosphate as a Primordial Energy Currency at the Origin of Life. *Orig. Life Evol. Biosph.*, *48*(2), 159-179.
- WHO. (2012). *WHO Guideline: sodium intake for adults and children*. <https://www.who.int/publications/i/item/9789241504836>
- WHO. (2013). *Global Action Plan for the Prevention and Control of NCDs 2013-2020*. <https://www.who.int/publications/i/item/9789241506236>
- Wu, B., Yang, D., Yang, S., & Zhang, G. (2021a). Dietary Salt Intake and Gastric Cancer Risk: A Systematic Review and Meta-Analysis. *Front. Nutr.*, *8*.



- Wu, S., Snajdrova, R., Moore, J. C., Baldenius, K., & Bornscheuer, U. T. (2021b). Biocatalysis: Enzymatic Synthesis for Industrial Applications. *Angew. Chem. Int. Ed.*, *60*(1), 88-119.
- Xu, J.-J., Elkaddi, N., Garcia-Blanco, A., Spielman, A. I., Bachmanov, A. A., Chung, H. Y., & Ozdener, M. H. (2017). Arginyl dipeptides increase the frequency of NaCl-elicited responses via epithelial sodium channel alpha and delta subunits in cultured human fungiform taste papillae cells. *Sci. Rep.*, *7*(1), 7483.
- Yagasaki, M., & Hashimoto, S.-i. (2008). Synthesis and application of dipeptides; current status and perspectives. *Appl. Microbiol. Biotechnol.*, *81*(1), 13-22.
- Yamada, H., & Kobayashi, M. (1996). Nitrile Hydratase and Its Application to Industrial Production of Acrylamide. *Biosci. Biotechnol. Biochem.*, *60*(9), 1391-1400.
- Yan, B., Ding, Q., Ou, L., & Zou, Z. (2014). Production of glucose-6-phosphate by glucokinase coupled with an ATP regeneration system. *World J. Microbiol. Biotechnol.*, *30*(3), 1123-1128.
- Yan, F., Cui, H., Zhang, Q., Hayat, K., Yu, J., Hussain, S., Tahir, M. U., Zhang, X., & Ho, C.-T. (2021). Small Peptides Hydrolyzed from Pea Protein and Their Maillard Reaction Products as Taste Modifiers: Saltiness, Umami, and Kokumi Enhancement. *Food Bioprocess Technol.*, *14*(6), 1132-1141.
- Yi, D., Bayer, T., Badenhorst, C. P. S., Wu, S., Doerr, M., Höhne, M., & Bornscheuer, U. T. (2021). Recent trends in biocatalysis. *Chem. Soc. Rev.*, *50*(14), 8003-8049.
- Yokoyama, K., Chiba, H., & Yoshikawa, M. (1992). Peptide Inhibitors for Angiotensin I-Converting Enzyme from Thermolysin Digest of Dried Bonitot. *Biosci. Biotechnol. Biochem.*, *56*(10), 1541-1545.
- Yokozeki, K., & Hara, S. (2005). A novel and efficient enzymatic method for the production of peptides from unprotected starting materials. *J. Biotechnol.*, *115*(2), 211-220.
- Yokozeki, K., & Abe, I. (2020). A novel route for aspartame production by combining enzymatic and chemical reactions for industrial use. *Biosci. Biotechnol. Biochem.*, *85*(2), 464-466.
- Yu, T., Huang, J., Liu, W., Pan, J., & Liu, J. (2020). *Preparation method of L-glutamic acid-L-tryptophan dipeptide by mutated L-amino acid ligase and enzymatic method* (China Patent No. CN110777123).
- Yu, T., Pan, J., & Liu, J. (2021). *Mutant enzyme and its application in catalyzing glycine, histidine and lysine to produce GHK* (China Patent No. CN112280755).
- Yushkova, E. D., Nazarova, E. A., Matyuhina, A. V., Noskova, A. O., Shavronskaya, D. O., Vinogradov, V. V., Skvortsova, N. N., & Krivoschapkina, E. F. (2019). Application of Immobilized Enzymes in Food Industry. *J. Agric. Food Chem.*, *67*(42), 11553-11567.
- Zhang, Y., Venkitasamy, C., Pan, Z., Liu, W., & Zhao, L. (2017). Novel Umami Ingredients: Umami Peptides and Their Taste. *J. Food. Sci.*, *82*(1), 16-23.
- Zheng, C., Qu, M., Liu, Y., Wang, J., & Ying, H. (2021a). Design and optimizing a new CDP-choline *in vitro* multienzyme producing process starts from D-ribose. *Biotechnol. Appl. Biochem.*
- Zheng, Y., Tang, L., Yu, M., Li, T., Song, H., Li, P., Li, K., & Xiong, J. (2021b). Fractionation and identification of salty peptides from yeast extract. *J. Food Sci. Technol.*, *58*(3), 1199-1208.
- Zhu, Y., Zhang, L., Sun, A., Bao, C., Zou, J., & Yu, Z. (2019). *One-step synthesis of L-carnosine using L-amino acid ligase* (China Patent No. CN109593805).
- Zucca, P., Fernandez-Lafuente, R., & Sanjust, E. (2016). Agarose and Its Derivatives as Supports for Enzyme Immobilization. *Molecules*, *21*(11), 1577.

## 11 Lebenslauf

Name Sven Ingo Bordewick  
Geboren 07.12.1989 in Hamburg

### Beruflicher Werdegang

---

seit 08/2022	<b>Wissenschaftlicher Mitarbeiter (100 %)</b> , Institut für Lebensmittelchemie, Leibniz Universität Hannover
01/2019 – 07/2022	<b>Wissenschaftlicher Mitarbeiter (50 %)</b> , Institut für Lebensmittelchemie, Leibniz Universität Hannover
08/2018 – 12/2018	<b>Wissenschaftliche Hilfskraft</b> , Institut für Lebensmittelchemie, Leibniz Universität Hannover

### Schule und akademische Laufbahn

---

seit 10/2018	<b>Promotion in Chemie</b> unter Prof. Dr. rer. nat. Dr.-Ing. habil. Ralf Günter Berger, Institut für Lebensmittelchemie, Leibniz Universität Hannover
01/2017 – 05/2018	<b>Orientierungsphase und Suche nach einer passenden Promotionsstelle</b>
10/2013 – 12/2016	<b>Master of Science Biochemie</b> , Universität Greifswald <ul style="list-style-type: none"> <li>▪ Note: 1,1</li> <li>▪ Abschlussarbeit: „Investigations of Baeyer-Villiger monooxygenases from <i>Yarrowia lipolytica</i>“ (Note 1,1)</li> </ul>
10/2010 – 09/2013	<b>Bachelor of Science Biochemie</b> , Universität Greifswald <ul style="list-style-type: none"> <li>▪ Note: 1,2</li> <li>▪ Abschlussarbeit: „Mutagenesis of Baeyer-Villiger monooxygenases to alter the NADH/NADPH specificity“ (Note 1,0)</li> </ul>
08/2000 – 06/2010	<b>Allgemeine Hochschulreife</b> , Gymnasium Barmstedt <ul style="list-style-type: none"> <li>▪ Note: 1,5</li> </ul>

### Stipendien und Auszeichnungen

---

09/2018	<b>GBM-Masterpreis für herausragende Masterarbeit</b> , Universität Greifswald/Gesellschaft für Biochemie und Molekularbiologie (GBM)
10/2014 – 09/2015	<b>Deutschlandstipendium für besonders leistungsstarke Studierende</b> , Universität Greifswald
2013	<b>Auszeichnung für besondere Leistungen in der Bachelorprüfung im Jahr 2013</b> , Gesellschaft Deutscher Chemiker (GDCh)

## 12 Liste der wissenschaftlichen Publikationen

Die vorliegende Dissertation basiert auf den folgenden Publikationen:

- **Bordewick, S.**, Mast, T. A., Berger, R. G., & Ersoy, F. (2021). Recombinant Production of Arginyl Dipeptides by L-Amino Acid Ligase RizA Coupled with ATP Regeneration. *Catalysts*, 11(11), 1290.
- **Bordewick, S.**, Berger, R. G., & Ersoy, F. (2021). Mutagenesis of the L-Amino Acid Ligase RizA Increased the Production of Bioactive Dipeptides. *Catalysts*, 11(11), 1385.
- **Bordewick, S.**, Berger, R. G., & Ersoy, F. (2022). Co-Immobilization of RizA Variants with Acetate Kinase for the Production of Bioactive Arginyl Dipeptides. *Molecules*, 27(14), 4352.

Die folgende Publikation ist während der Promotion entstanden, aber nicht Gegenstand dieser Dissertation:

- Berger, R. G., **Bordewick, S.**, Krahe, N.-K., & Ersoy, F. (2022). Mycelium vs. Fruiting Bodies of Edible Fungi—A Comparison of Metabolites. *Microorganisms*, 10(7), 1379.

Die folgenden Beiträge auf wissenschaftlichen Konferenzen sind im Rahmen der Promotion entstanden, aber nicht Gegenstand dieser Dissertation:

- **Bordewick, S.**, Diestelhorst, H., Vorwerk, K., Berger, R. G. Salzgeschmack verstärkende Peptide – Viele Optionen, ein Ziel. Vortrag auf der DLG-Think Food 2021 Online-Konferenz, 15. – 16. Juni 2021, Deutschland
- **Bordewick, S.**, Mast, T. A., Berger, R.G., Ersoy, F. Biocatalytic Production of Bioactive Dipeptides. Poster auf dem GDCh JCF Frühjahrssymposium 2022, 23. – 26. März, Hannover, Deutschland

Die folgenden Publikationen sind vor der Promotion entstanden und basierten auf Ergebnissen der Bachelor- und Masterarbeit:

- Beier, A., **Bordewick, S.**, Genz, M., Schmidt, S., van den Bergh, T., Peters, C., Joosten, H. J., Bornscheuer, U. T. (2016). Switch in Cofactor Specificity of a Baeyer-Villiger Monooxygenase. *ChemBioChem*, 17(24), 2312–2315.
- **Bordewick, S.**, Beier, A., Balke, K., Bornscheuer, U. T. (2018). Baeyer-Villiger monooxygenases from *Yarrowia lipolytica* catalyze preferentially sulfoxidations. *Enzyme Microb. Technol.*, 109, 31–42.